Bioactivity and bioaccessibility of novel rutin-protein composites incorporated into a functional dairy beverage

A thesis submitted in partial fulfilment of the requirements for the degree of Master of Food Technology

Massey University

Palmerston North, New Zealand

Anubhavi Singh

2022

Abstract

Rutin, a plant-derived bioactive compound is becoming increasingly popular as a natural ingredient in various nutraceutical, pharmaceutical, or cosmetic industries. However, because of its hydrophobic nature, rutin possesses a low solubility in both aqueous- and lipid-based systems; thereby, reducing its absorption in the gastrointestinal digestion tract. Such properties of rutin (i.e., poor solubility and low bioavailability) have been the main limiting factors against its use as a functional ingredient in the food industry so far. Pertaining to its functional attributes for exhibiting anti-oxidative potency coupled with its metabolic capacity that regulates cellular functions in the physiological system, previous research at Massey University invented a highly soluble form of rutin using a food protein (sodium caseinate). This delivery system safeguards rutin against undesirable changes that occur during the processing and storage of the food, as well as under the conditions of the upper part of the gastrointestinal system. This patented novel technology, known as 'FlavoPlus' existing in the form of two products (FlavoPlus 1™ and FlavoPlus 2™), can deliver rutin at the targeted sites in the gut and can substantially improve its bioavailability. Accordingly, the current research used FlavoPlus™ as a functional ingredient for the assessment of its functionality (bioactivity and bioaccessibility of rutin) in a protected form after its incorporation into a functional milk beverage. This study also aimed to assess the antioxidant capacity and the subsequent absorption using a Caco-2 cell model system.

This research was carried out in two phases. In Phase 1, the antioxidant potential of FlavoPlus 1 (FP1), FlavoPlus 2 (FP2), and rutin hydrate (RH) was investigated using DPPH (2,2-diphenyl-1-picryl-hydrazyl) assay, which attributed to the total antioxidant content present in these three samples. FP1 and FP2 had significantly ($p \leq 0.05$) higher scavenging abilities in a concentration-dependent manner than RH. Further, the total phenolic content (TPC) in FP1, FP2, and RH was measured by corresponding each concentration with rutin equivalent present in the three samples. RH consisted of 94% rutin equivalent per gram of sample whereas FP1 and FP2 had 46% and 27.3% rutin equivalent per gram of sample, respectively. Although RH contained higher rutin content (%), its antioxidant activity was lower than FP1 at 200 µg/mL. Further, FP1, FP2, and RH were subjected to an *in vitro* cell-based model to measure their cell viability and intracellular antioxidant potency using Caco-2 cells that were stimulated with 0.1% DMSO. With an increase in their concentration, FP1 and FP2 maintained cell viability

better than RH after four hours of incubation. As there were no significant ($p>0.05$) differences in cell viability, it was proposed that FP1 and FP2 protected Caco-2 cells without causing any toxicity even at higher concentrations. In addition, the intracellular antioxidant assay proposed that FP1 and FP2 exhibited higher antioxidative potency even at a low concentration of 0.5 µg/mL than RH in Caco-2 cells that were stimulated with a free radical generator (i.e., 2,2′-azobis(2-methylpropionamidine) dihydrochloride (AAPH)) during 0, 10, and 30 minutes of incubation. Thus, similar attributes were analysed after exposing FP1, FP2, and RH to *in vitro* gastrointestinal digestion, to understand the interactions between rutin-protein composites and the dairy beverage matrix.

In Phase 2, the rutin-protein composites and RH were incorporated into a dairy beverage to deliver rutin in the gut. Bigger particle size was observed for FP2 during both gastric and intestinal phases, when compared to FP1, thereby reducing the surface area. Whereas RH showed a decreasing trend for particle size from gastric to intestinal phase, which could be due to the aggregation of proteins as the result of pH change during both gastric and intestinal phases. Moreover, the bioaccessibility of FP1 and FP2 after digestion was estimated at 63% and 45%, respectively. These bioaccessible samples were subjected to transepithelial electrical resistance (TEER) estimation. The findings suggested that FP2 maintained the barrier integrity of Caco-2 cell monolayers even at high concentrations over 24 hours of incubation whereas, FP1 had a lower TEER value suggesting a disruption in the epithelial barrier. These results are in accordance with the findings obtained from the cell viability assay as FP1 and FP2 maintained the viability within a similar range of concentrations. In addition, the intracellular antioxidant assay proposed that FP2 exhibited higher antioxidant potency than either FP1 or RH during 0 and 10 minutes of incubation. With a longer incubation period, FP1 was stronger in scavenging AAPH even at a higher concentration of 25 µg/mL.

Taken together, the findings of this research confirmed that both FlavoPlus products could be delivered through a suitable dairy matrix (i.e., a milk beverage) as the carrier that attributes their high digestibility and enhanced functional properties within the gut without compromising human health and nutrition. Thus, based on the findings of this research, it can be concluded that FP1 and FP2 showed higher bioactivity than RH based on their antioxidant potential and cell viability of Caco-2 cells. The rutin-protein composites exhibited higher bioaccessibility when delivered through a dairy matrix and were found to

be non-toxic to Caco-2 cells at higher concentrations resulting in good barrier integrity for Caco-2 monolayers. However, further research is required to assess the bioavailability of rutin-protein composites after digestion within physiological systems *in vivo*.

Acknowledgement

This journey at Massey University has not been an easy one for me but I am in debt to many individuals for their help, guidance and positive encouragement while pursuing my master's degree. Firstly, I would like to thank Riddet Institute, AgResearch and High-Value Nutrition (HVN) for giving me an opportunity to work on this project by providing financial support.

I wish to express my sincere gratitude to my supervisor, Dr. Ali Rashidinejad for his suggestions, guidance, and much needed support throughout the project. I was not always the perfect student, yet he never gave up and was always patient. I would also acknowledge the help of Dr. Raise Ahmad, my co-supervisor, for his insights and assistance while drafting cell culture experiments and valuable contribution towards my project.

Furthermore, I want to thank Ajitpal Purba (Senior Technician, AgResearch) for helping me with solving all my problems while handling cells and making me feel confident throughout my project. I am also grateful for Maggie Zou (Riddet Institute) for always being there for me during the tough and happy times. I am thankful for Maggie's help in procurement of all the required materials and training me on various equipment's within the laboratories. I am profoundly grateful to Karen Pickering (Administrator, School of Food and Advanced Technology) for helping me during my thesis submission process. I am also grateful to Denise Martin (Administrator, AgResearch) for solving all my IT problems and making me feel welcome as a student at AgResearch. I would also like thank and acknowledge Tim O'Dea, Peter Jeffrey and Mark Adams for helping me with all my IT issues and acquiring licenses for the software packages.

I also want to express my profound thanks to Dr. Rachel Anderson (Team Leader, AgResearch) and Dr. Dulantha Ulluwishewa (Research Scientist, AgResearch) for their inputs during the absorption and co-culture mechanisms. I would also like to express gratitude to my mentor, Professor Matt Golding, for his encouragement and his valuable insights and knowledge on fundamentals of food science. I am grateful to Prof. Matt Golding for taking time out for me whenever I needed his advice and guidance for personal and professional development.

I would also like to thank all my friends for their constant support, motivation, and financial help during the tough times. Special thanks to Arushi, Olivia, Kshitiz, Fabian and Shorya for listening to my late-night rants despite your own problems and helping me cope up during the pandemic far away from home. I am also grateful to Akshay, Linda, Solita, Ngoc and Peng whom I have met in NZ and have helped me manage my anxiety and made me believe in myself more. I am also thankful to my batchmates Kizzy, Nan, Wenwen and Susan for brainstorming solutions while understanding food research gaps. I am grateful for my officemate, Amin who helped me with all my formatting issues during my thesis writing and feeding me food and driving me back home safely during all my late nights at the office.

Lastly, I would like to thank my brother, Kanishk for always being a protective big brother and helping me understand how the world works far away from home and making me more independent.

Forever grateful for all the sacrifices made by my parents.

I hope you will be proud of me, wherever you are.

Table of Content

List of tables

List of figures

List of abbreviations

Abbreviation	Terminology
A549	Adenocarcinoma human alveolar basal epithelial cells
AAPH	2,2′-azobis(2-methylpropionamidine) dihydrochloride
ANOVA	Analysis of variance
Aβ	B-amyloid peptides
BHT	Butylated hydroxytoluene
BSA	Bovine serum albumin
C6 glioma cells	Rat glioblastoma cell line
Caco-2	Colorectal adenocarcinoma cells
CAT	Catalase
COX-1	Cyclooxygenase-1
DAD	Diode-array detection
DCFH-DA	2′,7′-dichlorofluorescin diacetate
DHA	Docosahexaenoic acid
DMSO	Dimethyl sulfoxide
DPPH	1,1-diphenyl-2-picrylhydrazyl
EGCS	Epigallocatechin gallate
EPA	Eicosapentaenoic acid

EVOM	Epithelial Voltohmmeter
FBS	Fetal bovine serum
FC	Folin-Ciocalteu
FP1, FP2	FlavoPlus™ 1 , FlavoPlus™ 2
GIT	Gastrointestinal tract
GLUT	Glucose transporter
GRAS	Generally recognised as safe
G-rutin	4(g)-alpha-glucopyranosylrutin
GSH-Px	Glutathione peroxidase
HepG2	Hepatocellular carcinoma cell line
HPLC	High performance liquid chromatography
HT29	Human colorectal adenocarcinoma cell line
HUVEC	Human umbilical vein endothelial cells
IBD	Inflammatory bowel disease
IL-1B, IL-6, IL-8	Interleukin 1β, Interleukin-6, Interleukin-8
iNOS	Inducible nitric oxide synthase
LC-MS	Liquid chromatography mass spectrometry
LDL-C	Low-density lipoprotein cholesterol
LPS	Lipopolysaccharide
MEM	Minimum essential media

µg	Microgram
µM	Micromolar
mL	Millilitre
mins	Minutes
MTT	3-(4,5-dimethylthiazol-2-yl)-2,5-diphenyltetrazolium bromide
NaCas	Sodium caseinate
NEAA	Non-essential amino acids
NF-κB	Nuclear factor kappa b
NMR	Nuclear magnetic resonance
PBS	Phosphate-buffer saline
pH	Potential of hydrogen
Pen-Strep	Penicillin-streptomycin
RH	rutin hydrate
ROS	Reactive oxygen species
RPM	Revolutions per minute
SGF	Simulated gastric fluid
SGLT-1	Sodium glucose transport protein
SH-SY5Y	Triple cloned subline of neuroblastoma cell line SK-N-SH
SIF	Simulated intestinal fluid
SMEDDS	Self-emulsifying drug delivery system

SPSS	Statistical package for the social sciences
STZ	Streptozotocin
TEER	Transepithelial electrical resistance
TNF- α	Tumour necrosis factor alpha
TPC	Total phenolic content
T-SOD	Total superoxide dismutase
UV-Vis	Ultraviolet visible
Vc	Vitamin C

Introduction

1.1. Background

Diet and health are the major contributors to the onset of chronic diseases worldwide (Frutos et al., 2019). The industrial revolution has caused an advent in agriculture and the processing of food products, which risks the incidence of lifestyle-related diseases (Wu & Schauss, 2012). Most of the population globally suffers from diet-related chronic diseases caused by poor nutrition (e.g., a high-fat, sugar, and salt-rich diet) coupled with fewer levels of physical activity. This has increased the potential of changing food choices to promote healthy regulation of nutrients and dietary components (Ruiz-Cruz & Ornelas-Paz, 2017). Chronic diseases such as type-2 diabetes, arthritis, cancer, cardiovascular, and neurogenerative diseases induced by oxidative stress, uncontrolled inflammation, and mitochondrial dysfunction is a major contributor to mortality. According to World Health Organisation (WHO), the global mortality rate due to chronic diseases was around 71%, which demonstrates that, epidemiologically, a healthy diet is necessary to improve life expectancy and quality of life (Kyrø et al., 2013; McGuire, 2016; Organization, 2019). Subsequently, a variety of health-promoting foods that exhibit bioactive compounds have emerged in the format of "functional foods" (Roberfroid, 2002).

The Food and Nutrition Board of the National Academy of Sciences defines functional food as a potentially healthy product including "any modified food or food ingredient that may provide a health benefit beyond that of traditional nutrients it contains" (Milner, 2000). For a functional food product to achieve optimum nutrition, we need adequate scientific knowledge that satisfies the dietary need of all members of a population. Epidemiologically speaking, every functional food needs to be validated and biologically relevant for a specific health benefit it possesses. Functional foods can be designed to target specific functions or reduce the risk of disease with strong scientific evidence (Roberfroid, 2002). The simplest forms of functional foods available are vegetables and fruits. Nonetheless, there are commercial functional food products such as fortified drinks (e.g., products containing dietary fibres and additional fortified vitamins, green tea enriched with catechins), enriched food products (e.g., margarine with cholesterol-lowering agents), and enhanced food products (e.g., eggs with enriched omega-3

and yoghurts with prebiotics and probiotics) (Lau et al., 2012). The global market size of functional foods and beverages was USD 258 billion in 2020, which is set to increase by 9.5% in consecutive years (i.e., reaching USD 529 billion by 2028). Such an unprecedented demand in the functional food market was attributed to the global impact of COVID-19 (Supplements, 2021).

Traditionally, chronic diseases and inflammation have been treated with alternative medicine with historical roots such as Ayurveda and phytotherapy that uses naturally occurring plants and herbs (Sen & Chakraborty, 2017). These plant-derived fruits and vegetables are rich in bioactive moieties that are characterised by a wide variety of naturally occurring molecules that possess a polyphenolic structure (Hussain et al., 2019; Ignat et al., 2011). These molecules consist of several hydroxyl groups on aromatic rings. These polyphenols are further classified into flavonoids and phenolic acids (Ignat et al., 2011). Flavonoids consist of six sub-groups including flavones, flavonols, flavanol, isoflavones, and anthocyanins. These are found abundantly in fruits and vegetables such as plums, cherry, blueberries, celery, capsicum, soy, grapefruit, oranges, and plant-derived beverages such as wines, teas, and berry juices (Clifford, 2000; Hussain et al., 2019; Wang & Li, 2015). Phenolic acids, on the other hand, include tannins, lignans, and stilbenes. Major sources of phenolic acids are coffee, berries, grapes, cereals, spinach, and tomatoes (Naczk & Shahidi, 2006).

Rutin is a natural bioactive classified as a flavonol glycosidic derivative comprising of flavonol quercetin and disaccharide rutinose (Sharma et al., 2013). It is commonly found in buckwheat and grapes which are the major sources. Rutin can be extracted from different parts of plants (e.g., *Sophora Japonica*) including leaves, hulls, seeds, buds, peels, and dried sprouts, with the concentration found in the extract differing based on the variety of the plants (Frutos et al., 2019). Rutin has been reported for its antioxidant and free radical scavenging activity, and it exerts anti-inflammatory properties by reducing inducible nitric oxide synthase (iNOS) activity in cells and appears to mitigate the effect of pro-inflammatory cytokines (Yu et al., 2015).

Even though several studies have revealed rutin's capability to induce anticancer effect and scavenge radicals, it still possesses a challenge of low bioavailability due to hydrophobicity and inadequate absorption in the gastrointestinal tract (GIT) (Ben Sghaier et al., 2016; Hussain et al., 2019). Accordingly, due to its low bioavailability, a higher dose is required to induce the health-promoting properties in the body. There are various dosage forms of rutin available for

their respective treatment of diseases. Few studies have reported 1000 mg/day for its antioxidant action while others have suggested a variable range of 400-1000 mg/day for its blood vessel protection in cardiovascular diseases (Boyle et al., 2000; Hendler & Rorvik, 2008). In this regard, there are different oral dosage forms of rutin currently available in the market for various ailments; e.g., tablets, capsules, chewable, gels, powders, soft-gel capsules, suspensions, and ointment/creams (Sharma et al., 2013).

To achieve the effective bioavailability of a bioactive compound such as rutin, various delivery systems have been designed, which can increase the absorption rate of bioactives. The stability of a bioactive compound can be disrupted due to metabolic reactions that occur in the GIT. These reactions can affect the stereochemistry, molecular weight, and chemical structure of such a compound (Hussain et al., 2019). In order to avoid structural modification of rutin before absorption, it needs better stability and an enhanced biological delivery system. Such a system can likely be provided by protein-based nano-carriers such as albumin or milk-derived caseins, nano-emulsion encapsulation, or nanoparticles (Bordenave et al., 2014; Rashidinejad, 2020; Rashidinejad et al., 2019; Thiruvengadam et al., 2018). A protein-based encapsulation/delivery system can influence different electric charges based on varying pH.

The complexity of choosing a compatible food matrix is strongly influenced by the choice of encapsulation method or nano-carrier for the bioactive compound (Dima et al., 2020). In this research, it was hypothesised that the interactions between bioactive compound (i.e., rutin) and protein (i.e., caseinate) could improve the bioaccessibility of rutin incorporated into a functional food matrix and increase its bioavailability and absorption in a cell model system. It was already known that the development of such novel rutin-protein composites resulted in a highly dispersible powder comprised of sodium caseinate as the water-soluble dairy protein ingredient (Rashidinejad et al., 2019). By developing protein complexes/composites with hydrophobic bioactives, the requirement for high doses of such dietary supplements can be reduced by enhancing their bioaccessibility. Considering the interaction of rutin with milk proteins, and its stability under acidic systems with effective solubilisation of a hydrophobic compound, a milk beverage may be a suitable vehicle for delivering rutin in the gut with high digestibility and enhanced intestinal absorption. These novel rutin-protein composites may result in a functional antioxidant within the human physiological system and exhibit as a functional ingredient without compromising the desirable properties of the food product and human health.

1.2. Aims and objectives

The current study was undertaken to demonstrate and achieve the following aims:

1. To determine cell cytotoxicity and antioxidant potential of protected rutin (rutin-casein composites; FlavoPlus^{TM}) in comparison with rutin hydrate (RH), using an *in vitro* cell culture model of human intestinal epithelial cells (Caco-2).

2. To investigate the bioaccessibility, physicochemical properties, and intracellular antioxidant potential of FlavoPlus products incorporated into a functional milk product, using an *in vitro* gastrointestinal model.

To achieve these aims, the research was carried out with three objectives as follows:

- Determination of the free radical scavenging capacity, cell cytotoxicity, and intracellular antioxidant potential of rutin-casein composites (FlavoPlus^{TM} 1 and FlavoPlus^{TM} 2) in comparison to rutin hydrate.
- Incorporation of the novel rutin-casein composites into a milk beverage and investigation of the effect on its structural and analytical properties, as well as determination of the bioaccessible rutin using static *in vitro* gastro-intestinal model.
- Determination of the absorption and intracellular antioxidant potential of rutin in the fortified milk beverage using intestinal epithelial cell model (polarised Caco- 2 cells).

The schematic outline of the structure of the current research is presented in Figure 1.1.

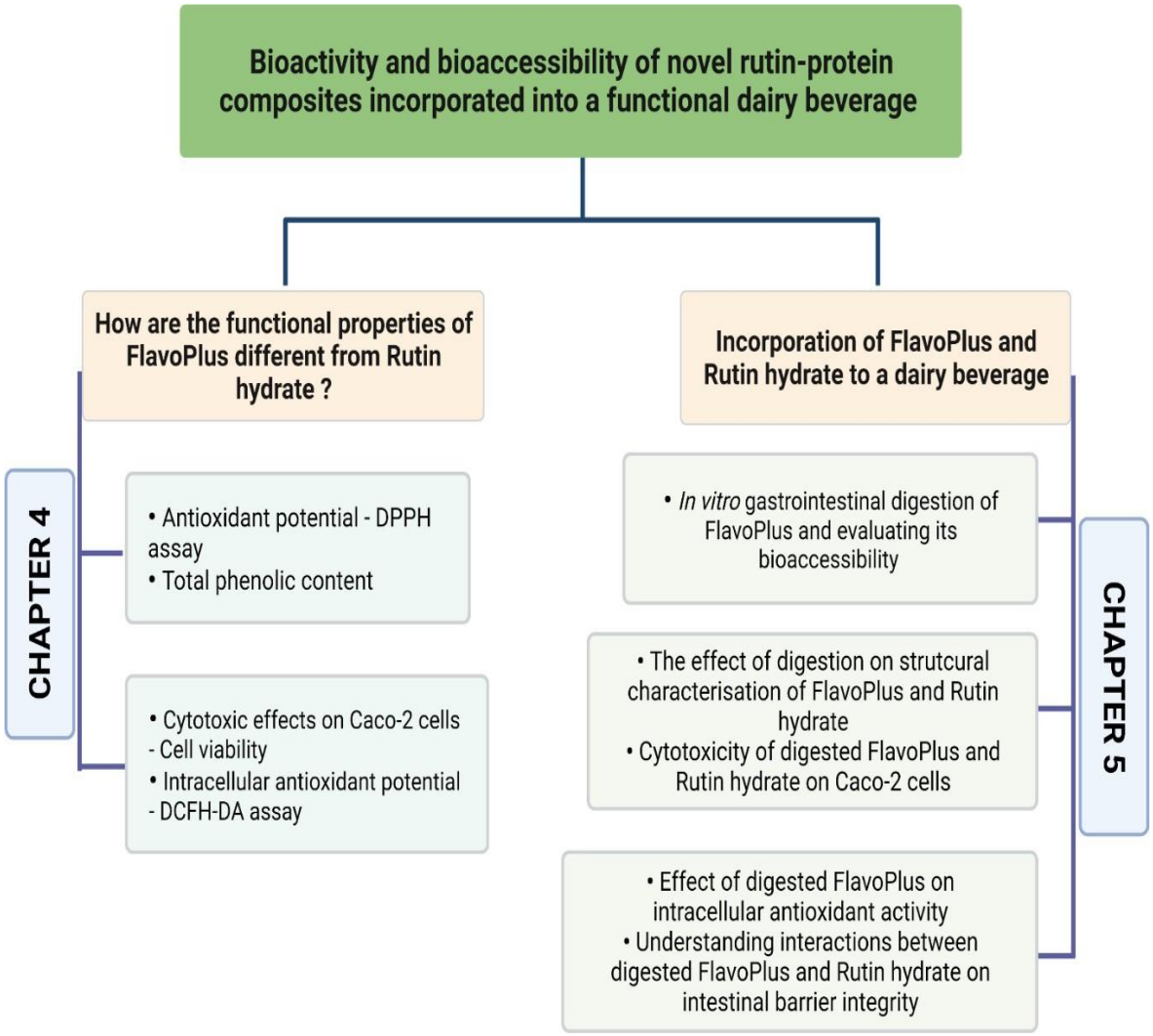

Figure 1.1 Schematic outline of the structure of the current research

Review of literature

2.1. Rutin

Rutin is a citrus flavonoid glycoside generally available in the form of a yellow powder. The name 'Rutin' was derived from a plant called *Ruta graveolens*, which is how the compound was discovered (Frutos et al., 2019; Yang et al., 2008b). Rutin is also known as rutoside, sophorin, quercetin-3-rutinoside, and vitamin P (Albu et al., 2013). This natural flavonol comprises quercetin and a disaccharide (i.e., rutinose), and is found abundantly in different plants, citrus fruits, vegetables, plant-derived beverages like buckwheat, apple, grape, tea, and wines. Various plant species with naturally occurring rutin are *Sophora japonica* (Fabaceae), *Canna indica* (Cannaceae), and *Eucalyptus spp.* (Myrtaceae) (Negahdari et al., 2021). These sources have a variable amount of rutin content due to their growing conditions with different environmental factors like ultraviolet radiation (UV), and temperature (Frutos et al., 2019).

Table 2.1 Rutin content in different plant-derived sources (Frutos et al., 2019)

Plant name	Plant part (s)	Rutin content (mg/100 g dry weight)	Reference
Rue (*Ruta graveolens* L.)	Leaves	3.1	(Proestos et al. (2006)
Common buckwheat (*Fagopyrum sculentum* Moench.)	Hulls Dried sprouts Seeds	3.25 157 10	(Glavač et al., 2017)
Tartary buckwheat (*Fagopyrum tataricum* Gaertn.)	Seeds	1250	(Fabjan et al., 2003)
Apples (*Malus pumila* L.)	Peel	800	(Wach et al., 2007)
Grapes (*Vitis vinifera* L.)		1.592	(Iacopini et al., 2008)
Sea buckthorn (*Hipppophae rhamnoides* L.)	Leaves	300	(Zu et al., 2006)
Amaranthus hybrid (*Amaranthus cruentus)*	Seeds Leaves	8 2.450	(Kalinova & Dadakova, 2009)

2.2. Chemistry of rutin

Flavonoids have a core structure based on the three-carbon bridge (C_6 -C_6 -C_6), which is cyclized with oxygen. Flavonoids provide color pigments like yellow, purple, red, and blue in plants and vegetables due to the presence of chemotaxonomic markers (Prasad & Prasad, 2019). Rutin was discovered in the 19th century in *Ruta graveolens* L. (*Rutaceace*) (Yang et al., 2008a).

2.2.1. Structural characteristics of rutin

As mentioned in the previous section, rutin glycoside is a combination of aglycone quercetin along with a disaccharide rutinose (rhamnose and glucose). In the proposed structure of rutin, there is the presence of two intramolecular hydrogen bonds between quercetin and the glucose moieties (Prasad & Prasad, 2019), along with a trans conformation between rhamnose and glucose moieties of rutin that makes it a rigid structure (Jin et al., 1990). Flavonols undergo methylation and hydroxylation reactions after glycosylation (Batra & Sharma, 2013). It has been demonstrated that rutin is synthesized by an enzymatic reaction where rhamnose is transferred from a sugar nucleotide moiety (thymidine diphosphate L-rhamnose) to form 3-quercetin-β-D-glucoside, which is also known as isoquercetin (a mono-glycoside form of quercetin). The formation of 3-quercetin-β-D-glucoside is catalyzed by hesperidinase, an enzyme that forms quercetin. The combination of these two systems completes the glycosylation of quercetin to rutin (de Araújo et al., 2013).

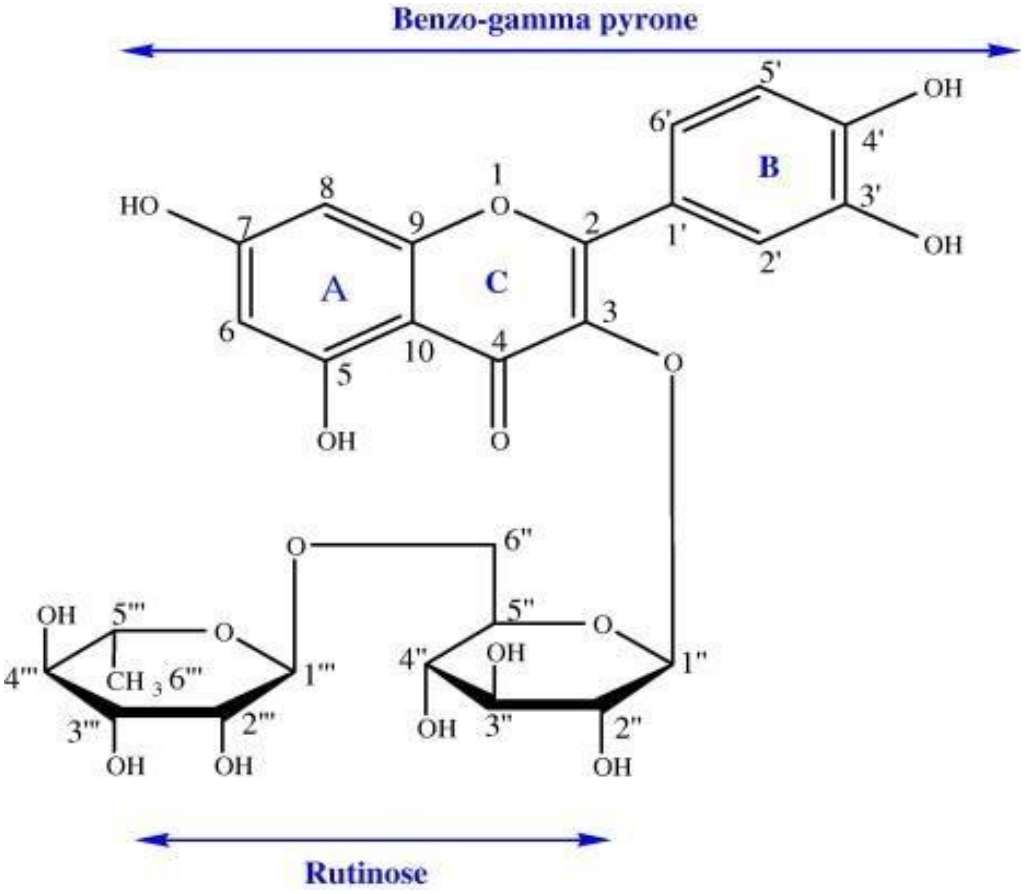

Figure 2.1 Chemical structure of rutin (quercetin-3-O-rutinoside). Source: (Ghiasi et al., 2012)

The glycosylation of flavonols also suggests a reduction in its antioxidant activity. Blocking of the 3-OH group on the C-ring can decrease the radical scavenging because, in order to achieve the maximum antioxidant effect, the 3-OH group needs to be attached to a 2,3-double bond which is adjacent to the 4-carbonyl (Figure 2.2) in the C-ring (Frutos et al., 2019; Panche et al., 2016; Rice-Evans et al., 1996). According to a study by Nguyen and Liu (2013), the formation of a complex with rutin and cyclodextrin molecules (which is a family of glucopyranose, that trap hydrophobic compounds (Szejtli, 1998)) not only enhanced the stability of rutin under oxidation, heat, light, and hydrolysis but also increased its capability to scavenge free radicals. The rutin-cyclodextrin complex required a concentration of 0.014 mg/mL (IC50) to scavenge 50% of DPPH (2,2-diphenyl-1-picryl-hydrazyl) radicals; whereas rutin in its free form needed a concentration of 0.022 mg/mL to scavenge 50% of DPPH radicals. These structural changes to rutin reflect strongly on its antioxidant activity (Ganeshpurkar & Saluja, 2017).

2.2.2. Stability of rutin

Rutin is susceptible to degradation under various reactions like thermal, oxidation, and light-induced decomposition (Chua, 2013; Nguyen et al., 2013). Thermal processes in an aqueous medium system such as cooking, frying, and boiling can degrade the functionality of a flavonoid. A study was undertaken by Buchner et al. (2006) where rutin and quercetin were heated at 100°C in an aqueous solution at pH 5 and pH 8, and the flavonols were perfused with air to initiate oxidation. At pH 5, quercetin concentration was decreased by 75% after 300 minutes, whereas the amount of rutin was reduced by only 20% at the same pH. This behaviour of rutin is due to its chemical structure also called rutinoside of quercetin or quercetin glycoside (Frutos et al., 2019), which is due to the blocked 3-OH group in the C-ring by a sugar moiety (Figure 2.2) that makes rutin more stable than quercetin against oxidation and weak basic conditions. The presence of two intra-molecular hydrogen bonds in the B-ring of rutin makes it more stable than quercetin (Zvezdanović et al., 2012). The conjugation of aromatic rings in rutin influences its stability towards oxidation and chemical transformation under the influence of pH (Prasad & Prasad, 2019; Suzuki et al., 2005).

2.2.3. Solubility of rutin

Rutin is a hydrophobic flavonoid in nature, but it can be solubilized in polar solvents such as methanol, ethanol, 1-propanol, acetone, 1- butanol, dimethyl sulfoxide (DMSO), and ethyl acetate with high temperatures (Zi et al., 2007). With the increase in demand for rutin to be used as a health-promoting agent in the food, pharmaceutical, and cosmetic industries, the use of organic solvents can cause toxicity in the food formulations and decrease in yield and purity of rutin. The hydrophobic nature of rutin causes low aqueous solubility in water and decreases membrane permeability, which hinders *in vitro* and *in vivo* studies (Chua, 2013). Moreover, the degradation of rutin can occur due to hydrolysis, oxygenation, and other enzymatic reactions in the gastrointestinal system (Rashidinejad et al., 2019). The solubility of rutin can be enhanced using a combination of 1% DMSO along with cell culture media for *in vitro* studies (Ravi et al., 2018). However, the use of nanoparticulate systems can enhance the solubility of bioactive compounds while exhibiting higher bioavailability and stability in the physiological systems (Gullón et al., 2017). In order to develop a highly dispersible form of rutin, studies have shown that nano-emulsions and nanocrystals in the aqueous phase protect

rutin from drastic morphological changes even after a change in pH treatment after crystallization reaction (Mauludin et al., 2009). A study by Kurisawa et al. (2003) produced a rutin-polymer that exhibited 50 times higher solubility than monomeric rutin by oxidative polymerization using a catalyst called *Myceliophthora* laccase in a methanol buffer.

2.2.4. Extraction of rutin

The efficient recovery of a bioactive compound like rutin from its natural sources has intrigued many researchers to find solutions regarding its bioaccessibility in food systems and bioavailability in physiological systems (Garcia et al., 2017; Hollman & Katan, 1999; Lee et al., 2007). Extraction is a critical step in insolating and purifying a bioactive compound, and its efficiency depends on a series of factors such as the type of organic solvent used, temperature, a change in the concentration gradients, and achieving maximum yield from the source (Ignat et al., 2011).

Over the years, multiple methods have been developed for the optimal extraction of rutin from various sources. Some of these include conventional solvent extraction techniques such as liquid-liquid extraction where one or more solutes would be thoroughly mixed with an immiscible solvent and result in an extract, which is a solvent-rich solution inclusive of the desired solute (Ignat et al., 2011; Müller et al., 2000). Liquid-liquid extraction is commonly used in the beverage industry for separating polyphenolic compounds (Bucić-Kojić et al., 2007). Another extraction technique commonly used in the food industry is solid-liquid extraction, where a solid matrix is mobilized into a solvent and an extract is recovered through a mass transport phenomenon (Bucić-Kojić et al., 2007; Corrales et al., 2009).

These conventional extraction techniques have been evaluated for the efficient extraction of rutin using different types of solvents, which sometimes are also mixed with water as well because using a small amount of water helps in the diffusion of flavonoids through the plant tissues, which increases the surface area for easier contact between the solvent and solute and maximize the yield of the extract (Altıok et al., 2008; Kim et al., 2005). Major solvents that have been used for the extraction of rutin are methanol, ethanol, diethyl ether, ethyl acetate, and acetone (Stalikas, 2007). Polar alcoholic solvents such as ethanol and methanol have been reported to increase the extraction yield of rutin (Fathiazad et al., 2010). According to a study that was carried out long ago by Sando and Lloyd (1924), a method was developed where rutin

was extracted using 95% alcohol from the flowers of elder (*Sambuscus canadensis* L. (Adoxaceae)), which was later patented by further research in 1948.

There are other significant factors that affect the extraction process of rutin; e.g., temperature and time. Conventionally, high temperature and longer extraction time enhance mass transfer during a heat reflux extraction but rutin undergoes thermal degradation after 100°C in an aqueous system (Buchner et al., 2006; Nguyen et al., 2013). However, this might decrease the concentration of rutin concerning its extraction time at higher temperatures (Chua, 2013), resulting in a loss of its bioactivity.

Extraction cycles are also considered significantly important and effective for an extraction process used for rutin. Xie et al. (2011) extracted rutin from *Hibiscus mutabilis* L., where two extraction cycles of 10 and 5 minutes at 25°C achieved an increase in the extraction yield, which was more than 90% of the total yield. Thereby, successive extraction helps in increasing the efficiency of extraction for bioactive compounds (Altıok et al., 2008; Chua, 2013). Innovative extraction techniques, such as pressurized liquid extraction, are being used (Zhang et al., 2008) to ensure a good quality substrate or a product.

2.2.5. Detection and quantification of rutin

There are different types of highly sensitive techniques and analytical methods being used for the quantitative and qualitative analysis of polyphenols, which can provide solutions for the separation of polyphenols and their detection in different groups (Ignat et al., 2011; Q. Liu et al., 2008). Spectrophotometric methods are being used for quantitative and qualitative analysis of different classes of polyphenols. Spectrophotometric methods such as UV-Vis and colorimetric assays are simplistic and low in cost, but they have limited functionality because they neither quantify individual polyphenols nor separate them (Ignat et al., 2011).

Method development for high-performance liquid chromatography–diode array detection (HPLC-DAD) has been modified over the years to improve its efficacy and reduce its analysis time. For detection, separation, and quantitative analysis of rutin, HPLC has been commonly used (Acevedo-Fani et al., 2021; Babazadeh et al., 2017). The chromatographic conditions of HPLC commonly used for rutin include a reverse-phase C18 column, which enhances the

separation of different classes of polyphenolic compounds mostly polar and hydrophobic compounds with a faster equilibrium process. The ultraviolet-visible (UV-Vis) diode array detector, where a deuterium lamp is used as a source of UV light, can determine rutin in a food matrix with a range of wavelength from 190 to 490 nm. A mobile phase consists of a binary solvent system; an organic polar solvent such as methanol or acetonitrile as Solvent A and acidified water containing acetic acid or formic acid as Solvent B (Ignat et al., 2011; Nollet & Toldrá, 2012). Some studies have suggested that the detection of rutin generally occurs between 258-358 nm at a retention time of 4.8 minutes, which is considerably lower than other reports (e.g., 16.17 minutes (Brolis et al., 1998), 19 minutes (Deineka et al., 2004), and 27.2 minutes (Buchner et al., 2006), indicating that this method can be applied to rutin to determine its release from food products (Acevedo-Fani et al., 2021; Babazadeh et al., 2017; Rashidinejad et al., 2019). There are other techniques like liquid chromatography-mass spectroscopy (LC-MS) and nuclear magnetic resonance (NMR), which offer a better analytical approach to understanding bioactive compounds and their structures from different biological resources (Bureau et al., 2009; E.-H. Liu et al., 2008).

2.3. The antioxidant property of rutin

The generation of free radicals in humans can occur because of abnormal metabolic health, which is caused by the consumption of inherent oxygen in the cells leading to oxidative stress. Oxidative stress releases a range of free radicals and reactive oxygen species (ROS) such as superoxide, hydroperoxides, and hydroxyl causing cytotoxicity in normal cells by reacting with nucleic acids and proteins in the physiological system (Benavente-García et al., 1997; Sáez-Tormo et al., 1994). The antioxidant potential of rutin is well reported using different methods; either through biochemical estimations by measuring its capacity to scavenge stable DPPH free radical or through *in-vitro* cell-based intracellular antioxidant assays (Prior et al., 2005; Yang et al., 2008a). Its antioxidant effect can be due to its hydrogen donating ability towards the DPPH free radical, which accepts electrons to become a diamagnetic stable molecule. This helps the rutin molecules to have easier access to the DPPH molecules present in a solvent interface (Chat et al., 2013). A study was performed under *in vitro* conditions where rutin and butylated hydroxytoluene (BHT), a phenol derivative, were used at a concentration of 0.05 mg/mL. This resulted in 90.4% and 58.8% inhibition of DPPH radicals, respectively. The inhibitory action of rutin towards the DPPH molecule had a concomitant increase; whereas,

BHT exhibited poor antioxidant activity (Yang et al., 2008a). According to a previous study (Boyle et al., 2000), rutin was used as a supplement to understand its antioxidant effects. Following a 6-week trial of 500 mg rutin supplementation/day, there was a 2.5-fold increase in the plasma levels of quercetin when compared to the Week 0 samples (Boyle et al., 2000). Rutin exhibited a protective effect against the toxicity of ROS that leads to oxidative damage in the physiological systems (Manach et al., 1997). In an *in vitro* intracellular antioxidant assay, rutin showed reliable cell permeability, which resulted in scavenging of induced hydroxyl radicals in a hepatocellular carcinoma cell line (HepG2 cells), indicating that rutin could exhibit antioxidant activity against oxidative stress-induced ROS. This behavior of rutin could be due to a combination of chelating activity by Cu^{2+} or free radical scavenging activity (Kim et al., 2011). Table 2.2 summarizes several other previous studies that demonstrated the antioxidant effects of rutin. The recommended daily intake of rutin is 500 mg/d (Sattanathan et al., 2011), which is a challenge to be delivered via food.

Table 2.2 Evidence of in vitro and in vivo studies demonstrating antioxidant effects of rutin and rutin-protein complexes

Experimental design	Dosage and duration	Observations	Proposed suggestions (if any)	Reference
		***In vitro* studies**		
Rutin-phospholipid (soya lecithin) complex and pure rutin subjected to DPPH assay	10-90 µg/mL for 30 minutes	Rutin-phospholipid complex exhibited higher radical scavenging activity in comparison to pure rutin.	Improving the lipophilicity of rutin enhances its free radical scavenging property.	Jain et al. (2012)
Rutin, Vc, and BHT were investigated for the potential antioxidative effect	5,20,30,50,75 µg/mL for 30 minutes	Inhibition rate for rutin was 90.4%, Vc (92.8%) and BHT (58.8%). Free radical scavenging increased with an increase in concentration.		Yang et al. (2008a)
Preventative effect on hemoglobin glycosylation by rutin	0.5,5,10 µg/mL for 72 hours	Inhibition of glycosylation by rutin for tested concentrations was 11%, 27%, and 42% respectively.	To understand the effect of structural activity different aglycones and glycosides should be compared.	Asgary et al. (1999)
Effect of rutin on superoxide anion production in HT29 cells, A549 cells, and Caco-2 cells	5-100 µM for 45 minutes	Against HT29, A549, and Caco-2 cells, rutin reduced ROS production by 64.41%, 56.65%, and 31.12% respectively.		Ben Sghaier et al. (2016)
		In vivo studies		

STZ (60 mg/kg) induced renal injury in diabetic rats	3 doses of 10, 30, and 90 mg/kg for 10 weeks	Significant increase in the activity of CAT, GSH-Px, and T-SOD resulting in strong antioxidative effect by rutin.		Hao et al. (2012)
Hypercholesterolemia-induced male rats	10 or 100 mg/kg in a high cholesterol diet for 4 weeks	Rutin reduced total cholesterol, LDL-C levels, and liver enzymes at 100 mg/kg supplementation in 1 mL/100g of diet.		Ziaee et al. (2009)
Hyperammonemia-induced male Wistar albino rats	100 mg/kg body weight for 8 weeks	Increased antioxidant levels were observed at 50 mg/kg body weight.		Mahmoud (2012)
STZ (60 mg/kg) induced male Wistar rats	20% casein diet supplemented with 0.2% G-rutin for 4 weeks	G-rutin suppressed glycation of tissue proteins in diabetic rats.	The behavior of rutin under elevated activation of the polyol pathway can help in understanding its role in diabetes.	Nagasawa et al. (2002)

DPPH: 2,2-diphenyl-1-picrylhydrazyl; Vc: Ascorbic acid; BHT: butylated hydroxytoluene; HT29 cell line: human colorectal adenocarcinoma cell line; A549 cell line: adenocarcinoma human alveolar basal epithelial cells; Caco-2 cell line: human epithelial cells; STZ: streptozotocin; CAT: catalase; GSH-Px: glutathione peroxidase; T-SOD: total superoxide dismutase; LDL-C: low-density lipoprotein cholesterol; G-rutin: 4(G)-alpha-glucopyranosylrutin.

2.4. Pharmacokinetics of rutin and its association with human health

Rutin has been known to possess various biological activities such as antioxidant, antimicrobial, anti-inflammatory, anti-ulcerogenic, and chemo-preventative (Albu et al., 2013; Ben Sghaier et al., 2016; Ponnusamy et al., 2015; Sharma et al., 2013; Yu et al., 2015). These properties have been researched for pharmacological applications through animal models and *in vitro* cell models for various chronic diseases and conditions like neurogenerative disorders, cardiovascular diseases, diabetes mellitus, many types of cancers, and inflammatory bowel diseases (IBD) (Sharma et al., 2013). The use of rutin as a potent bioactive compound that exhibits strong antioxidant properties, may also explain its compatibility being complex with proteins and nanoparticles. Thus, enhancing its bioaccessibility through the gastrointestinal tract (GIT) without inducing any toxicity in the body (Sharma et al., 2013).

2.4.1. Metabolic health and inflammation

Although rutin and its associated compounds and complexes have been studied mostly as antioxidant compounds, their anti-inflammatory action has found higher relevance in clinical trials. According to Oboh et al. (2015), rutin could inhibit pro-oxidants such as Fe^{2+}, induced during lipid peroxidation in rat pancreas homogenates, where it was significantly more effective than quercetin.

The important mediators of inflammation are transcription factor, NF-κB, and TNF-α (tumour necrosis factor-alpha) as they regulate pro-inflammatory transcriptional factors that activates pro-inflammatory cytokines such as IL-1β, IL-6, and IL-8, which in turn, lead to an inflammatory response that can be either acute or chronic inflammation (Serhan et al., 2010). As inflammation involves the production of pro-inflammatory cytokines, enzymes such as cyclooxygenase-1 (COX-1), and other chemical mediators, the imbalance between the cytokines may lead to some chronic inflammatory responses in the human physiological system, resulting in endothelial dysfunction in the cells (Jiang et al., 2019). It has been found that rutin suppresses the inflammatory responses in an *in vitro* Caco-2 cell culture model, where it may prevent intestinal dysfunction and cardiovascular diseases linked to chronic inflammation (Morales et al., 2018).

2.4.2. Absorption and transepithelial transport of bioactives

Rutin is hydrophobic and possesses difficulty in diffusion through cell membranes that reduce the absorption of the bioactive molecules in the stomach. The structure of bioactive compounds changes in the colonic region of the body due to microbial enzymes, thus resulting in glycosylation (Németh et al., 2003). Differentiated Caco-2 cells have been used typically to compare the absorption of a bioactive from the apical compartment to the basolateral compartment of monolayers. For a flavonoid glycoside such as rutin, a study by Németh et al. (2003) reported that the transfer of aglycones and its metabolites from the apical compartment after 4 hours of incubation was almost 90% and 70% respectively when quantified through HPLC-DAD. The evidence to prove that efficient absorption of dietary flavonoid glycosides takes place due to glycosylation has been reported by several researchers (Zhang et al., 2013). But the limitations to increasing the concentration of dietary flavonoids may result in longer incubation periods for absorption studies *in vitro*, thereby also increasing the risk of cytotoxicity in cells. With a polarised Caco-2 cell culture model, it mimics the characteristics of gut epithelium and hence it may be relevant to understanding the transport and potential absorption dynamics of rutin in the gut. The transepithelial absorption of rutin was observed at different time intervals of 2, 4, 6, 8, 12, and 24 hours to characterise the effect of rutin throughout the incubation time periods. The maximum transport through the monolayers from the apical compartment to the basolateral compartment was observed at 12 hours, after which there was a decrement in the transport of rutin that passed to the basolateral compartment of the cells (Jiang et al., 2019).

There have been certain enzymes reported which are present in the small intestine that enhance the absorption of dietary flavonoids by hydrolysis, known as β-glucosidase. This enzyme has also been particularly known to enhance the absorption of lactose (the sugar present in milk that gives glucose and galactose upon hydrolysis) in the gut through sugar transporters such as SGLT-1 (sodium-glucose transport proteins) and GLUT (glucose transporter) that facilitate membrane diffusion within the cell monolayers (Németh et al., 2003). Transmembrane diffusion of rutin complexed with proteins or nanoparticles has its advantages as they extend the release of bioactives by being carriers for hydrophobic compounds and delivering the encapsulated or entrapped bioactives at the target area of the gut (Negahdari et al., 2021). To study the transport of hydrophobic compounds like rutin, the integrity of the monolayers is measured by monitoring the permeability of the compounds through transepithelial electrical

resistance (TEER) values. These values indicate the barrier integrity of the cells during the transport/diffusion of compounds across different barrier models such as GIT and the blood-brain barrier (Srinivasan et al., 2015). The transport characteristics depend on the concentration of the compounds, temperature, incubation time, and pH (He & Zeng, 2005). According to Zhang et al. (2013), accumulation of rutin through intracellular absorption can be dependent on time and concentration, along with metabolic enzymes that help in mediating rutin across the apical membrane of the monolayers to the basolateral membrane.

2.5. Cytotoxicity of bioactives

The intake of bioactives in substantial amounts through fruits and vegetables as a natural source has been a common practice. However, recent research trend has focused on developing flavonoid-enriched products with higher functional, biophysical, and bioaccessibility attributes (McClements, 2021). The potency of rutin was determined by how effectively it was responsible for the mechanisms that affected cytotoxicity within the body. Any healthy cells cultured *in vitro* with flavonoids triggers several metabolic activities such as cell proliferation, cell death, and apoptosis that are comparable to the physiological system in our body, as cells tend to respond and act against different stimuli (Sak, 2014). To characterize *in vitro* functional activities of these supplements using cell models, their cytotoxicity needs to be evaluated. This can help in finding effective concentration in the *in vitro* cell-based functional assays.

To evaluate purified rutin or any functional foods fortified with rutin that have any cytotoxic effects on cultured cells, an effective and nontoxic concentration needs to be evaluated. The solubility of hydrophobic compounds can be overcome using solvents such as DMSO, methanol, or ethanol and they have severe cytotoxic effects on the cells (Hollebeeck et al., 2011). This also increases the need to evaluate the role of delivering rutin through a protected matrix to minimise any toxic effect on the physiological system (Knekt et al., 2002). In this regard, as presented in Table 2.3, the *in vitro* studies demonstrated that rutin can protect against induced cytotoxicity and mitochondrial dysfunction in different cell models, thus maintaining cellular homeostasis.

Table 2.3 Evidence from the cytotoxic and protective effect of rutin in cell lines and animal models

Experimental design	Dosage and duration	Observations	Reference
Rutin exposed to Caco-2 cells for cytotoxicity	25 µM – 250 µM for 72 hours	96.5% cell viability at 150 µM, without any significant cytotoxicity.	Kuntz et al. (1999)
Effect of rutin on LPS-induced HUVECs	2.5 µM - 100µM for 6 hours. LPS treatment at 100 ng/mL	Decreased LPS-induced toxicity in cells in a dose-dependent manner without reducing cell viability.	Lee et al. (2012)
Cell viability of rutin on HepG2 cells	0.1 µM- 100 µM for 4 hours and 24 hours	No significant effect on cell proliferation after 24 hours. But, at 48 h inhibition in cell growth was observed at 100 µM, 50 µM, and 10 µM doses.	Alía et al. (2006)
Effect of rutin on Aβ42-induced SH-SY5Y cells	2, 10, and 20 µM treatment of Aβ42 with and without rutin for 48 hours	Aβ42 reduced cell viability, while rutin attenuated the Aβ42-induced cytotoxicity at 2, 10, and 20 µM by 14%, 20%, and 23% respectively.	Wang et al. (2012)
Rutin inhibits cell proliferation of rat C6 glioma cells	50 µM of rutin treatment for 24 hours	Rutin reduced cell proliferation by 24.81%.	da Silva et al. (2020)

HT29 cells: human colorectal adenocarcinoma cell line; HepG2 cells: human hepatoma cell line; Caco-2 cells: human epithelial cells; HUVECs: human umbilical vein endothelial cells; LPS: lipopolysaccharide; Aβ: β-amyloid peptides; SH-SY5Y cells: triple cloned subline of neuroblastoma cell line SK-N-SH; C6 glioma cells: Rat glioblastoma cell line

As shown in Table 2.3, rutin has been a promising bioactive possessing antioxidant potential that reduces the risk of accelerating any chronic diseases and strengthening its free radical scavenging capacity in the physiological systems. To increase the functional effect of rutin without altering its structure, the formation of covalent bonds has been reported by former researchers (Afanas'eva et al., 2001). As per previous studies on quercetin's strong potency as an antioxidant, it cannot be manifested as a protective compound due to its cytotoxic and genotoxic behaviour in comparison with rutin over longer incubation time periods with high concertation during *in vitro* experiments (Alía et al., 2006).

The increasing interest of consumers in plant proteins has boosted the use of bioactives such as rutin to form complexes with different food materials that could enhance their limiting properties (e.g., hydrophobicity) via their delivery in fortified functional foods (Rashidinejad

et al., 2019). To overcome the limited bioavailability of rutin, some formulations have been developed where rutin has been used in combination with other ingredients in herbal remedies and multivitamin supplements (Erlund et al., 2000). Some studies have revealed a dose of rutin that is considered safe without initiating any toxicity or adverse health risks at 2000 mg/kg and 5000 mg/kg. This, in turn, helps in creating more efficient formulations in the future to deliver rutin as a functional ingredient (Patil et al., 2012; Suzuki et al., 2015; Tiwari et al., 2020).

2.6. Incorporating rutin into functional foods

As consumers are becoming more aware of food ingredients and supplements, for health benefits that are scientifically proven or claimed, there has been a rise in the demand for functional foods. These foods exhibit higher nutritional values along with sustainable impacts on the environment (Gimenez-Bastida & Zielinski, 2015). Because of its higher nutritive value and health benefits, rutin has become an essential part of the diet through different sources such as fruits and vegetables or buckwheat (Frutos et al., 2019). However, dietary rutin is poorly soluble in both water and oil and possesses high hydrophobicity, low bioavailability, and limited membrane permeability, thus, the lower absorption in the body (Gullón et al., 2017). Therefore, by reducing its hydrophobicity and developing hydrophilic modified rutin fortified functional foods, we can increase its bioavailability and functionality.

To develop a food carrier for loading rutin into the food matrix, there are various delivery systems such as lipid-based nano emulsions, that can be used in fortifying rutin within any beverages, as well as maintaining high stability and increased bioavailability (Dima et al., 2020). The most common encapsulating materials for bioactives such as rutin are milk proteins as they are hydrophilic and nontoxic. Some of the commonly used milk proteins used for this purpose are casein, whey proteins, lactoferrin, sodium caseinate, and β-lactoglobulin. The major advantage of choosing proteins for bioactive encapsulation may be due to their polyelectrolyte structure, which can help in maintaining the charge within the carrier and help to stabilise the entrapped bioactive compound (Dima et al., 2020; Rashidinejad et al., 2019). A research study by Barbé et al. (2013) observed that kinetics of milk protein digestion and the absorption of amino acids for unheated milk, heated skim milk, milk with rennet, and milk without rennet gelation had different results. Therefore, the gelation of milk decreased the outflow of the food from the stomach and thus the subsequent absorption of amino acids, which

indicates the resistance of caseins and β-lactoglobulin towards hydrolysis under acidic conditions within the stomach (Moughan, 2020).

To develop gels fortified with bioactives, natural biopolymers (e.g., polysaccharides) are used that generally have a negative charge after interacting with proteins as they form electrostatic complexes. Some examples of polysaccharides used for this reason are cellulose, xanthan, pectin, and carrageenan. Polysaccharides are broken down by amylase during digestion in the GIT, and subsequently, are fermented by colonic microbiota (Dima et al., 2020).

2.6.1. Enhancing the bioavailability of rutin through delivery systems

As discussed previously (Section 2.6), the major disadvantage of delivering rutin itself is directly linked to its poor solubility (Gullón et al., 2017). There have been different approaches to increasing the solubility of rutin after studying its biological characteristics and maximising its potential in the food industry for food fortification and developing new functional foods (Dima et al., 2020).

As shown in Table 2.4, many approaches have been used to encapsulate bioactive compounds to overcome their poor solubility (Nguyen et al., 2013). Novel delivery systems have been designed to deliver bioactives through the GIT, which have made it possible to discover new methods to improve their therapeutic potential, without limiting their efficacy, cytotoxicity, and structural integrity (Negahdari et al., 2021). These advances in delivery systems have made rutin an attractive target for commercial fortified functional foods. Formulations based on nano-carriers such as lipids have significantly improved aqueous solubility and facilitated emulsification, thereby, increasing its absorption in the body (Sharma et al., 2013).

Importantly, every product introduced into the market needs to have approved regulatory requirements, sensorial attributes, storage, and high-temperature stability along with mitigating oxidation due to variable environmental conditions. The issue of delivering bioactive compounds within the GIT is that it needs a food matrix that can enhance its bioactivity and ensure that interactions between the encapsulating agent and the bioactive result in a controlled release when ingested (Moughan, 2020). The food matrix also affects the GIT after delivering fortified foods, due to the breakdown of the matrix loaded with bioactives. There are mineral ions, proteins, surfactants, and other conjugates formulated with bioactives that are released in the gut along with gastric and intestinal fluid, which are then absorbed by the surface of the gut

upon their breakdown. The release of the bioactives after the breakdown of its food matrix changes the physicochemical characteristics of the released compound and affects its transport mechanism through the junctions of the intestinal epithelium cells (Liu et al., 2017; Zhang & McClements, 2016). Table 2.4 discusses the interactions between encapsulating material and bioactives through common delivery systems, which have been used to enhance bioaccessibility and absorption of bioactives such as rutin, curcumin, and β-carotene.

Table 2.4 Delivery systems designed to enhance bioaccessibility and bioavailability of bioactives

Encapsulating nanomaterial	Bioactive compound	Impact of the delivery system	Reference
Cyclodextrins (α, β, ɣ) complex	Rutin, Curcumin, Lycopene, Resveratrol	Increased dissolution rate; Stable in the GIT after oral administration (*in vivo*); Increased antioxidant capacity; Protection against UV and heat treatments; Controlled release in the gut; Increased bioaccessibility; Maintaining oxidative and thermal stability.	Nguyen et al. (2013); Sri et al. (2007); Paczkowska et al. (2015); Celik et al. (2015); Chen et al. (2020); Liu et al. (2016); Shi et al. (2015)
Phospholipid complex	Rutin, EGCG, β-Carotene	Increased permeability and intestinal absorption in Caco-2 cells; Increased oxidative stability; Heat stabilized; Increased solubility; Maintaining antioxidant potential and bioactivity.	Granja et al. (2019); Alexander et al. (2016); Das and Kalita (2014); Singh et al. (2012); Gutiérrez et al. (2013); Shpigelman et al. (2012); Kidd and Head (2005)
Nanoparticulate systems (nanoemulsions, nanocapsules, SMEDDS, polymeric nanoparticles, nanocrystals)	Rutin, EGCG, β-carotene, EPA, DHA, Vitamin D_3	Enhanced physicochemical properties; heat stabilized; Re-dispersible and higher dissolution activity; Prolonging release in the GIT; Enhanced bioaccessibility after *in vitro* digestion; Enhanced absorption in everted sac models *in vivo*; Improving cellular uptake in Caco-2 cells; Bioaccessibility was improved after *in vitro* digestion.	Mauludin et al. (2009); Babazadeh et al. (2016); Dey et al. (2019); Dima and Dima (2020); Kumar and Bhopal (2012); Walia and Chen (2020); Yang et al. (2016); Yuan et al. (2019) Rashidinejad et al. (2019); Zhang and Han (2018)

GIT: gastrointestinal tract; UV: ultraviolet; EGCG: epigallocatechin gallate; Caco-2 cells: human epithelial cells; SMEDDS: self-emulsifying drug delivery systems; EPA: eicosapentaenoic acid; DHA: docosahexaenoic acid.

2.6.2. Functional foods enriched with bioactives

The role of a novel food-grade delivery system is to overcome issues of bioaccessibility, bioavailability, and cytotoxicity, to develop new food products that can have a similar sensorial property, stability, or shelf-life without altering the biological functions of the bioactives or the sensorial and structural properties of the food they are incorporated into.

2.6.2.1. Enriched dairy products

Milk and its product derivatives are commonly consumed as part of a staple diet worldwide; however, these products are perishable as they have a short shelf life. To improve these limitations, researchers have developed formulations in the dairy industry to improve their physicochemical properties, rheological attributes, and textures along with sensorial properties to satisfy consumers (Dima et al., 2020). Hydrocolloids have been extensively used to create complexes with proteins, particularly casein micelles, which are used in the dairy industry. There have been various hydrocolloids such as carrageenan, xanthan, carboxyl methylcellulose, and pectin that are complexed with different proteins for the application of dairy derivatives such as yoghurt, cheese, ice cream, and butter milk (Yousefi & Jafari, 2019).

Researchers have explored dairy products containing a protected form of hydrophobic flavonoids such as rutin. For example, a study by Acevedo-Fani et al. (2021) revealed that incorporating rutin complexed with sodium caseinate in a yoghurt resulted in better stability during *in vitro* gastrointestinal digestion. Moreover, it impacted the release of rutin from the food matrix, by making it more bioaccessible after gastrointestinal digestion. Thus, fortified dairy foods are suitable models for understanding the influence of the food matrix in which bioactives are encapsulated/protected for prolonging their release in the gut and enhancing their functional attributes such as antioxidant potency or stability under the conditions of food storage and digestive system (Helal & Tagliazucchi, 2018).

Research Methodology

3.1. Introduction

The experimental methodology in the current research was divided into 2 phases, with each phase serving its categorical objectives. **Phase 1** demonstrated the potential antioxidant effect of the two rutin-casein composites (FlavoPlus 1™ and FlavoPlus 2™) on human intestinal epithelial cells (Caco-2) through biochemical assays. In **Phase 2**, a functional milk product (banana-flavored milk beverage) fortified with both rutin-casein composites was prepared and digested using an INFOGEST *in-vitro* digestion model. Subsequently, this milk product was characterised by the effect of the incorporated composites on its physicochemical properties and intracellular antioxidant potential.

3.2. Cellular and biochemical estimation of antioxidant potential of FlavoPlus 1™ and FlavoPlus 2™ through *in vitro* studies

The human intestinal epithelium cell line, Caco-2 was used to test the antioxidant activity of rutin-casein composites (FP1 and FP2). Caco-2 cells were cultured in Minimum Essential Media (MEM) for 72 hours and always maintained at 37°C in a 5% CO_2-humified incubator. Cells were treated with DMSO at doses varying from 0% to 5% before testing the cytotoxic effect of FP1, FP2, and RH. The optimisation of DMSO concentration on Caco-2 cells was tested by investigating the cell viability through various experimental trials. Simultaneously, the cytotoxic effect of FP1, FP2, and RH on Caco-2 cells was determined by MTT assay, as demonstrated in Section 3.2.2.1.

Evaluation of the *in-vitro* antioxidant activity of FP1 and FP2 in comparison to RH through the Caco-2 cellular model was determined by a fluorescent antioxidant assay. 2′,7′-Dichlorofluorescin diacetate (DCFH-DA) is a fluorescent dye that helps in the detection of ROS in cells. Cells were pre-treated with various concentrations of antioxidant medium containing FP1, FP2, and RH for 1 hour. DCFH-DA dye was added to these pre-treated cells and incubated for 1 hour, where it converts into an oxidisable form of DCFH. To determine the effective intracellular antioxidant activity of FP1, FP2, and RH, a free-radical generator, called 2,2′-Azobis(2-methylpropionamidine) dihydrochloride (AAPH) was added to these pre-treated

cells and relative fluorescence over 1 hour is monitored to indicate any antioxidant activity within the cells.

3.2.1. Cell line, medium, and reagents

Caco-2 cells (ATCC ®; American Tissue Culture Collection, # HTB-37) with passage number 19 were kindly provided by Dr Rachel Anderson (AgResearch, Palmerston North, New Zealand). Cells were maintained and cultured in complete minimum essential media (MEM) and seeded in a 96-well plate for the experiment at 70% confluency.

3.2.2. Cell culture medium and reagents preparation

3.2.2.1. Complete Minimum essential media

Complete MEM was prepared by supplementing Gibco™ MEM (L-Glutamine; Catalogue number 11095080, ThermoFisher Scientific™, Waltham, MA, USA) with a 10% Fetal Bovine Serum (FBS, Australian sourced, ɣ-radiated, Catalogue number FBSF, Thermo Fisher Scientific, Waltham, MA, USA), 1% NEAA (MEM non-essential amino acids 100x solution; Catalogue #11140-050), and 1% penicillin-streptomycin (Pen-Strep, 10,000units/mL penicillin G sodium salt and 10,000 µg/mL streptomycin sulfate in 0.85% saline) were procured from Gibco, Invitrogen, MA, USA. Cells were sub-cultured every third day using trypsin (TrypLETM, Gibco™, Invitrogen Corporation, Carlsbad, CA, USA), and Gibco™ PBS (Phosphate buffer saline), pH 7.4 (catalogue #10010023). The complete MEM was stored at 4°C.

3.2.2.2. 3-(4,5-Dimethylthiazol-2-Yl)-2,5-Diphenyltetrazolium Bromide (MTT) stock solution

3-(4,5-Dimethylthiazol-2-Yl)-2,5-Diphenyltetrazolium Bromide (MTT) stock solution was prepared by dissolving 5 mg of the dye (Catalogue #M6494, Invitrogen by Thermo Fisher Scientific™, Waltham, MA, USA) in 1 mL of phenol-free Gibco™ MEM. The solution was syringe-filtered (0.22 µm) and stored at -20^{0}C until further use. The working solution of MTT dye was prepared by diluting the stock solution by 10-fold (1:10) in phenol-free MEM. The stock solution was covered in the foil due to MTT's light-sensitive nature.

3.2.2.3. Dimethyl sulfoxide (DMSO)

A stock solution of 0.3% DMSO (Catalogue #D4540, Sigma-Aldrich®, St. Louis, MO, USA) was prepared, which was further diluted in phosphate buffer saline (PBS), pH 7.4 (Catalogue #10010023), before being syringe-filtered (0.22 µm) and stored at -20°C until used.

3.2.2.4. DCFH-DA/Cellular antioxidant assay

All reagents and buffers for the DCFH-DA assay were prepared according to the method reported by Ma et al. (2018)

2′,7′-Dichlorofluorescin diacetate (DCFH-DA) stock solution

To prepare a 12.5 mM stock solution, 12.182 mg of DCFH-DA (Catalogue #4091-99-0, Sigma-Aldrich®, St. Louis, MO, USA) was dissolved in 2 mL of DMSO (Catalogue #D4540, Sigma-Aldrich®, St. Louis, MO, USA) and stored in 100 µL single-use aliquots at -20°C to avoid repeated freeze-thaw cycles.

2,2′-Azobis(2-methylpropionamidine) dihydrochloride (AAPH) stock solution

To prepare a 60 mM stock solution, 32.542 mg of AAPH (Catalogue #2997-92-4, Sigma-Aldrich®, St. Louis, MO, USA) was dissolved in 2 mL of Gibco™ HBSS (Catalogue #14175095, Thermo Fisher Scientific™, Waltham, MA, USA) and stored in 100 µL single-use aliquots at -20°C to avoid repeated freeze-thaw cycles.

3.2.2.5. Preparation and resuspension of bioactive compounds

Rutin hydrate stock solution

A stock solution of rutin hydrate (≥94%; Catalogue #207671-50-9; Thermo Fisher Scientific™, Waltham, MA, USA) was prepared by dissolving 1 mg of the powder in 0.3% DMSO solution before further dilution in treatment medium. The solution was syringe-filtered (0.22 µm) and stored at -20°C until used.

Rutin-casein composites (FP1 and FP2) stock solutions

The composition of food-grade FP1 powder included: sodium caseinate (NaCas; 46%), rutin (46%), and dipotassium phosphate (8%). This powder was developed and manufactured in our laboratory by Rashidinejad et al. (2019). The manufacturing procedure for FlavoPlus 1™ and FlavoPlus 2™ was described in a patent by Thompson et al. (2020). A stock solution was prepared by dissolving 2 mg of the powder in 1 mL Ultrapure water (Millipore Corp., SAS –

#67120, Bedford, MA, USA) before further dilution in the treatment medium. The solution was then syringe-filtered (0.22 µm) and stored at -20°C until use.

FP2 was composed of sodium caseinate (54.5%), rutin (27.3%), and dipotassium phosphate (18.2%). This powder was previously developed and manufactured in our laboratory (Rashidinejad; et al., 2022). A stock solution was prepared by dissolving 2 mg of the powder in 1 mL Milli-Q (Millipore Corp., SAS – 67120, Bedford, MA, USA) water before further dilution in the treatment medium. The solution was syringe-filtered (0.22 µm) and stored at -20°C until use.

3.2.2.6. DPPH stock solution

The DPPH stock solution was prepared by dissolving 0.025 g DPPH reagent (procured from Sigma-Aldrich Co., Inc. Darmstadt, Germany) in 100 mL methanol (Analytical grade, Catalogue #67561, Sigma-Aldrich®, St. Louis, MO, USA). The stock solution was covered by aluminium foil, due to its light sensitivity and stored in a dark and cool place until used.

3.2.2.7. Total phenolic content (TPC) stock solution

Folin-Ciocâlteu (FC) reagent (Merck Co., Inc. New Jersey, USA) was mixed with Milli-Q water in a ratio of 1:1 to generate a stock solution. The stock solution was covered by aluminium foil due to its light sensitivity and then was stored in a dark place and at 4°C until used.

3.3. Methods

3.3.1. Maintenance and culture of Caco-2 cells

The Caco-2 cells were grown and maintained in the complete MEM at 37°C, 5% CO_2 in a humified incubator (Heracell™ VIOS 160i CO_2 Incubator, Thermo Fisher Scientific™, Waltham, MA, USA). The growth of cells was monitored daily under an inverted microscope (Nikon Eclipse TS100, Japan) until it reached 70% confluency. Cells were sub-cultured every third day by washing with PBS (pH 7.4; Catalogue #10010023), and incubating with trypsin for 4 minutes to remove adherent cells from the surface of the flasks (TrypLETM, Gibco™, Invitrogen Corporation, Carlsbad, CA, USA). The cells were then centrifuged at 110 RCF for 4 minutes (MegaFuge™ 8 centrifuge, Thermo Fisher Scientific™, Waltham, MA, USA) and resuspended in MEM medium. Subsequently, they were seeded into 96 well plates for the corresponding assays (Natoli et al., 2012).

3.3.2. Differentiation of Caco-2 cells

Differentiation of Caco-2 cells was done to perform absorption experiments and barrier integrity assessment of the cell monolayer. The cells were tested for viability using trypan blue solution (0.4%, Catalogue #T10282, Invitrogen™ Thermo Fisher Scientific™, Waltham, MA, USA) where the cell suspension was mixed with trypan blue dye in a 1:1 ratio and mixed in Eppendorf tube. About 12 µL of the sample was loaded onto a disposable Countess™ chamber slide (ThermoFisher Scientific™, Waltham, MA, USA) and observed under a Countess™ automated cell counter (ThermoFisher Scientific™, Waltham, MA, USA). Live and viable cells were transparent and clear while dead cells were stained blue with trypan blue.

Caco-2 cells were seeded at a density of 8×10^4 cells/ Transwell (6.5 mm, polyester, 0.33 µm pore size; Corning® Inc., Catalogue #CLS3470, ThermoFisher Scientific™, Waltham, MA, USA). The volume of fresh MEM medium in the apical compartment was 200 µL and the basolateral compartment was 810 µL. The plates were incubated in humified incubators at 37°C at 5% CO_2. The medium in the transwell was changed after every second day. Differentiation of Caco-2 cells occurs after 15-17 days of incubation. The background transepithelial electrical resistance (TEER) across the Caco-2 cell monolayer was measured after cells reached confluency using the EndOhm TEER cup (World Precision Instruments, Sarasota, FL, USA) connected to the Epithelial Voltohmmeter ($EVOM^2$) (World Precision Instruments, Sarasota, FL, USA), to determine the barrier integrity of the cells before absorption experiments.

3.3.3. Treatment of Caco-2 cells with rutin-casein composites

Caco-2 cells were treated with FP1, FP2, and RH at various concentrations ranging from 0.1 µg/mL to 50 µg/mL. These concentrations were achieved after dilutions from the stock solutions in a fresh MEM medium. To understand the effect of the samples, the control vehicles such as DMSO were optimised at varying concentrations from 0.01% to 5%. The concentration of DMSO used in diluting RH corresponds to the concentration range of DMSO used for its optimisation. After seeding cells at a density of 4×10^5 cells/mL in a 96-well plate (Corning® Co-star 3596 Inc., Catalogue # 07-200-90, ThermoFisher Scientific™, Waltham, MA, USA), the incubation of 24 hours was needed for the cells to adhere to the surface of the well. After incubation, the cells were treated with DMSO (0.01% to 5%). These cells were quickly assessed via MTT Assay to optimise the cytotoxic concentrations of DMSO.

3.3.4. MTT Assay

After the treatment with DMSO, FP1, FP2, and RH, the cells are washed with a phenol-red-free MEM medium. The MTT dye working solution (0.5 mg/mL) was added to each well and incubated for 3-4 hours. The negative control was DMSO+cells, the positive control was without any samples, and blank wells were regarded as wells without cells. After incubation, the wells had a dark blue/purple formazan crystal precipitation. After carefully aspirating the MEM medium from the wells, 100 µL/well DMSO was added. Further incubation of 10 minutes with occasional shaking at 37°C was needed to dissolve the formazan crystal formation. Absorbance was measured at 570 nm using a microplate reader (FlexStation 3™ Multi-Mode Microplate Reader, Bio-Strategy, NZ). The cell viability was calculated using Equation 1. This method was adapted from Kuntz et al. (1999) with some modifications.

$$\% \text{ Cell viability} = \frac{Absorbance\ of\ sample - Absorbance\ of\ blank}{Absorbance\ of\ control - Absorbacnce\ of\ blank} \times 100 \quad \text{.....(Eq. 1)}$$

3.3.5. Intracellular antioxidant activity (DCFH-DA assay)

Intracellular antioxidant activity was measured using a 2′,7′-Dichlorofluorescin diacetate **(**DCFH-DA) assay as mentioned by Wan et al. (2015) with slight modifications. The cells were seeded at a density of 6×10^5 cells/mL in a 96-well plate (Corning® Co-star 3596 Inc., Catalogue #07-200-90, ThermoFisher Scientific™, Waltham, MA, USA), where the incubation of 24 hours was needed for the cells to adhere to the surface of the well. After the incubation, the MEM medium was discarded and the cells were washed with Gibco™ PBS, pH 7.4 (Catalogue #10010023, ThermoFisher Scientific™, Waltham, MA, USA). All the reagents were stored at 4°C and were equilibrated to room temperature before use. The assay was performed by applying the method developed by Ma et al. (2018) with some modifications. The cells were treated with 100 µL of samples in conjunction with 25 µM DCFH-DA (Catalogue #4091-99-0, Sigma-Aldrich®, St. Louis, MO, USA) dye solution, which was incubated at 37°C for 1 hour. After an incubation of 1 hour, the cells were washed with PBS 3 times. After washing the cells, 100 µL of (600 µM) AAPH (Catalogue #2997-92-4, Sigma-Aldrich®, St. Louis, MO, USA) was added into a 96 well-plate. The fluorescence intensity was immediately measured at 37°C with an excitation of 480 nm and emission wavelength of 530 nm by a fluorescence micro-plate reader (FlexStation 3™ Multi-Mode Microplate Reader, Bio-Strategy, NZ) for every 5 minutes for 1 hour. The control group was without any samples and blank group was

without AAPH and samples; only PBS treatment was regarded as blank. The fluorescence intensity of the samples was calculated using Equation 2.

$$\text{Fluorescence intensity } \% = \frac{F_{sample}}{F_{control}} \times 100 \quad \textbf{(Eq. 2)}$$

where, F_{sample} is the fluorescence of the sample and $F_{control}$ is the fluorescence of the control.

3.3.6. UV-Spectrophotometric DPPH Assay

DPPH (2,2-diphenyl-1-picryl-hydrazyl) free radical scavenging method (Vogrincic et al., 2010) was used to test the antioxidant scavenging capacity of FP1, FP2, and RH via UV-spectrophotometric chemical-based assay.100 µL of each sample was mixed with 1:10 dilution of the DPPH stock solution in a cuvette and was then incubated in the dark for 30 minutes at room temperature (25°C) until the recording of the absorbance. For the control sample, 3.9 mL of the DPPH solution was added to the cuvette and its absorbance was recorded immediately at 517 nm using a spectrophotometer (Multiskan™ GO Microplate spectrophotometer, ThermoFisher Scientific™, Waltham, MA, USA). The blank sample consisted of water with DPPH solution. With the increase in the concentration of the bioactive compound (i.e., rutin), stable DPPH radical was reduced to its non-radical form changing the colour of the solution from purple to yellow. The scavenging activity or inhibition% was calculated against the control using the following Equation 3.

$$\text{Scavenging activity (\%)} = \frac{Absorbance\ of\ control - Absorbance\ of\ sample}{Absorbance\ of\ control} \times 100 \quad \textbf{(Eq. 3)}$$

where, the absorbance of the control is at t= 0 minutes and the absorbance of the sample is at t= 30 minutes. All measurements were carried out at room temperature.

3.3.7. Total phenolic content (TPC) estimation

To evaluate the TPC values in FP1, FP2, and RH, the method adapted from Gangwar et al. (2014) was applied using FC's reagent (procured from Merck Co., Inc. New Jersey, USA). An aliquot of 0.1 mL was taken from the sample stock and 2.5 mL of FC reagent was added and incubated for 10 minutes. After the incubation, 2 mL of sodium carbonate (75 g/L) was added, and samples were vortexed and incubated in dark at room temperature for 2 hours. The absorbance was measured by spectrophotometer at 765 nm (Multiskan™ GO Microplate

spectrophotometer, ThermoFisher Scientific™, Waltham, MA, USA). The absorbance values were compared with the gallic acid standard (50-300 µg/mL) curve to express the results as µg of the gallic acid equivalent of the sample.

3.4. Preparation of banana-flavored milk beverage fortified with rutin-casein composites and characterisation of its physicochemical and antioxidant properties

This part of the study aimed at preparing a banana-flavoured milk beverage fortified with FP1, FP2, and RH. The milk beverage was developed with a concentration of 7.32 g/L for 500 mg rutin per serving of 250 mL of banana-flavoured milk. This banana-flavoured milk was digested using an *in vitro* static digestion model. The *in vitro* digestion was performed to understand the changes in the structural and functional properties of bioaccessible rutin in the banana-flavoured milk beverage. High-performance liquid chromatography (HPLC) was used for the quantification of rutin in the samples at 0, 30, 60, and 120 minutes after digestion; i.e., to study the release of rutin, which determines the bioaccessible amount of rutin available after digestion. Subsequently, a bioaccessible amount of the samples was added to a differentiated Caco-2 cell monolayer to assess the impact on cytotoxicity, barrier integrity, and intracellular antioxidant activity.

3.4.1. Materials, chemicals, and reagents

Commercial banana-flavoured milk used in the experiments was purchased from a local supermarket (Pak n Save, Palmerston North, New Zealand), the composition and nutritional information of which are presented in Table 3.1.

Table 3.1 Composition/nutritional information of the banana-flavoured milk used for the experiment

Composition	Average quantity per 250mL serving	Average value per 100 mL	% Daily intake per serving
Energy	650 kJ	260 kJ	7 %
Protein	11 g	3.3 g	4.4 %
Fat, total	3.8 g	1.5 g	5 %
- saturated	2.3 g	0.9 g	10 %

Carbohydrate	18.8 g	7.5 g	6 %
- sugars	18.8 g	7.5 g	21 %
Sodium	90 mg	35 mg	4 %
Calcium	365 mg	145 mg	46 % RDI
Vitamin D	1.3 mg	0.5 mg	13 % RDI

The enzymes used in the *in vitro* digestion were of porcine origin; pepsin (Catalogue #P7012-5G, Sigma-Aldrich®, St. Louis, MO, USA) was stored at 0°C, pancreatin (Catalogue #P7545-100G, Sigma-Aldrich®, St. Louis, MO, USA) was stored at 0°C, and bile salts (Catalogue #B8631-100G) was stored at room temperature. Milli-Q water (Millipore Corp., SAS – 67120, Bedford, MA, USA) was used for the preparations of all the solutions. High purity (HPLC grade) rutin and quercetin standards were purchased from Sigma-Aldrich®, St. Louis, MO, USA. All chemicals and reagents used for this study were of analytical grade.

3.5. Methods

3.5.1. Preparation of banana-flavoured milk fortified with rutin composites and rutin hydrate

To prepare banana-flavoured milk fortified with FP1, FP2, and RH, a dosage of 500 mg rutin per serve of 250 mL of milk was chosen, and 400 mL of the fortified milk was prepared. The concentration of the powders in the milk product was 7.32 g/L. The powders were stirred at 1200 revolutions per minute (RPM) into the milk for 15 minutes and the mixture was heated at 70°C for 30 minutes and cooled before storage. Fortified milk was then bottled and stored at 4°C until further use.

3.5.2. *In vitro* digestion of rutin-fortified milk

The *in-vitro* digestion of the banana-flavoured milk fortified with FP1, FP2, and RH was performed according to a method published by Minekus et al. (2014) with some modifications. Freshly made fortified banana-flavoured milk beverage was used for the *in vitro* digestion studies (in triplicates). The milk samples fortified with FP1 and FP2 were compared to the milk fortified with RH. The milk without fortification was used as the control, along with Milli-Q water being regarded as the blank. Three aliquots were taken for each time point to generate

enough samples for further experiments, while two tubes were used for performing *in vitro* digestion for each replicate. A shaking water bath was maintained at 37±1°C, in order to maintain the human body temperature.

A 10 mL volume of each sample was mixed with simulated gastric fluid (SGF) to a final ratio of 1:1 containing 5 µL $CaCl_2$, 8 mL SGF, and 0.5 mL pepsin (at a final pepsin activity of 2000 U/mL), and the pH of the tubes was adjusted to 3 ± 0.1. The first time point (at 0 minutes) marked the initiation of the gastric phase in this experiment. During the gastric phase, samples were collected at 0, 30, 60, and 120 minutes. In the case of the intestinal phase, the samples were obtained from the remaining tubes in the water bath, which had a final volume of 20 mL from the gastric phase. The digesta was mixed with simulated intestinal fluid (SIF) to a final ratio of 1:1 containing 40 µL $CaCl_2$, 2.5 mL bile salts (at 10 mM), and 5 mL pancreatin (at a final 100 U/mL trypsin activity), and the pH of the tubes was adjusted to 7±0.1 with regular stirring at 27 RPM. During the intestinal phase, samples were collected at 0, 30, 60, and 120 minutes.

To stop the enzymatic reactions, enzyme inhibitors were immediately added to the samples. 10 µL of Pepstatin A (Catalogue #ab141416, Abcam, UK) in methanol (0.5 mg/mL) was added to every 1 mL of gastric digesta sample taken and 0.45 mL of the protease inhibitor cocktail (1 tablet in 50 mL Milli-Q water; Sigmafast®, Catalogue #S8820, Sigma-Aldrich®, St. Louis, MO, USA) solution was added to every 1 mL of the intestinal digesta sample. All digesta samples were stored at -20°C for further experimental analysis.

3.5.3. High-performance liquid chromatography (HPLC)

Rutin and quercetin standards were analysed at concentrations of 105-421 ppm and 10-40 ppm, respectively, based on the methods reported by Naveen et al. (2017) and Acevedo-Fani et al. (2021) with slight modifications. An Agilent 1200 series, HPLC machine equipped with UV/visible diode array detector (Agilent Technologies, 1200 Series, Santa Clara, CA, USA) and Kinetex XB-C18 column (100 A°, 100 mm × 4.6 mm, 2.6 µm pore size) was used to measure the amount of rutin bioaccessible in the banana fortified milk product after extraction. The mobile phases were composed of two different solutions: acetic acid 0.5% acting as A and acetonitrile acting as B. The flow rate was 1 mL/min with a sample injection volume of 5 µL. The column temperature was maintained at 26°C and the UV detector was set at 356 nm. Rutin was detected at 356 nm and peak height and peak area were obtained by integration using EZ

Chrome software (Agilent OpenLab Technologies, USA). The identification of rutin was dependent on the retention time of the peaks and their spectra compared with the calibration curve made from standards (105-421 ppm).

3.5.4. Particle size

The particle size of the samples was obtained after the *in vitro* digestion using a Mastersizer (Malvern MasterSizer Hydro 2000MU, Malvern Instruments Ltd., Malvern, UK) with two laser sources. The refractive index used was 1.460 for milk and 1.33 for water at an obscuration level maintained at 9.5%. A small amount (2-3 mL) of digested milk sample was added to the measurement cell containing 800 mL of water to reach the obscuration level.

3.5.5. Zeta potential

The zeta potential of the samples was determined by Zetasizer Nano ZS (Malvern Panalytical Ltd, UK) at 25°C. The milk samples were diluted with deionised water before analysis to prevent multiple scattering events during the experiment. The samples were equilibrated for 2 minutes before measurement.

3.5.6. MTT assay

The procedure of MTT assay was previously described in Section 3.2.3.4. The cells were treated with a bioaccessible amount of FP1, FP2, and RH after the *in vitro* digestion, and their cell viability was calculated by measuring absorbance at 570 nm using a microplate reader (FlexStation 3™ Multi-Mode Microplate Reader, Bio-Strategy, NZ). The cell viability was calculated using Equation 1.

3.5.7. Intracellular antioxidant assay (DCFH-DA assay)

After quantification of cell viability, the cells were seeded on Transwell inserts (6.5 mm, polyester, 0.33 μm pore size; Corning® Inc., Catalogue #CLS3470, ThermoFisher Scientific™, Waltham, MA, USA) to become a differentiated cell monolayer after 15-17 days. The procedure of DCFH-DA assay was previously described in Section 3.2.3.5. DCFH-DA assay quantifies the intracellular antioxidant capacity of the bioaccessible samples after 24 hours of absorption on the Caco-2 monolayer with a change in its fluorescence values.

3.5.8. Transepithelial electrical resistance assay (TEER)

Caco-2 cells were seeded at a density of 8×10^4 cells/Transwell (6.5 mm, polyester, 0.33 μm pore size; Corning® Inc., Catalogue #CLS3470, ThermoFisher Scientific™, Waltham, MA, USA) in Gibco™ MEM medium in an apical compartment with 200 μL and a basolateral compartment with 810 μL. The plates were incubated in humified incubators at 37°C at 5% CO_2 (Heracell™ VIOS 160i CO_2 Incubator, ThermoFisher Scientific™, Waltham, MA, USA) and the medium in the transwell was changed after every second day. Differentiation of Caco-2 cells occurred after 15-17 days of incubation. After reaching confluency, the transepithelial electrical resistance across the Caco-2 cell monolayer was measured using an EndOhm TEER cup (World Precision Instruments, Sarasota, FL, USA) connected to the EVOM^2 Epithelial Voltohmmeter (World Precision Instruments, Sarasota, FL, USA) to determine the barrier integrity of the cells. With preliminary tests, the cells were considered confluent when TEER was higher than 500 Ω/cm^2. The TEER values were regularly noted every 2 hours for the next 12 hours, and the final reading was taken at 24 hours. Resistance values are calculated using Equation 4.

$$\text{TEER } (\Omega/cm^2) = Raw\ TEER\ value\ (\Omega) \times surface\ area\ of\ insert\ (cm^2) \ldots\ldots \text{(Eq. 4)}$$

3.6. Statistical analysis

All the experiments were replicated at least three times. The results were expressed as mean±standard error of the mean. One-way ANOVA (Analysis of variance) was used to determine the effect of FP1, FP2, and RH on the various biochemical and physicochemical properties of the banana-flavoured milk at $\alpha \leq 0.05$. For multiple comparisons, Tukey's post hoc test was employed to determine the significant differences among the means of these three sample groups (i.e., FP1, FP2, and RH) ($P \leq 0.05$) using the IBM SPSS statistical software (Version 26, Armonk, NY., USA). Graphs were analysed and created using ORIGIN software (OriginPro, Version 9.7.0.185, 64-bit, 2020, Northampton, MA, USA) and Microsoft Excel (Version 2111, 64-bit, 2021, Redmond, Washington, USA).

Results and discussion

4.1. Behaviour of rutin-protein composites on the antioxidant properties

In this chapter, the antioxidant potential of natural rutin hydrate (RH) was compared with rutin-protein composites (i.e., FP1 (FlavoPlus 1) and FP2 (FlavoPlus 2)), and its correlation with the total phenolic content was also determined. Furthermore, the effect of the novel composites on human intestinal epithelial cells (Caco-2) was investigated. The cytotoxicity was observed through an MTT assay along with determining the intracellular antioxidant activity using a fluorescent-based assay on undifferentiated Caco-2 cells.

4.1.1. DPPH radical scavenging activity

The antioxidant activity of FP1 1 and FP2 was evaluated and compared with RH using the DPPH free radical scavenging assay. This assay is used to evaluate the antioxidant potential of foods by testing their ability to act as free radical scavengers and hydrogen atoms (Pyrzynska & Pękal, 2013). The composition of FP1 and FP2 powders supplemented with sodium caseinate had a varying amount of rutin, as mentioned in Section 3.2.2.5. In the case of both FP1 and FP2 powders, they presented a significantly ($p<0.05$) higher DPPH scavenging ability than RH. However, when the two rutin composites (FP1 and FP2) were compared together, there was no significant difference seen, due to their similar composition. These results suggest that the addition of caseinate has improved the antioxidant properties of rutin. This is in line with the findings from a previous study carried out by Jain et al. (2012), where rutin-phospholipid complexes were formed to enhance the *in vitro* antioxidant activity of rutin. The significant impact of rutin equivalent on the DPPH and TPC values is evident from the results obtained in this study. The DPPH free radical scavenging assay revealed that both FP1 and FP2 powders, enriched with varying levels of rutin and supplemented with sodium caseinate, exhibited markedly higher DPPH scavenging abilities compared to the reference substance, RH. This enhanced scavenging ability suggests that the incorporation of rutin, particularly in the presence of caseinate, has led to improved antioxidant properties in FP1 and FP2.

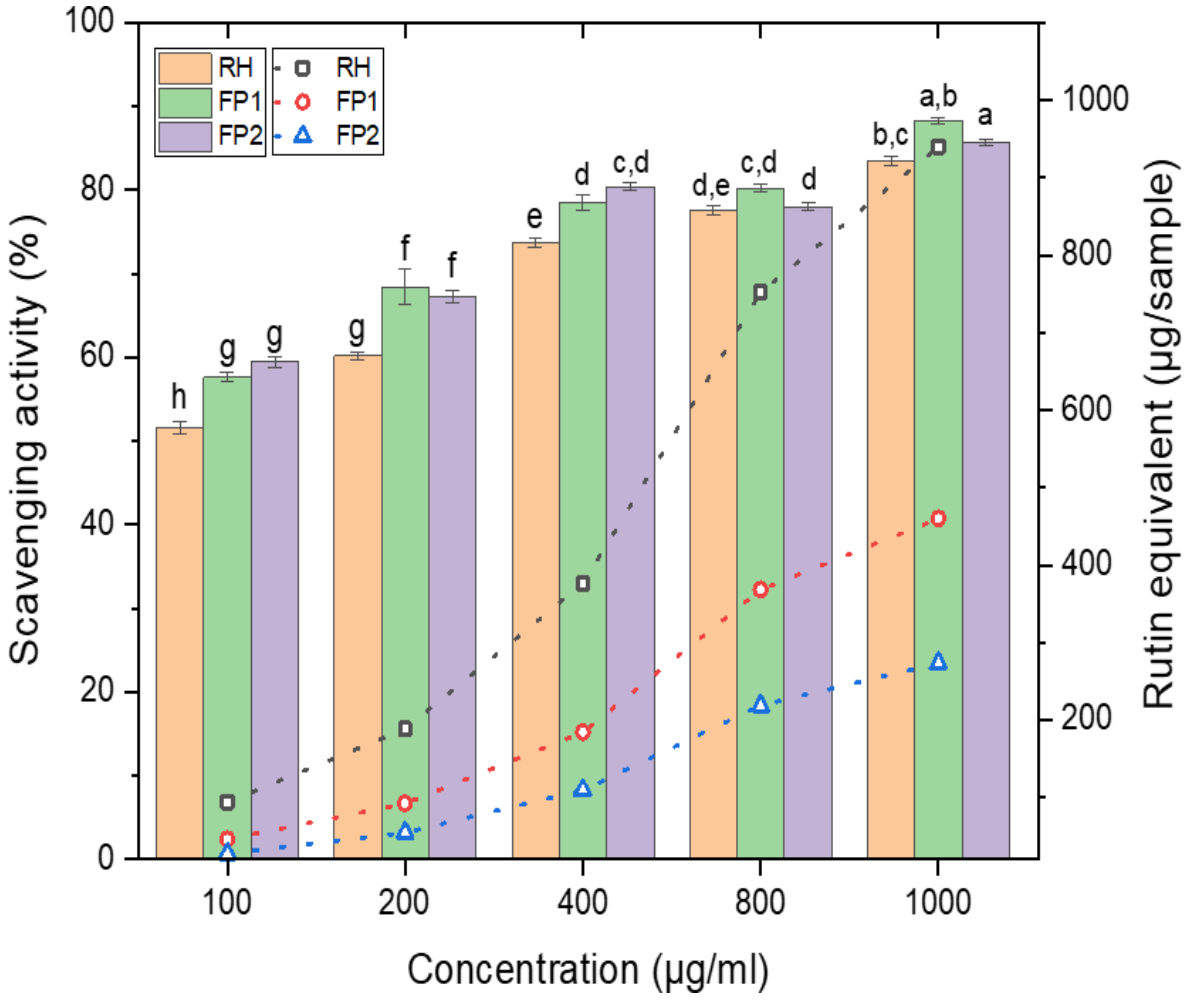

Figure 4.1 The DPPH (2,2-diphenyl-1-picryl-hydrazyl) antioxidant activity (an equivalent amount of rutin, ug/mL) of FlavoPlus1 (FP1) and FlavoPlus2 (FP2) vs rutin hydrate (RH). **Note:** Data represents the mean of six replicates with error bars corresponding to the standard error of the mean. Columns that do not share the same letters are significantly different ($p \leq 0.05$).

Based on these results, RH showed lower antioxidant activity compared to both rutin-protein composites, which can be due to its structural characteristics of having fewer hydrogen donor atoms reflecting electrostatic interactions with free DPPH radicals, as the result of less solubility in the aqueous medium. The modified rutin-protein complexes illustrate a significant increase in their scavenging ability in a concentration-dependent manner. The resulting scavenging effect of RH and rutin in the rutin-protein composites is largely due to the hydrophobic and electrostatic interactions of bioactive compounds, which modulate the reduction of free DPPH radicals. Many researchers (Celik et al., 2015; Nguyen et al., 2013; Sharma et al., 2013) have investigated rutin-cyclodextrin complexes to improve the hydrophobicity of rutin and eventually enhance its antioxidant property. The results of the current study suggest that the rutin-protein complex might have improved the stability of rutin

within an aqueous system, resulting in increased interaction with a protein source and improved antioxidant potential. This is in line with the previous reports about rutin complexed with other protein sources and its stability in an aqueous system (Nguyen et al., 2013; Ye et al., 2021) Ye et al. (2021) investigated a similar rutin-protein complex in which they acknowledged the impact of rutin-soy protein isolate to improve the stability of a rutin-protein complex within an aqueous system, which significantly increased the interaction between rutin and protein source. Nguyen et al. (2013) worked on creating a rutin-cyclodextrin complex that protected rutin from heat and UV degradation. Similar to the results of the current experiment, their rutin-cyclodextrin complex also enhanced the antioxidant capacity of rutin when compared to free rutin in a similar system. This strongly indicates the importance of developing complexes with bioactive compounds such as rutin to enhance their stability and significantly improve their interactions within a continuous aqueous system.

4.1.2. Total phenolic content (TPC)

The TPC values of FP1 and FP2 were compared with RH, which attributes to the presence of rutin as the phenolic compound in these samples (Figure 4.2). This superiority is due to the higher solubility of these two composites when compared to the untreated form of rutin (i.e., RH). The dose-dependent effect of FP1 and FP2 seen in Figure 4.2 further confirms the antioxidant potency of these samples. Based on the formulations of the samples discussed in Section 3.2.2.5, the amount of rutin equivalent present in the three samples was 46%, 27.3%, and 94% for FP1, FP2, and RH, respectively. These values correspond with their phenolic activity for the concentrations shown in Figure 4.2. After the determination of TPC values for FP1 and FP2, there was a positive correlation (R^2 = 98%) found between the TPC values and the antioxidant scavenging activity (DPPH values) of the rutin-protein composites. With an increase of 50 µg/mL after each concentration, RH corresponded with the amount of rutin present in the sample. Although RH contained a higher rutin equivalent at 200 µg/mL concentration, its TPC value was lower than FP1 (Figure 4.2), which could be due to its lower aqueous solubility and stability at room temperature for over 2 hours during incubation. The significant increase in TPC values for FP1 at a concentration of 200 µg/mL and the insignificant difference between FP1 at 200 µg/mL and FP1 at 300 µg/mL can be attributed to several factors related to the solubility, stability, and concentration of rutin, and the primary phenolic compound present in the samples.

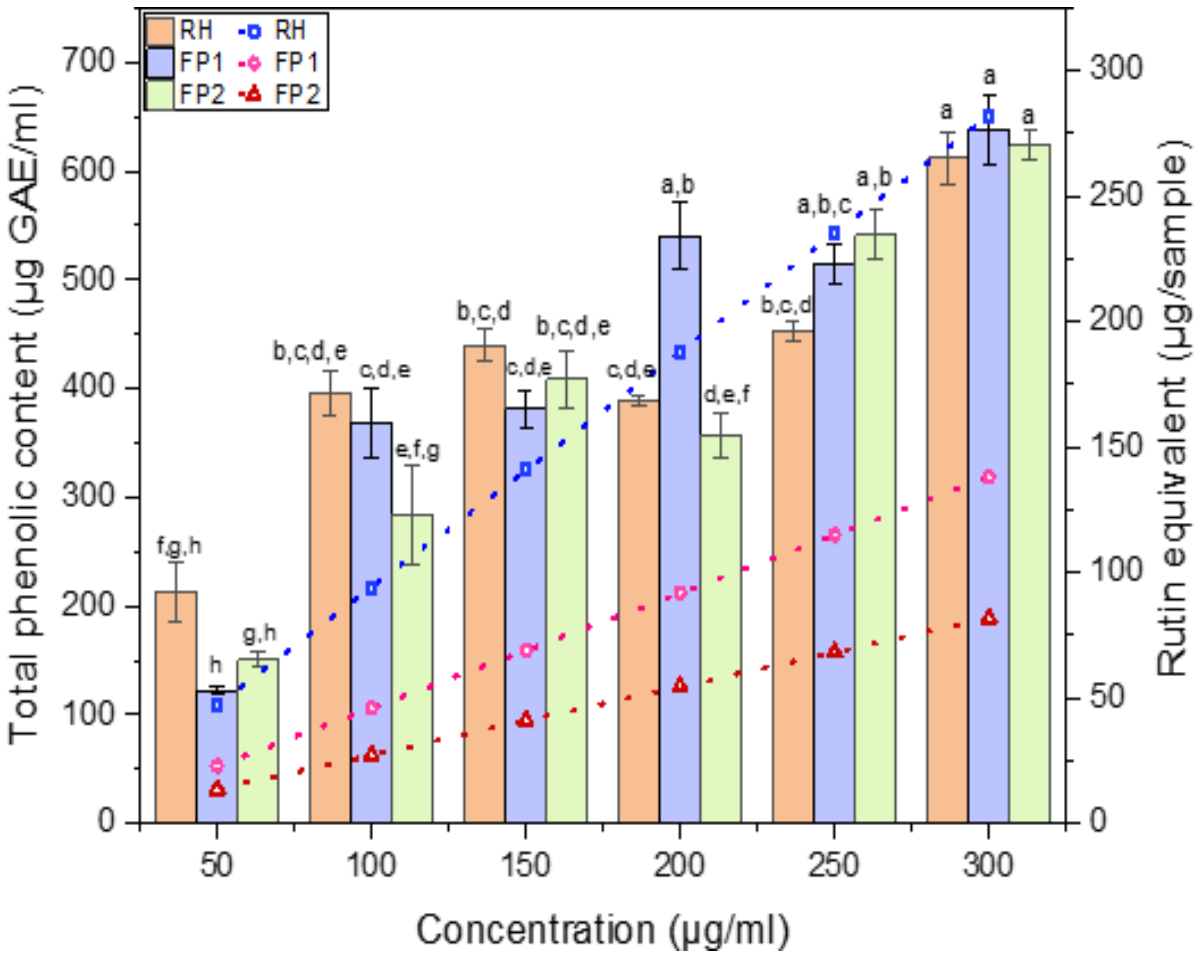

Figure 4.2 The total phenolic content of FlavoPlus1 (FP1) and FlavoPlus2 (FP2) vs rutin hydrate (RH), expressed as rutin equivalent (µg/ml). **Note:** Data represents the mean of three replicates with error bars corresponding to the standard error of the mean. Samples (FP1, FP2, RH) that do not share the same letters are significantly different ($p \leq 0.05$).

The conjugation between rutin and caseinate protein in a flavonoid-complex system results in higher functional properties, along with noncovalent complexes due to the hydrophobic nature of rutin (Horincar et al., 2019). In similar flavonoid complexes, the protein was compared with a non-covalent complex of whey protein isolate and rutin, which exhibited higher antioxidant and stable food complexes when investigated (Wei et al., 2015). FP1 and FP2 were systemically compared at every concentration, which led to a characteristic observation that due to modification in the caseinate protein, stronger binding affinities between the complexes could lead to higher phenolic content within the samples.

4.1.3. Cytotoxic effect of DMSO on rutin-protein composites and rutin hydrate in Caco-2 cells

Because of rutin's highly hydrophobic nature, it was resuspended in dimethyl sulfoxide (DMSO) for the *in vitro* cellular assays. DMSO is highly toxic to the cells (Hollebeeck et al., 2011), and therefore, the concentration required to resuspend rutin must be optimised for Caco-2 cell viability and structural integrity. It was investigated that the dose-dependent effects of dimethyl sulfoxide (DMSO) should range from 0% (control) to 5% on the Caco-2 cell line, to find the safe/non-toxic dose for rutin resuspension. This study examined the cytotoxic behaviour of DMSO as a vehicle carrier, which could further confirm whether DMSO has any background effects on Caco-2 cells while measuring the cytotoxic behaviour of FP1, FP2, and RH on Caco-2 cells. The cell viability of Caco-2 cells was dependent on the concentration of DMSO over an exposure period of 4 hours. Thus, it was important to identify optimum concentration where Caco-2 cells were healthy with good viability percentage following stimulation with DMSO.

Based on the results observed in Figure 4.3, the cell viability of Caco-2 cells in response to DMSO was quantified from Equation 1 (Section 3.2.3.4). The stimulation of Caco-2 cells with different concentrations (0-5%) of DMSO for 4 hours resulted in a dose-dependent decrease in the cell viability (Figure 4.3). The control was the concentration of 0% (without DMSO) which was significantly different from post-treatment of the cells with DMSO at a concentration of 0.1%. This resulted in better viability which indicates healthy cells and their resistance toward DMSO as a vehicle solvent. Moreover, an increase in the doses of DMSO concentration after 0.1% resulted in more stress leading to >50% cell death, thereby, reducing cell viability. Similar results were observed by Hollebeeck et al. (2011) where a dose-dependent response at 0.05-1% DMSO stimulated inflammatory response in confluent Caco-2 cells.

As seen in Figure 4.3, with an increase in the concentration of DMSO, a decrement in cell viability was observed. This decrease in cell viability could be a result of cell death by the cytotoxic effect of DMSO via degrading the metabolic health of cells and damaging the cell membrane. Therefore, it was important to account for the activity of DMSO as it was used as a vehicle solvent for dissolving the hydrophobic RH while assessing the antioxidant properties of Caco-2 cells.

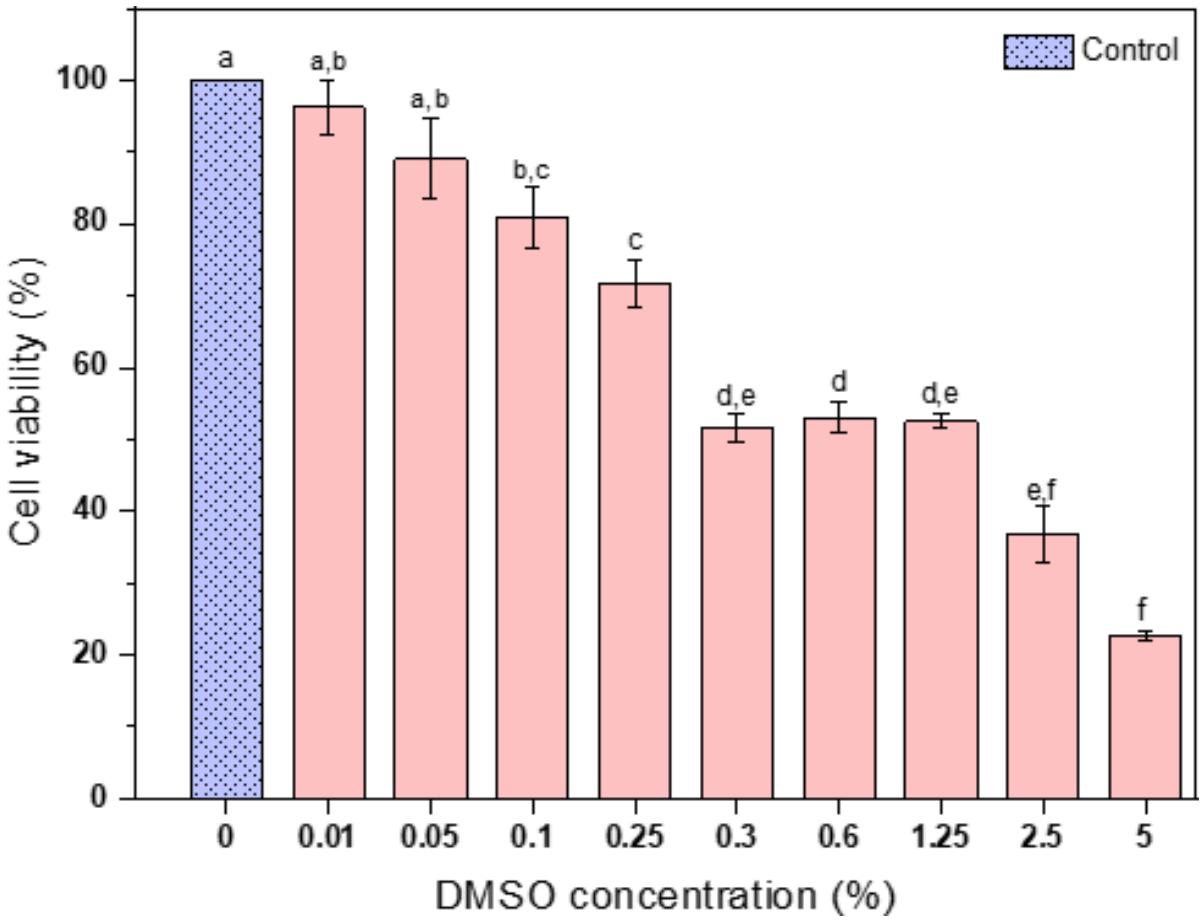

Figure 4.3 The effect of dimethyl sulfoxide (DMSO) concentration on Caco-2 cell viability. **Note:** Data represents the mean of three biological replicates with four replicates in each assay with error bars corresponding to the standard error of the mean. Columns that do not share the same letters are significantly different at $p < 0.05$ based on one-way analysis of variance (ANOVA) followed by Tukey's post hoc test.

4.1.4. The effect of rutin-protein composites on the viability of Caco-2 cells

As described in Section 3.5.6, the effect of FP1, FP2, and RH on the cell viability of Caco-2 cells through an MTT assay was assessed. The cells were incubated with 4 different concentrations (0.1, 0.5, 15, and 25 µg/mL) that showed changes in cell viability post-incubation for 4 hours. As shown in Figure 4.4A, the concentration of 0.1 µg/mL showed at least 75% cell viability for RH, whereas in the case of FP1 and FP2, the cell viability was observed to be >80%. This decrease in cell viability for RH could be due to a mechanism related to active or passive penetration of a higher amount of rutin in cells that could pertain to cytotoxic effects being generated in healthy Caco-2 cells after being exposed for 4 hours. As discussed in Section 3.2.2.5, the amount of rutin present in RH was higher than that in FP1 and FP2; thereby, the results suggest a degree of cytotoxicity based on the formulations

of the samples, although the amount of water-soluble rutin in both rutin-protein composites was higher than RH.

As shown in Figure 4.4B, the effect of RH at 0.5 µg/mL on the cells showed at least 80% cell viability, but FP1 and FP2 had higher cell viability, which could be due to the increase in concentration from 0.1 µg/mL to 0.5 µg/mL. However, in Figure 4.4C, the cell viability was reduced drastically for RH and FP2, which could be due to cellular damage in the system with a high dose of 15 µg/mL. A similar effect was not shown by FP1 after 4 hours of exposure to the cells, as it maintained cell viability of above 80%. The cytotoxic effect of rutin at a higher dose could be explained by the exposure duration as well, i.e., a higher exposure time could result in the degradation of cellular membranes leading to more ROS generation. Despite FP1 and FP2 having strong antioxidant potential as discussed in Section 4.1.1, they could have a cytotoxic effect on cells, which restricted cell proliferation.

A research study by Sak (2014) has shown that dietary flavonoids such as rutin, quercetin, and naringin could display a dual activity by inhibiting the cytotoxicity in Caco-2 and HepG2 cells, as well as causing some genotoxic damage to the healthy cells. This may connect with the results observed in Figure 4.4D, where cell viability was recorded at 80% with a stable proliferation of Caco-2 cells but with a concentration of 25 µg/mL. There could be some genomic variations that lead to the activation of some transcriptional regulators, which initiate antioxidant enzymes to prevent the cells from oxidative stress.

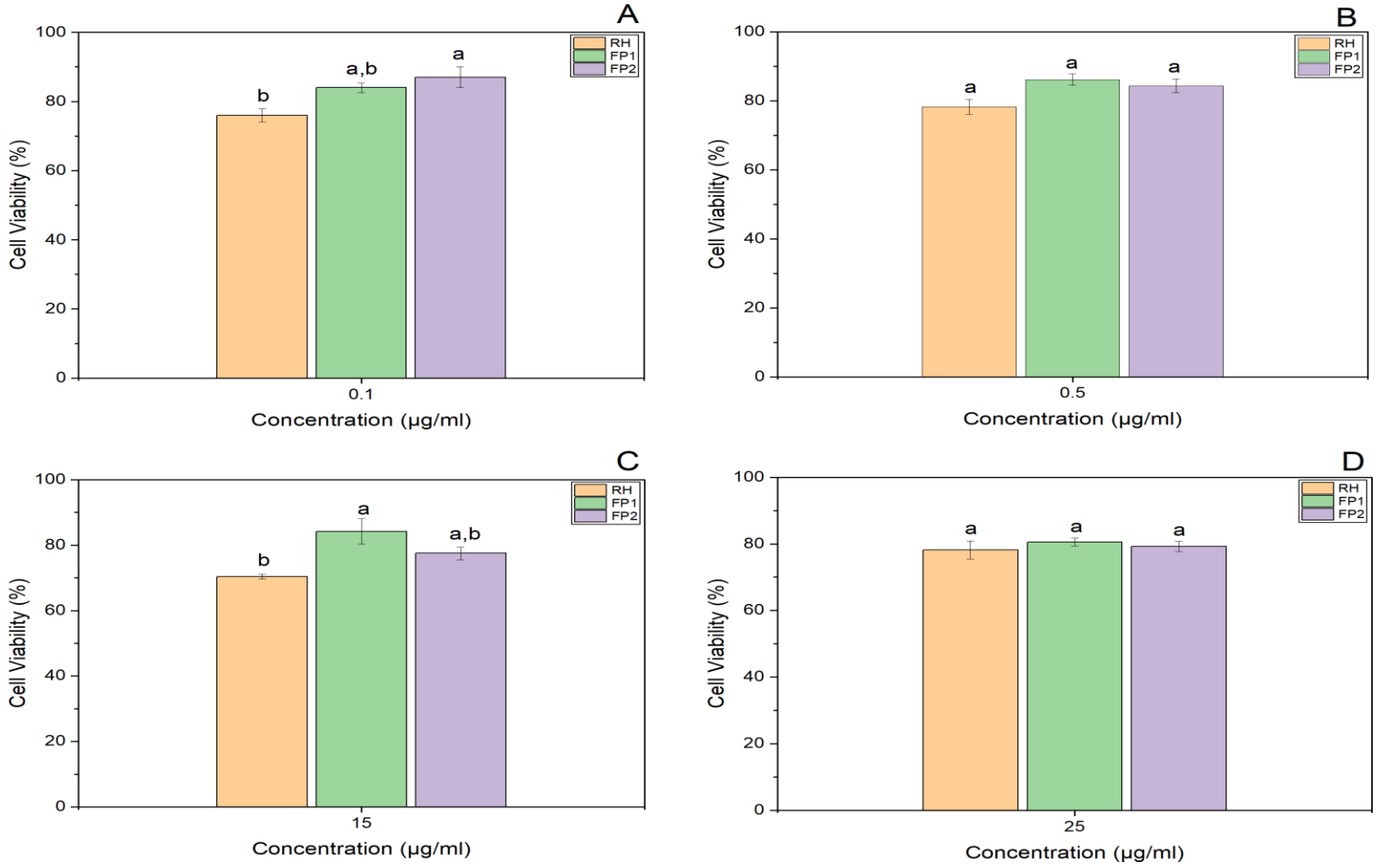

Figure 4.4 The effect of FlavoPlus1 and FlavoPlus2 vs rutin hydrate on cell viability. **Note: A,B,C,D** represent different concentrations in the assay. Data represents the mean of four biological replicates with three replicates in each assay. Error bars correspond to the standard error of the mean. Columns that do not share the same letters are significantly different ($p \leq 0.05$).

As shown in Figure 4.4, the cell viability in the system is maintained with a range of concentrations of FP1, FP2, and RH along with 0.1% DMSO as a vehicle carrier for RH with an exposure time of 4 hours. This resulted in preventing cell death and reducing ROS generation, which favoured cell proliferation for the cells. Thus, a similar range of concentrations was considered for further *in vitro* analysis. In addition to observing the protective effect of FP1 and FP2 on cell viability, the underlying mechanisms for understanding how structural moieties of rutin may affect cellular damage in differentiated Caco-2 cells may enhance our understanding of how rutin-protein composites highlight antioxidant capacity at a cellular level.

4.1.5. Intracellular antioxidant activity of rutin composites vs rutin hydrate in Caco-2 cells

The ability of rutin-protein composites studied in this experiment (i.e., FP1 and FP2) to induce an antioxidant response was investigated using DPPH radical scavenging assay in Section 4.2.1, where an increase in the concentration (µg/mL) of such composites was able to scavenge more reactive oxygen species. Additionally, to understand the effect of rutin-protein composites on a cellular level, an intracellular antioxidant potential was measured through *in vitro* cellular antioxidant assay (DCFH-DA method). For this reason, Caco-2 cells were incubated with FP1, FP2, and RH for 1 hour and subsequently treated with DCFH-DA (as a fluorescent marker) at a concentration of 25 µM for 30 minutes, which detects the ROS in the cell (Kim et al., 2011). The cells were washed with PBS three times to prevent any debris from FP1, FP2, and RH, and they were then exposed to 100 µL of AAPH for inducing oxidative stress. The results were obtained after fluorescence was measured on the plate reader for 60 minutes with an interval after every 5 minutes to monitor the optimal incubation time, concerning the changes in fluorescence intensity.

Figure 4.5 shows that at 4 different concentrations ranging from 0.5 µg/mL to 200 µg/mL, the change in fluorescence corresponds with the cellular antioxidant activity over 60 minutes. The concentration and time-dependent increases in fluorescence signal were observed with a peak at 60 minutes for FP1 at 0.5 µg/mL, suggesting that FP1 at 0.5 µg/mL was not able to inhibit the presence of AAPH (inducer of oxidative stress) in the cells, resulting in a lower cellular antioxidant activity. Therefore, the cellular antioxidant activity at 60 minutes was lower when compared to 0 and 10 minutes. An increased quenching of ROS was observed at 0 minutes and 10 minutes whereas, and with an increase in the incubation time from 10 minutes to 30 minutes,

the fluorescence was observed at the higher range at the lowest concentration of 0.5 µg/mL. This could be due to the strength of the DCFH dye, which has an absorption period of 30 minutes to detect any ROS in the cell system (Kim et al., 2011). The observed fluorescence signal was caused by the samples in response to their free radical quenching effect of ROS, which was significantly lower at 60 minutes even at the highest concentration of 200 µg/mL for all three treatments (i.e., FP1, FP2, and RH).

According to Figure 4.5, the fluorescence observed at 30 minutes showed maximum quenching of ROS at 200 µg/mL for all three samples, meaning that they behaved as potent antioxidant compounds. The fluorescence (%) was particularly in the same range for FP1, FP2, and RH at 50 µg/mL, 100 µg/mL, and 200 µg/mL after 30 minutes of incubation under induced oxidative stress. Even after 30 minutes of incubation, both rutin-protein composites showed protective activity against AAPH in comparison to RH (Figure 4.5). This proves their efficiency at permeating the intestinal barrier in the Caco-2 cells which results in a functional antioxidant at the cellular level.

At 0 and 10 minutes, the activity of FP1, FP2, and RH varied concerning their concentrations. At 0.5 µg/mL, for example, FP2 showed similar antioxidant activity to that observed at 0 and 10 minutes; however, FP1 had higher antioxidant activity at 0 minutes with some minor decrement after 10 minutes. Both rutin-protein composites attributing to the cellular antioxidant activity at such a low concentration, predict an effective absorption of FP1 and FP2 in the Caco-2 cell model. In comparison with FP1 and FP2, RH showed lower antioxidant activity at both incubation periods of 0 and 10 minutes, but it demonstrated even lower antioxidant activity at a longer incubation period of 30 and 60 minutes.

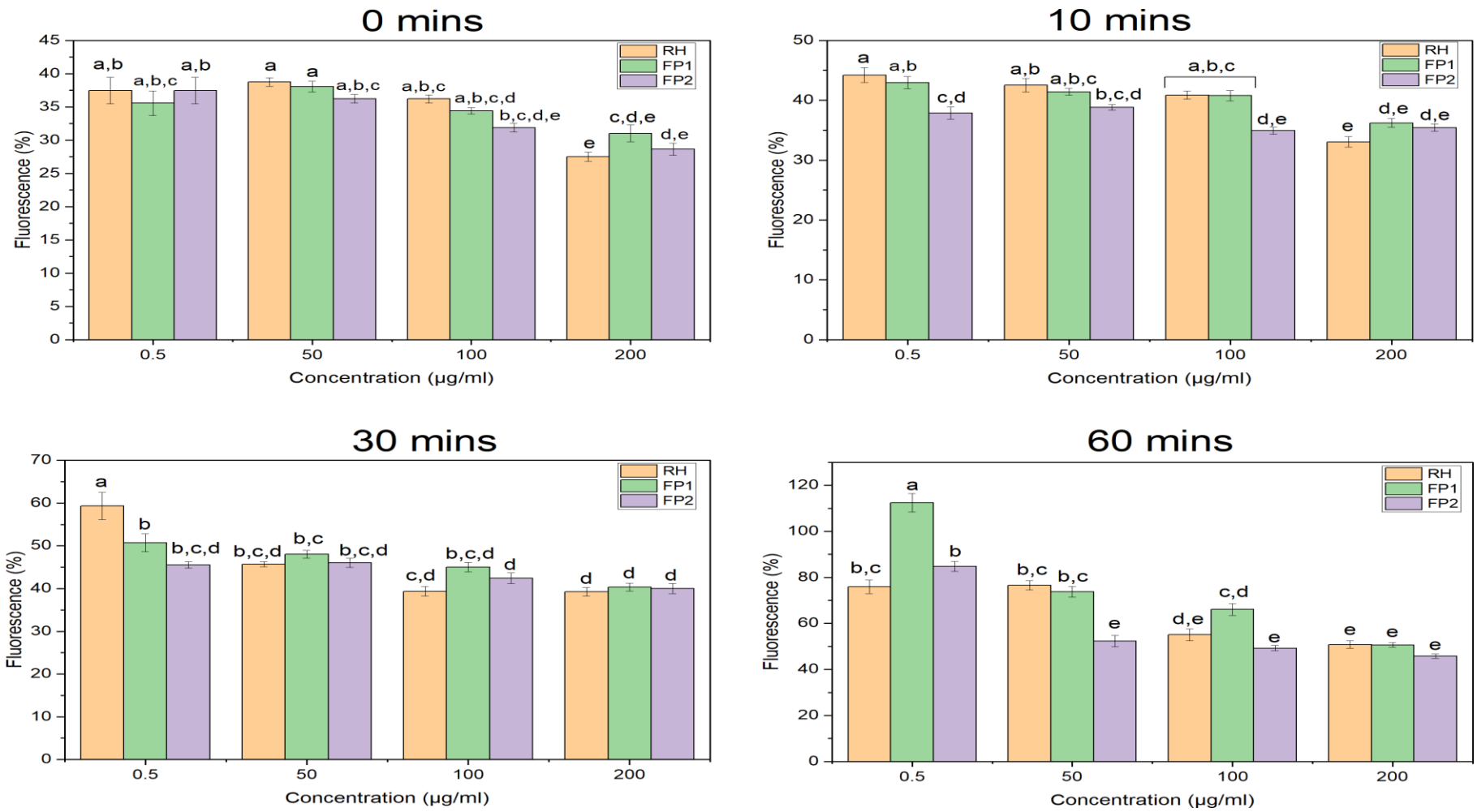

Figure 4.5 Effect of FlavoPlus1 (FP1) and FlavoPlus2 (FP2) vs rutin hydrate (RH) on intracellular antioxidant activity over 60 minutes. Intracellular antioxidant activity was quantified with a 2′,7′-Dichlorofluorescin diacetate (DCFH-DA) assay using relative fluorescence values of the samples. **Note:** Data represents the mean of three biological replicates with three replicates in each assay. Error bars correspond to the standard error of the mean. Columns that do not share the same letters are significantly different ($p \leq 0.05$).

Based on these results, the incubation period was optimised, and 60 minutes was chosen to show the maximum fluorescence that was recorded during the experiment. Having a median time interval of 30 minutes depicted how stable the rutin-protein composites were to reflect their antioxidant activity with a sensitive fluorescent probe like DCFH. In the case of assessing the cellular antioxidant activity for biological replicates, this may have a decreasing tendency with greater incubation periods - it could leak into the cells and reflect a very low antioxidant response from the samples, which in turn, could result in unreliable results and demonstrating low reproducibility (Wan et al., 2015).

Both rutin-protein composites (i.e., FP1 and FP2) in the current study showed a similar cellular antioxidant activity ($p \leq 0.05$) at early incubation time periods by effectively quenching peroxyl radicals generated by AAPH. This antioxidant activity of FP1 and FP2 reflected at 0 and 10 minutes could be due to their action of penetrating within the cell membranes to quench the induced peroxyl radicals, and thereby, it was reflected by the fluorescent indicator DCF, which is highly sensitive to quenching of peroxyl radicals. Meanwhile, the oxidation of the non-polar DCFH-DA dye that was diffused into the cell membranes to form DCFH by cellular esterase was inhibited by the rutin-protein composites resulting in less fluorescence. However, in the case of RH, the cells showed higher fluorescence, which pertains to the generation of DCF (i.e., the polar and oxidised form of DCFH). Similar studies have shown fluorescent DCF as an indicator of oxidative stress within an *in vitro* cell model (Kellett et al., 2018; Wan et al., 2015; Wolfe & Liu, 2007).

4.1.6. Summary

The findings of antioxidant activity and total phenolic content of the two novel rutin-protein composites measured via the *in vitro* cell and biochemical assays demonstrated a higher antioxidant potential for both novel rutin-protein composites (FP1 and FP2) when compared with RH. These results suggest that FP1 and FP2 were more efficient in scavenging free radicals than RH during the DPPH assay, which attributed to the higher solubility of rutin in these samples. Further, the cell viability assay suggested that with an increase in the concentration from 0.1 µg/mL to 25 µg/mL, the rutin-protein composites were maintaining better cell viability than RH even after an exposure of 4 hours. In addition, intracellular DCFH-DA assay results suggest that FP1 and FP2 exhibit higher antioxidant activity in comparison to RH after inducing oxidative stress for 60 minutes. Importantly, the novel food-grade rutin-protein composites were significantly efficient in scavenging ROS at a low concentration of 0.5 ug/mL when compared with RH at 0, 10, and 30 minutes of the incubation period. These superior properties of the novel composites vs untreated rutin (i.e., RH) demonstrated the successful delivery of rutin in form of these composites. This, in turn, suggests the strong potential of the incorporation of such composites in functional food and beverages.

4.2. *In vitro* bioaccessibility of rutin from rutin-protein composites incorporated into the functional milk product

In this section, the results are presented for a banana-flavoured dairy beverage (milk) that was enriched with rutin-protein composites to deliver 500 mg rutin per serve of 250 mL milk. During the gastric and intestinal digestion of the enriched dairy beverage, the product was characterised for particle size and its zeta potential, as well as the determination of the bioaccessibility of rutin. In addition, using *in vitro* model of polarized intestinal epithelium cell line (Caco-2), the cytotoxicity, paracellular absorption, and intracellular antioxidant potential of the digested milk containing FP1, FP2, and RH were determined.

4.2.1. Effect of *in vitro* digestion on the particle size and surface charge of rutin-protein composites and rutin hydrate

The particle size was analysed for different incubation times of the stimulated gastric and intestinal digestion. Characterisation of FP1 for particle size was carried out at room temperature and they were expressed as volume-weighted mean, which pertains to the size of particles that constitute the centre within the particle distribution system of the whole volume. As shown in Table 4.1, FP1 had an increasing particle size concerning the incubation times while undergoing *in vitro* digestion. During the gastric phase, there was a gradual increase in particle size from 38.95 to 49.42 µm, from the initial time point of 0 to 120 minutes, respectively. Whereas, in the case of the intestinal phase, the particle size increased from about 64.39 to about 264.48 µm, leading to a decrease in the surface area of the particles from 0.42 to 0.10 m^2/gm. This increase in particle size could be due to the aggregation of sodium caseinate from the protein complex and casein from the banana-flavoured dairy beverage.

The difference in particle size between the gastric and intestinal phases was mainly based on the pH and the effect of enzymes such as protease, which could break the structure of the rutin-protein complex within the casein matrix. This resulted in larger particles flocculating within the particle distribution, which might block the detection of smaller particles present in the system.

The zeta potential for FP1 during the gastric phase was between 4.23 and 3.53 mV, and for the intestinal phase, it was in the range of -18.35 to -5.95 mV. As the shift in particle size was evident in both phases of digestion, the particle charge was therefore also influenced by the degradation of casein from the dairy beverage over time; the rutin-protein complex consisting of NaCas was broken down by the enzymatic reactions occurring within both digestion phases.

Table 4.1. The particle size, specific surface area, and zeta potential of digested fortified banana-flavoured milk containing FlavoPlus 1 (FP1). **Note:** Data represents the mean of three replicates with error bars corresponding to the standard error of the mean. Values in the three columns that do not share the same letters are significantly different ($p \leq 0.05$).

Sample – FP1	**D [4,3] (µm)**	**Zeta potential (mV)**	**Specific surface area (m^2/gm)**
Gastric 0 minutes	38.95 ± 0.44^{c}	4.23 ± 0.23^{a}	0.31 ± 0^{c}
Gastric 30 minutes	43.38 ± 1.89^{c}	3.6 ± 0.80^{a}	0.32 ± 0.02^{c}
Gastric 60 minutes	$51.57 \pm 14.75^{b,c}$	4.91 ± 0.65^{a}	0.32 ± 0.01^{c}
Gastric 120 minutes	$49.42 \pm 6.68^{b,c}$	3.53 ± 0.27^{a}	0.29 ± 0.01^{c}
Intestinal 0 minutes	64.39 ± 2.35^{b}	-18.35 ± 1.82^{c}	0.42 ± 0.02^{b}
Intestinal 30 minutes	40.67 ± 9.02^{c}	-18.38 ± 1.70^{c}	$0.45 \pm 0.05^{a,b}$
Intestinal 60 minutes	61.87 ± 13.03^{b}	-13.01 ± 1.89^{c}	0.49 ± 0.04^{a}
Intestinal 120 minutes	264.48 ± 10.24^{a}	-5.95 ± 0.14^{b}	0.10 ± 0^{d}

As shown in Table 4.2, the particle size for FP2 was higher when compared to FP1 during both gastric and intestinal phases, which could be linked to the breakdown of casein from the milk beverage matrix and an early release of rutin from the protein in which rutin was entrapped. The amount of rutin present in FP2 fortified banana milk was lowest in comparison to FP1 and RH but there was 54.5% of NaCas which was dissociated from rutin as caseins present in the food matrix could be hydrolysed within the gastric phase due to the highly acidic conditions over 120 minutes, this could result in proteolytic cleavage of casein protein from the milk

matrix. The surface charge of the particles was positive within the 120 minutes of gastric phase digestion from 4.23 to 3.53 mV. A trend was observed in the present study for characteristics of FP1 and FP2, exhibiting an increased particle size thereby, also increasing the charge in the intestinal phase at 0 minutes where the digested milk containing FP1 and FP2 are subjected to highly alkaline conditions. Such alkaline conditions have shown a dissociation of NaCas from rutin, which could be the reason for the spike in particle size at 0 minutes during the intestinal phase and subsequent decrease in size over a longer incubation time. A similar trend was also observed by Dammak and do Amaral Sobral (2017), who confirmed the dissociation of NaCas from rutin at high alkaline conditions during *in vitro* digestion and its re-association after neutral pH was achieved in the system.

Table 4.2. The particle size, specific surface area, and zeta potential of digested fortified banana-flavoured containing FlavoPlus 2 (FP2). **Note:** Data represents the mean of three replicates with error bars corresponding to the standard error of the mean. Values in the three columns that do not share the same letters are significantly different ($p \leq 0.05$).

Sample - FP2	D [4,3] (µm)	Zeta potential (mV)	Specific surface area (m2/gm)
Gastric 0 minutes	369.36±19.12^{a}	4.30±0.20^{a}	0.19±0.01^{e}
Gastric 30 minutes	181.39±3.97^{b}	3.35±0.13^{a}	0.28±0.01^{a}
Gastric 60 minutes	186.11±9.93^{b}	2.66±0.16^{a}	0.23±0.01^{c,d}
Gastric 120 minutes	169.81±2.74^{b}	2.39±0.19^{a}	0.26±0^{a,b}
Intestinal 0 minutes	371.68±16.16^{a}	-13.55±0.47^{b,c}	0.21±0.01^{d,e}
Intestinal 30 minutes	345.88±32.11^{a}	-11.5±0.29^{b}	0.24±0.25^{b,c}
Intestinal 60 minutes	353.15±10.48^{a}	-17.33±2.14^{c}	0.27±0.01^{a}
Intestinal 120 minutes	369.59±10.70^{a}	-11.32±1.53^{b}	0.27±0.02^{a}

As shown in Table 4.3, the particle size of RH was higher during the gastric phase and had a subsequent decrement during the intestinal phase over 120 minutes. The amount of rutin present in the RH fortified banana milk was higher than FP1 and FP2, which could have

resulted in larger crystal formation, thereby, having a large particle size even at the initial time of gastric digestion. During the fortification of milk with RH, the dispersibility was low due to its hydrophobic nature, which resulted in a non-homogenous distribution of particles within the system. This is because both FP1 and FP2 had much higher solubility than RH, which resulted in their complete dispersibility in the milk system. The larger particle size could be a result of flocculation of casein particles from the dairy beverage during activation of protease resulting in the breakdown of proline. As the particle size varied from 274.61 to 78.25 µm, the particle charge was negative from the gastric to intestinal phase, within a range of -1.64 to -16.1 mV. The reduction of particle size during the intestinal phase may also result in a higher surface area (between a range of 0.41 to 0.48 m^2/gm). This effect in the surface charge of the particles could also be due to the change in pH from acidic to alkaline conditions, as rutin has been reported to have a higher affinity towards protein at the isoelectric point during low pH units (Naczk et al., 2006) (Yildirim-Elikoglu & Erdem, 2018).

Table 4.3. The particle size, specific surface area, and zeta potential of digested fortified banana-flavoured containing rutin hydrate (RH). **Note:** Data represents the mean of three replicates with error bars corresponding to the standard error of the mean. Values in the three columns that do not share the same letters are significantly different ($p \leq 0.05$).

Sample - RH	D [4,3] (µm)	Zeta potential (mV)	Specific surface area (m2/gm)
Gastric 0 minutes	274.61 ± 8.74^{a}	-1.64 ± 0.15^{a}	0.13 ± 0^{d}
Gastric 30 minutes	279.72 ± 8.322^{a}	-1.52 ± 0.12^{a}	0.16 ± 0^{d}
Gastric 60 minutes	138.62 ± 32.05^{b}	-1.37 ± 0.14^{a}	0.22 ± 0.02^{c}
Gastric 120 minutes	$95.09 \pm 18.14^{c,d}$	-1.88 ± 0.15^{a}	0.21 ± 0.01^{c}
Intestinal 0 minutes	$73.04 \pm 10.59^{d,e}$	-15.88 ± 0.48^{b}	0.41 ± 0.02^{b}
Intestinal 30 minutes	60.06 ± 2.68^{e}	-15.8 ± 0.61^{b}	0.43 ± 0.01^{b}
Intestinal 60 minutes	104.22 ± 23.28^{c}	-15.2 ± 0.77^{b}	$0.44 \pm 0.03^{a,b}$
Intestinal 120 minutes	$78.25 \pm 15.33^{c,d,e}$	-16.1 ± 0.41^{b}	0.48 ± 0.05^{a}

Table 4.4. The particle size, specific surface area, and zeta potential of digested unfortified banana-flavoured. **Note:** Data represents the mean of three replicates with error bars corresponding to the standard error of the mean. Values in the three columns that do not share the same letters are significantly different ($p \leq 0.05$).

Sample- Milk	**D [4,3] (µm)**	**Zeta potential (mV)**	**Specific surface area (m2/gm)**
Gastric 0 minutes	96.97 ± 10.04^{a}	-1.09 ± 0.05^{a}	0.19 ± 0^{b}
Gastric 30 minutes	$80.20 \pm 9.45^{a,b}$	-1.06 ± 0.04^{a}	0.21 ± 0.02^{b}
Gastric 60 minutes	$60.67 \pm 8.41^{b,c}$	-1.13 ± 0.05^{a}	0.26 ± 0.01^{b}
Gastric 120 minutes	$55.66 \pm 5.51^{c,d}$	-1.15 ± 0.06^{a}	0.27 ± 0.01^{b}
Intestinal 0 minutes	$64.23 \pm 17.13^{b,c}$	-15.85 ± 0.49^{b}	0.66 ± 0.06^{b}
Intestinal 30 minutes	$54.17 \pm 16.73^{c,d}$	-15.48 ± 0.42^{b}	6.47 ± 4.23^{a}
Intestinal 60 minutes	$74.6 \pm 12.33^{b,c}$	-15.46 ± 0.30^{b}	7.96 ± 0.62^{a}
Intestinal 120 minutes	39.35 ± 2.75^{d}	-14.8 ± 0.40^{b}	0.44 ± 0^{b}

The characterisation of banana-flavoured beverage for the size and surface charge of its particles was carried out to understand the effect of food matrix alone before the incorporation of the composites or RH. As shown in Table 4.4, the banana-flavoured milk showed a decrement in particle size from about 96.97 to about 39.35 µm during the gastric and intestinal digestion phases. This affected the charge of the particles present within the system and the surface area consequently. This increase in the particle size during the gastric phase could be due to the dissociation of casein protein into its monomeric forms resulting in an aggregation of proteins. Thereby, the reduction of particle size after the intestinal digestion contributes to the increase in surface area from 0.19 to 0.44 m^2/gm of the homogenous milk beverage, which could slow the rate of hydrolysis.

4.2.2. Bioaccessibility of rutin during *in vitro* digestion

The bioaccessibility of rutin in the fortified banana-flavoured beverage may indicate the amount of rutin that is available for absorption in the body. By understanding the effect of *in vitro* digestion on the size, composition, and structure of rutin-protein composites, the bioaccessibility of rutin can be enhanced. After the gastric digestion, FP1 and FP2 were subjected to intestinal digestion, which consisted of enzymatic stimulation by pancreatin and bile salts, to mimic the kinetics of *in vivo* digestion process. The recovery of rutin from the digested milk at the intestinal phase was quantified using HPLC. To understand the behaviour of FP1 and FP2 after intestinal digestive degradation, the concentration of rutin present in the initial samples prior to *in vitro* digestion was compared with the recovered amount of rutin from the digested milk.

The bioaccessible amount of rutin present in FP1 at 0 minute was significantly different from other time periods, which could be due to a pH change in the interface of the food matrix from acidic to alkaline (Rashidinejad et al., 2022). However, the protection of rutin throughout the gastric phase was due to the complex protein structure formation of casein and NaCas, which prevents the destabilisation of rutin by delaying proteolysis resulting in a prolonged release of rutin during the intestinal phase. A similar trend was observed by Lamothe et al. (2014), where green tea polyphenols were added to a milk matrix, which resulted in improved bioaccessibility (by 42%) after intestinal digestion.

The recovery of rutin from FP1 was prominent within a range of 43% to 48% throughout the intestinal digestion from 30 minutes to 120 minutes, whereas FP2 showed a consistent recovery of rutin in the range of 45% to 42% from 0 to 120 minutes. As some proportion of rutin was present in the gastric phase, both phases were analysed for bioaccessibility. These digestion phases were differentiated into soluble and insoluble fraction after centrifugation, and the soluble fraction of the digested milk was used to determine the bioaccessibility of rutin released from FP1 and FP2.

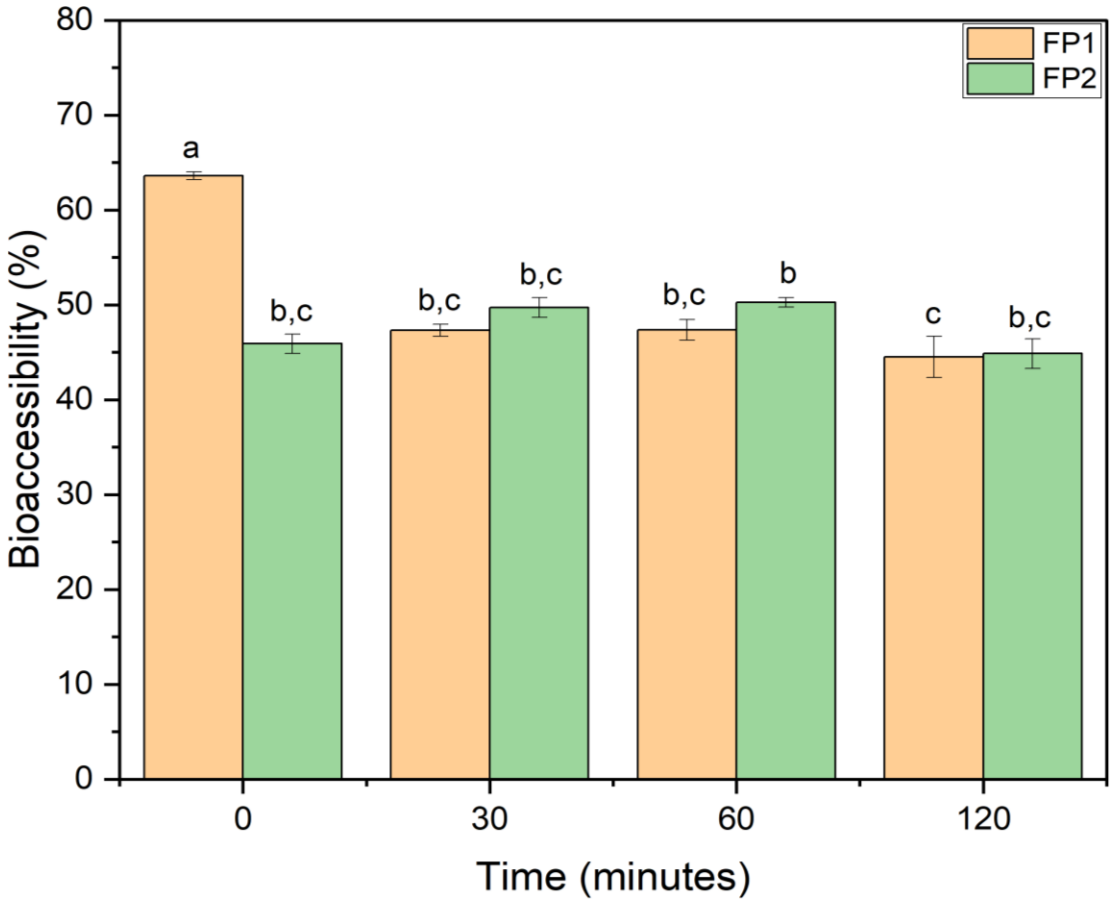

Figure 4.6. Bioaccessible rutin available in FlavoPlus1 (FP1) and FlavoPlus2 (FP2) obtained during the *in vitro* intestinal digestion phase. **Note:** Data represents the mean of three replicates with error bars corresponding to standard error of mean. Samples that do not share the same letters are significantly different ($p \leq 0.05$).

As Figure 4.6 indicates, the soluble fraction from FP1 was significantly higher at 63% at 0 minutes in comparison with FP2 which showed about 45% bioaccessibility. However, after 120 minutes of intestinal digestion, the soluble fraction from digested milk containing FP1 and FP2 was bioaccessible within a range of 45 to 47%. This indicates a loss of 16% to 18% of bioaccessible rutin over the intestinal digestion phase for FP1, but in the case of FP2, this loss was only 3% to 4%. Therefore, the total amount of digesta quantified for bioaccessibility was 0.5 mL, in which FP1 and FP2 had an average concentration of 641.31 ppm and 263.28 ppm, respectively, and based on these concentrations, FP1 and FP2 were evaluated for their potential epithelial absorption by diffusion across polarised Caco-2 cell monolayer.

4.2.3. Effect of digested milk containing rutin-protein composites on the barrier integrity of Caco-2 cell monolayer integrity

The bioaccessible fractions of FP1, FP2, and RH were investigated for their permeability by measuring the transepithelial electrical resistance across Caco-2 cell monolayers. As shown in Figure 4.7, the cells were differentiated and polarised for the diffusion of rutin from the bioaccessible fraction across the monolayers, and to determine the effect of digested milk containing FP1, FP2, and RH on the intestinal epithelium barrier integrity.

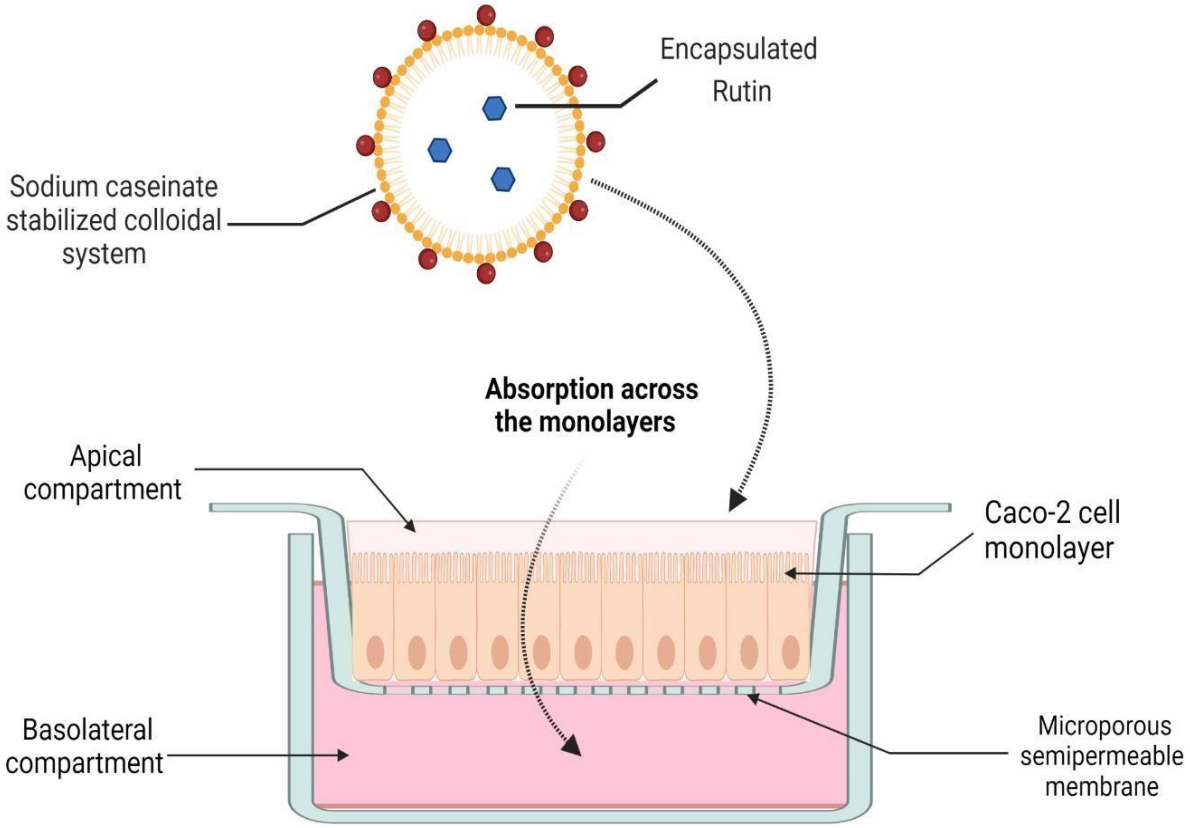

Figure 4.7. A schematic representation of *in vitro* absorption of novel rutin-protein composites across Caco-2 cell monolayers in transwell (Created with BioRender)

To determine the effect of FP1 digesta on barrier integrity of Caco-2 cells, they were treated with four different concentrations (0.1, 10, 50, and 200 µg/mL) for 24 hours. As shown in Figure 4.8, there was a reduction in TEER values at a concentration of 200 µg/mL during 10 hours of the incubation period. This reduction in TEER value may destroy the epithelial barrier of the Caco-2 cell monolayers, which could cause cytotoxicity in the cells and damage the barrier function of the epithelium. In comparison with the control, 0.1 µg/mL had the highest TEER over the 24 hours of incubation, thereby, expressing the tight junction barrier across the cell monolayers. The control had a TEER value above 1100 Ω/cm^2, which indicated that the differentiated Caco-2 cells had tight junctions and an intact monolayer suitable for diffusion.

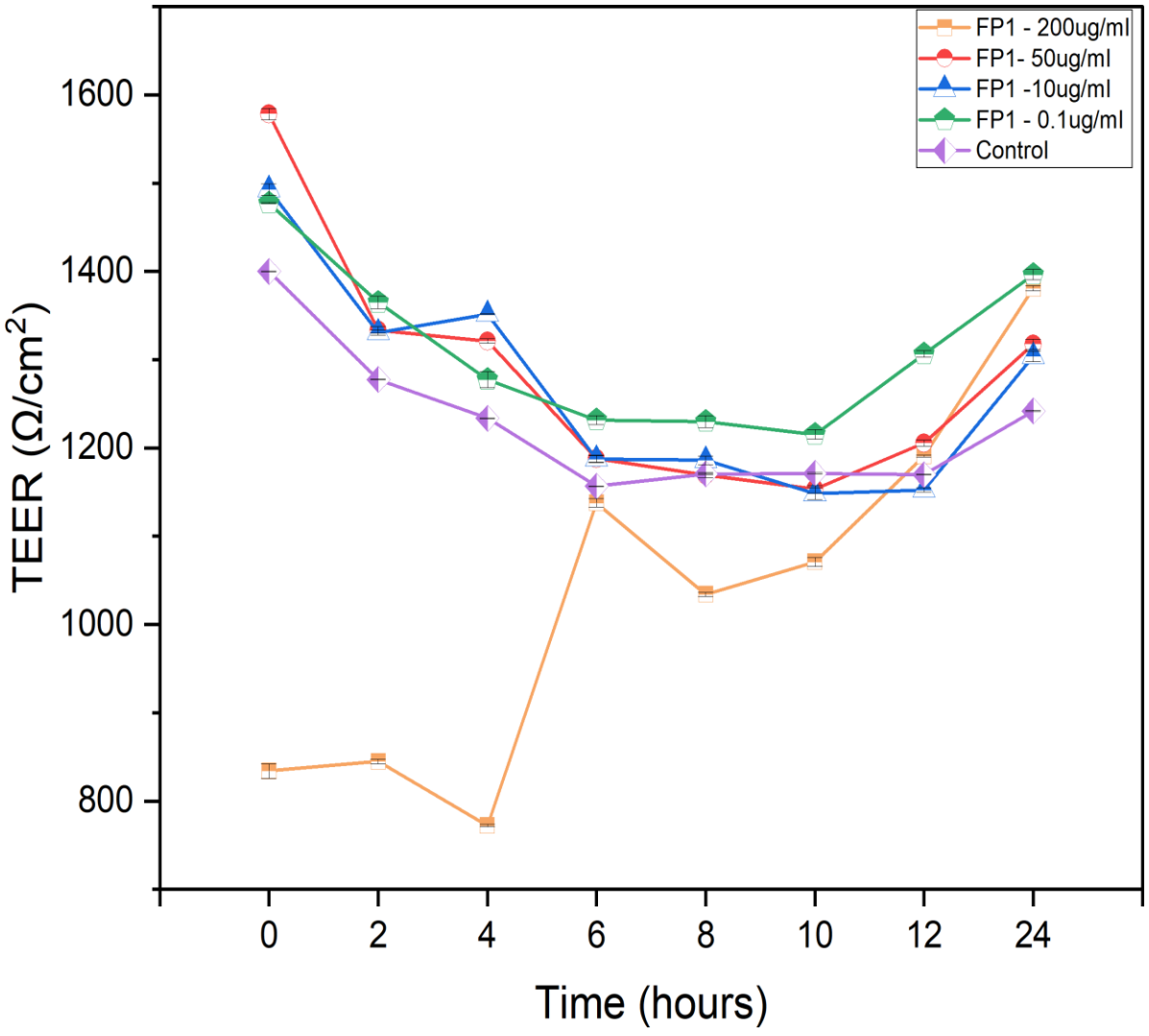

Figure 4.8. Transepithelial electrical resistance (TEER) of differentiated/polarized Caco-2 cells monolayer after every two hours with digested banana-flavoured milk containing FlavoPlus 1 (FP1) over a 24-hour incubation period. **Note:** Data represents the mean of two biological replicates with three replicates in each assay. Error bars correspond to the standard error of the mean.

At concentrations of 10 µg/mL and 50 µg/mL, the TEER values were similar, although there was a reduction in values between 4 and 8 hours of the incubation period. This reduction in TEER values could be due to the diffusion of the larger particles such as digestive enzymes, bile salts, and milk proteins from the digesta, which were bound to FP1, to penetrate through the monolayers causing a barrier disruption. The effectiveness of these two concentrations (i.e., 10 µg/mL and 50 µg/mL) after 24 hours of incubation suggest that tight junctions of the monolayers are intact, which can facilitate diffusion of FP1.

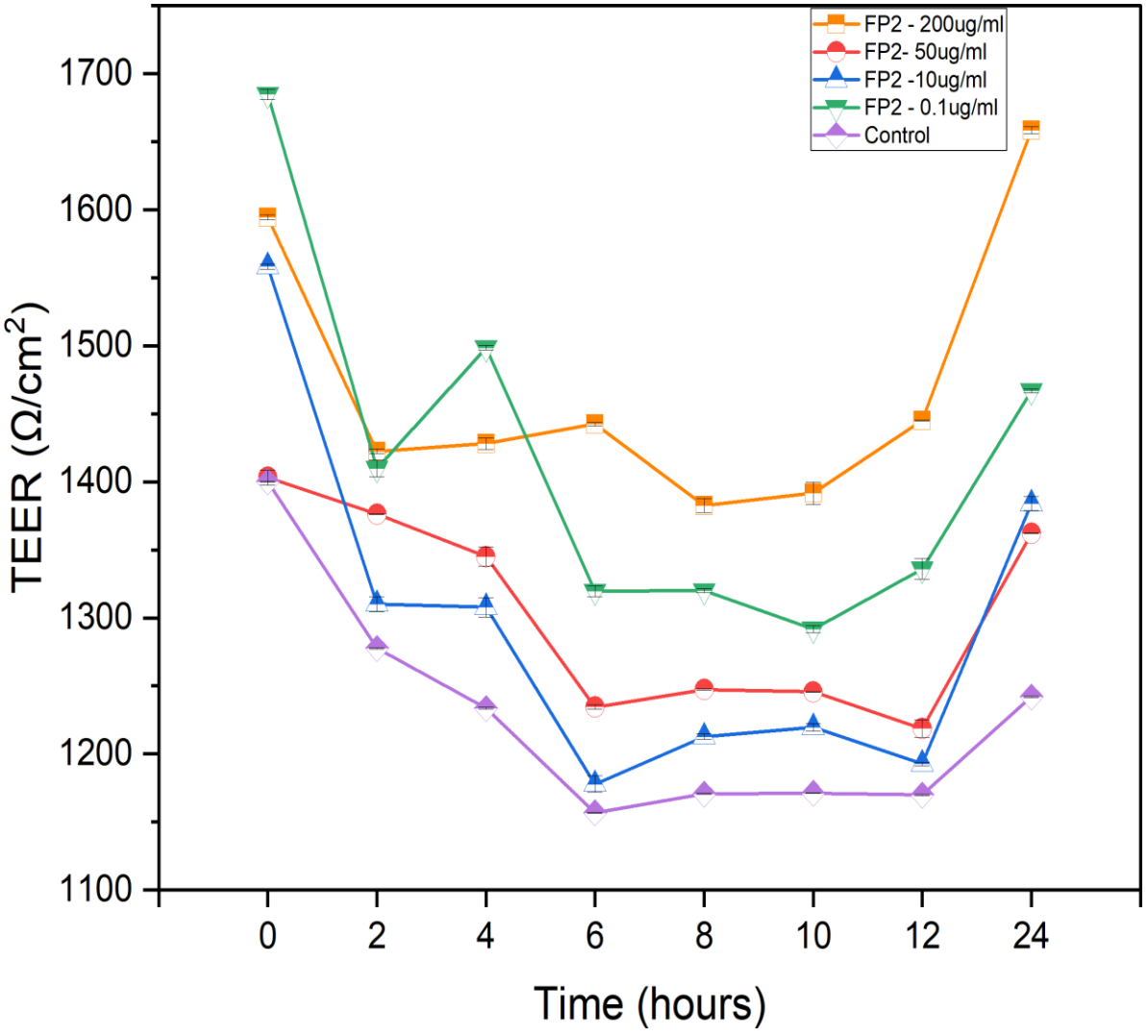

Figure 4.9. Transepithelial electrical resistance (TEER) of the differentiated Caco-2 cells monolayer after every two hours with digested banana-flavoured milk fortified with FlavoPlus 2 (FP2) over a 24-hour incubation period. **Note:** Data represents the mean of two biological replicates with three replicates in each assay. Error bars correspond to the standard error of the mean.

As FP2 was subjected to the differentiated Caco-2 cells for 24 hours, at the lowest concentration of 0.1 µg/mL the TEER value was the highest when compared with control for 4 hours of incubation. Nonetheless, as shown in Figure 4.9, there was a gradual increase in TEER value at 200 µg/mL concentration after 2 hours of incubation, which maintains the barrier integrity of the monolayers even at the highest concentration in comparison to the lower concentrations of FP2 (e.g., 10 µg/mL and 50 µg/mL), showed higher TEER values for 24 hours. These observations suggest that there might be an uptake of FP2 even at the highest concentration of 200 µg/mL during the 24 hours of incubation without disrupting the tight junctions that could help with facilitating the absorption/diffusion of rutin across the monolayers.

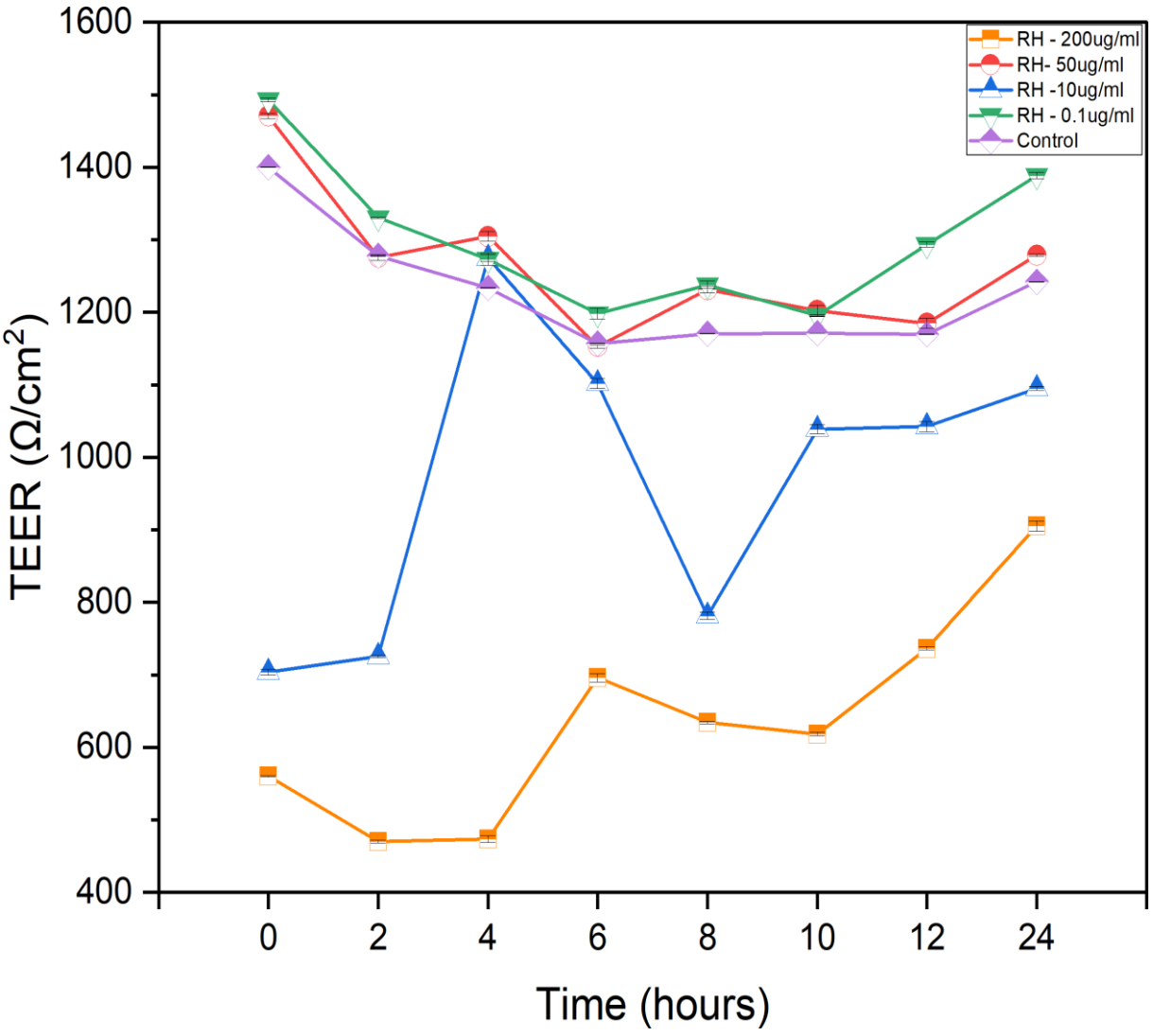

Figure 4.10. Transepithelial electrical resistance (TEER) of differentiated Caco-2 cells after every two hours with the digested banana-flavoured milk fortified with rutin hydrate (RH) over a 24-hour incubation period. **Note:** Data represents the mean of two biological replicates with three replicates in each assay. Error bars correspond to the standard error of the mean.

The barrier integrity of Caco-2 cell monolayers was maintained over 24 hours of incubation period after digested milk containing FP1 and FP2 was incubated with cells. Even if disruption of the tight junction was only observed for highly concentrated FP1 digesta at 200 µg/mL, which could indicate its cytotoxic effect on monolayers at high concentrations. The effect of digested milk containing RH on barrier integrity of Caco-2 cells monolayers was shown in Figure 4.10, the control was above the baseline of TEER value (1100 Ω/cm^2) suggesting a healthy and differentiated monolayer. As discussed previously in Section 4.2.1, RH was not completely dispersible during the incorporation into the dairy beverage, which resulted in a loss throughout the *in vitro* digestion. As observed in Figure 4.10, RH at a concentration of 200 µg/mL had the lowest TEER value ranging from 570 Ω/cm^2 to 900 Ω/cm^2 within 24 hours of incubation period in comparison to the control. Due to its low TEER values, the barrier integrity of the monolayers is obstructed resulting in a leaky epithelium, which makes it less likely for uptake of rutin to happen during absorption.

The low doses of RH (0.1 µg/mL and 50 µg/mL) that maintained the TEER value above 1200 Ω/cm^2 suggest that RH at low amounts might be digested rapidly by digestive enzymes in the GIT. Accordingly, this can reduce the amount of rutin present in the matrix before it reaches the epithelium barrier for absorption. However, in the case of a higher dose of 10 µg/mL, the TEER values were drastically reduced from 1200 Ω/cm^2 to 800 Ω/cm^2 during the incubation period of 2 to 8 hours. Taken together, these results suggest that owing to the hydrophilic nature of FP1 and FP2, they maintained barrier integrity even at higher concentrations. Whereas, RH resulted in reduced barrier integrity at higher concentrations, which could be due to the cytotoxic effects of the digestive enzymes and bile salts.

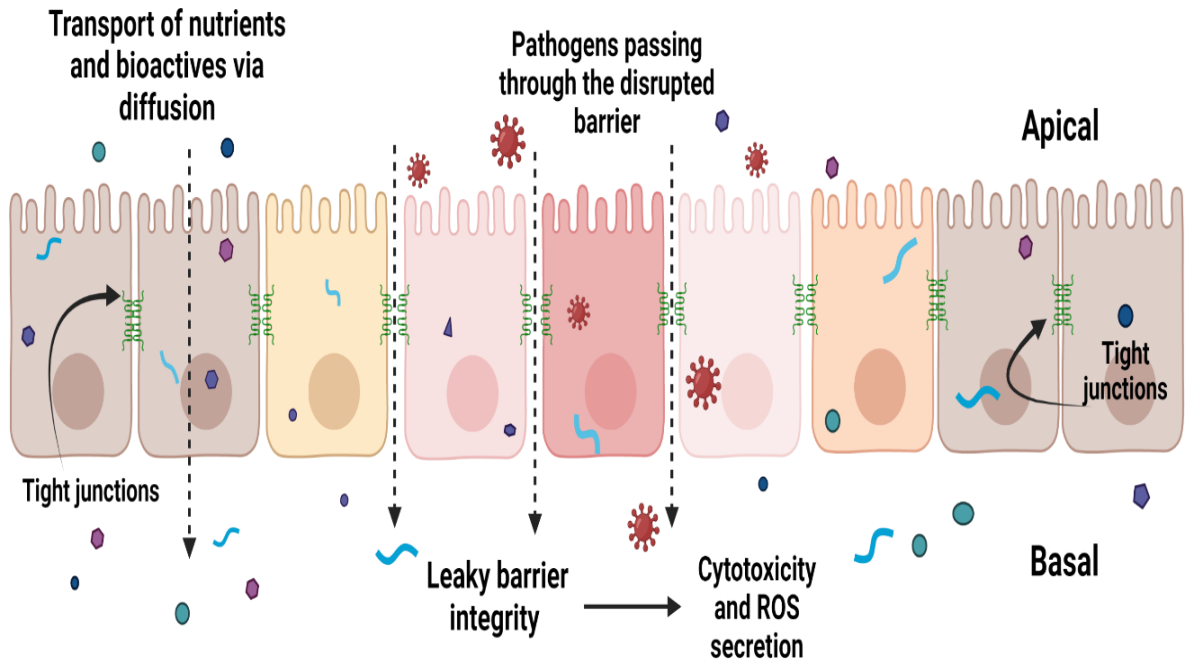

Figure 4.11. A schematic representation of the mechanism of absorption of Caco-2 cell monolayer. (Created with BioRender)

4.2.4. Cytotoxic effects of digested rutin composites vs rutin hydrate on Caco-2 cells

Based on the optimised concentration of FP1, FP2, and RH in Section 4.1.3, the cell viability at a concentration of 0.1 µg/mL after 4 hours of incubation was 80%. As shown in Figure 4.12, the digested milk containing FP1, FP2, and RH was investigated for cell viability through an MTT assay. The cell viability for digested milk containing FP1, FP2, and RH was expressed relative to the control, which was at 100%. At 0.1 µg/mL concentration, FP2 had the highest proliferation of cells >80% when compared to FP1 and RH. The amount of rutin present in the three samples after *in vitro* digestion would be lower in comparison to the amount present before digestion, which could result in increased cell viability. Though, as all three samples (i.e., FP1, FP2, and RH) were subjected to digestive enzymes and bile salts, it could induce cytotoxicity to the cells even at lower concentrations.

At 0.5 µg/mL concentration, FP1 and FP2 were statistically similar but there was a reduction in cell viability (<80%). Meanwhile, RH inhibited the proliferation of Caco-2 cells by having lower viability (<70%) at the same concentration, which could be due to its insoluble-bound form during digestion. The interactions between the food matrix and digestive enzymes could

also be responsible for reducing the cell viability of Caco-2 cells. This anti-proliferative effect was observed in Figure 4.12 for higher concentrations such as 15 µg/mL and 25 µg/mL, where FP1, FP2, and RH were not significantly different ($p>0.05$), but RH had the lowest cell viability (<70%). Increasing the concentrations of both FP1 and FP2 decreased the cell viability, but in comparison to RH values, they had lower cytotoxic potential on Caco-2 cells over 4 hours of the incubation period.

Gera et al. (2020) suggested 0.5 µg/mL as the safe concentration of rutin nanosuspension, as it maintained the cell viability of human osteosarcoma cells (MG-63). However, at a lower concentration of 0.3 µg/mL, there was a reduction in cell viability, which contrasts with the results observed in the current study, where 0.1 µg/mL was considered a safer concentration for digested milk containing rutin-casein composites. A research study by Olejnik et al. (2016) also reported that digested purple carrot extracts reduced cell viability with an increase in concentration on normal human colon epithelial cells (NCM460). These results demonstrate that both FP1 and FP2 had a similar effect on Caco-2 cells, which could be due to their structural modification, as rutin was protected by NaCas in these products, which most likely reduced the hydrophobicity, increased the solubility, and enhanced the bioaccessibility of rutin within the GIT thereby making it more bioavailable and less toxic than pure RH.

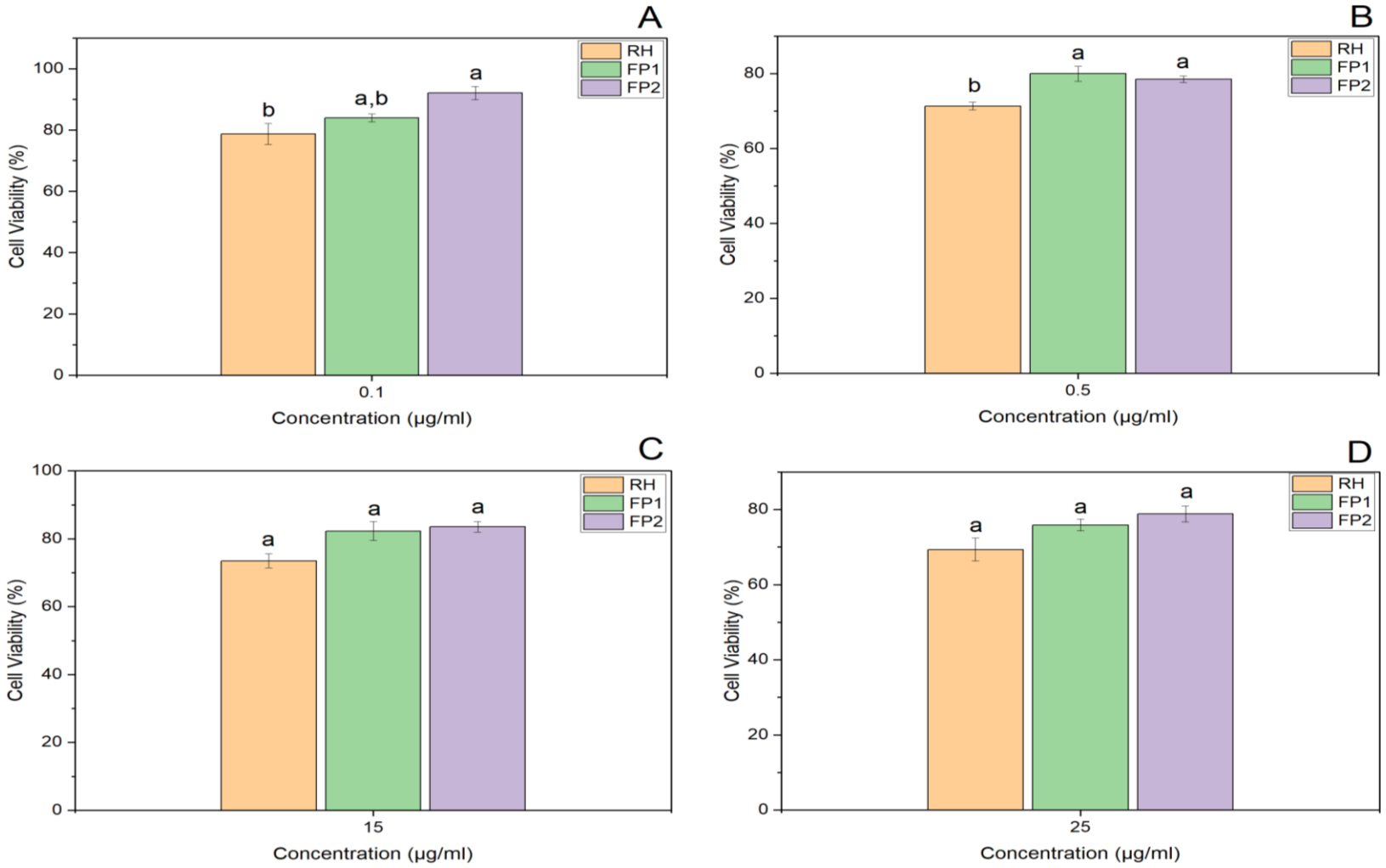

Figure 4.12. The effect of digested banana-flavoured milk fortified with FlavoPlus1 (FP1) and FlavoPlus2 (FP2) vs rutin hydrate (RH) on the viability of Caco-2 cells. **Note: A,B,C,D** represent different concentrations in the assay Data represents the mean of four biological replicates with three replicates in each assay. Error bars correspond to the standard error of the mean. Samples that do not share the same letters are significantly different ($p \leq 0.05$).

4.2.5. The *in vitro* intracellular antioxidant activity of digested rutin composites vs rutin hydrate on differentiated Caco-2 cells

The intracellular antioxidant activity of rutin-protein composites before being incorporated into milk was evaluated on Caco-2 cells in Section 4.1.5, where FP1 and FP2 showed higher antioxidant activity at the 0.5 µg/mL concentration during 0 and 10 minutes of the incubation period. However, with increasing the concentration and incubation time, there was a decrement in the intracellular antioxidant activity as shown in Figure 4.5.

In this section, the intracellular antioxidant activity of digested milk containing FP1, FP2, and RH over the 60 minutes of incubation was assessed on the differentiated Caco-2 cells using the same concentration range to investigate whether more bioaccessible rutin in both composites (i.e., FP1, FP2) exhibited stronger antioxidant activity as compared to pure RH.

As shown in Figure 4.13, at 0 minute of the incubation period, the fluorescence (%) was highest when compared to 10, 30, and 60 minutes. In the case of 0.5 µg/mL concentration, RH had the lowest antioxidant activity as the fluorescence (%) was highest which shows its less quenching ability against AAPH-induced ROS. The antioxidant effect of digested milk containing FP1 and FP2 against induced ROS was higher than RH by 30% at 0.5 µg/mL. A similar effect was observed at 25 µg/mL, where FP2 was significantly ($p<0.05$) more effective than both FP1 and RH. As Figure 5.5 shows that at the higher dose of 50 µg/mL, the digested RH was significantly lower ($p>0.05$) in reducing oxidative stress. At the maximum concentration of 200 µg/mL, all three digested milk samples were high in terms of quenching the ROS and indicating their antioxidant potency, but the effect was statistically non-significant ($p>0.05$).

After 10 minutes of incubation with AAPH, at 0.5 µg/mL, RH had the lowest antioxidant activity in comparison to FP1 and FP2 moreover, a similar trend was observed at 25 µg/mL concentration. As concentration was increased from 25 µg/mL to 50 µg/mL, RH was ineffective in inhibiting ROS production after 10 minutes of incubation. However, at the 200 µg/mL concentration, all three samples, including RH, FP1, and FP2, were statistically insignificant ($p>0.05$) but their antioxidant potency was higher than the 50 µg/mL concentration. As incubation time increased from 10 to 30 minutes, at the 0.5 µg/mL concentration, there was no significant difference ($p>0.05$) between the two time points. Thus,

this indicates that lower concentrations for the digested milk containing RH, FP1, and FP2 were ineffective against inhibiting oxidative stress in the induced differentiated Caco-2 cells.

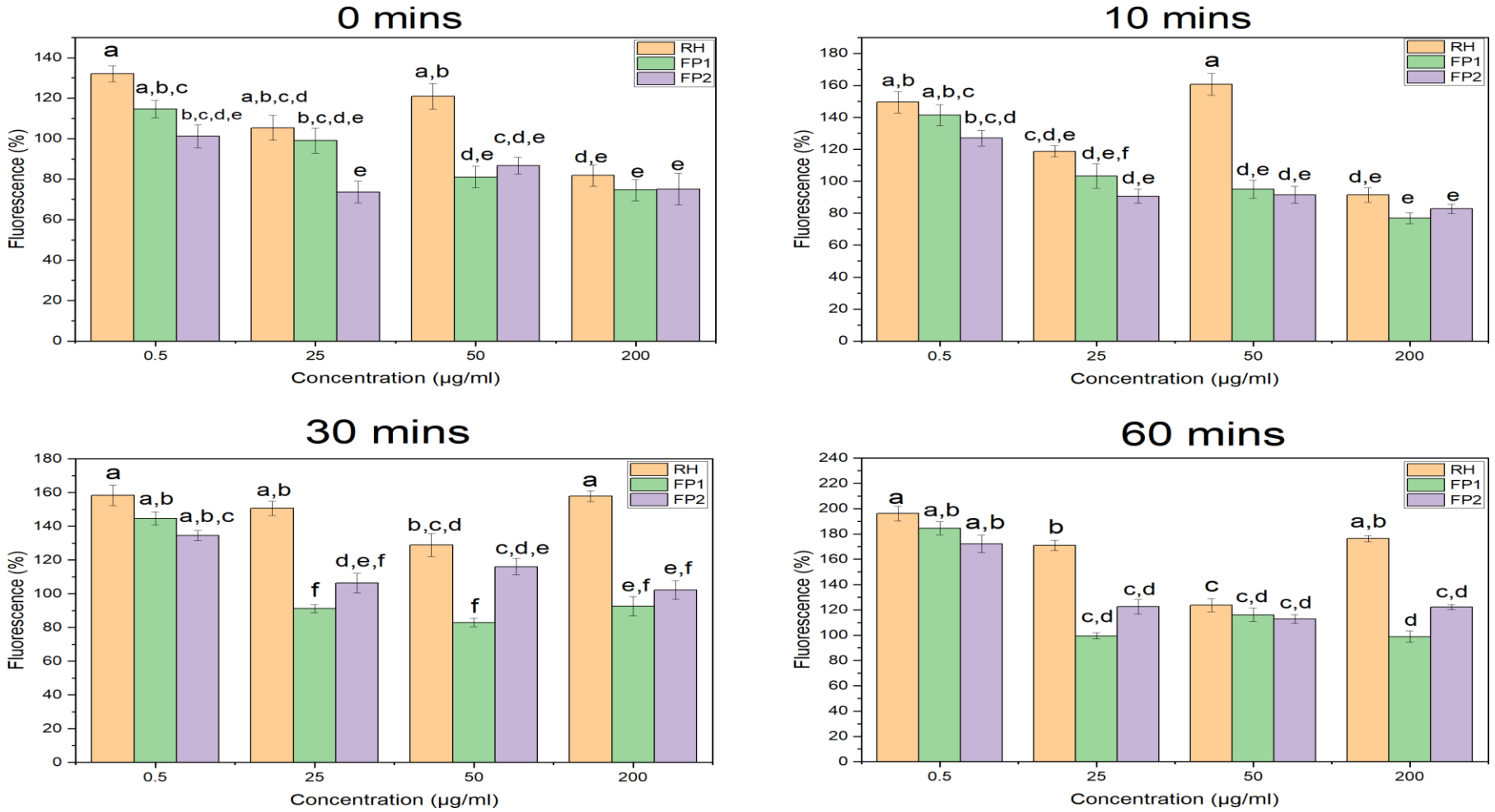

Figure 4.13. The effect of digested banana-flavoured milk fortified with FlavoPlus1 (FP1) and FlavoPlus2 (FP2) vs rutin hydrate (RH) on intracellular antioxidant activity over 60 minutes in the differentiated Caco-2 cells. Intracellular antioxidant activity was quantified with DCFH-DA assay using relative fluorescence values of the samples. **Note:** Data represents the mean of three biological replicates with three replicates in each assay. Error bars correspond to the standard error of the mean. Samples that do not share the same letters are significantly different ($p \leq 0.05$).

The scavenging activity exhibited by digested milk containing FP1 and FP2 was higher than that the digested milk containing RH at 25, 50, and 200 µg/mL as RH was significantly lower at exhibiting antioxidant potency at these three concentrations, respectively. But, with increasing the incubation time from 30 to 60 minutes, FP1 exhibited higher intracellular antioxidant potency by ameliorating ROS by 40%, when compared to FP2. The higher antioxidant potency of FP1 could be due to a higher amount (46%) of rutin being present in the digested milk, while FP2 had a lower rutin content (27.3%). On the contrary, digested milk containing RH was significantly lower ($p>0.05$) at scavenging ROS attributed to its lower antioxidant potency. This could be due to the low dispersibility of RH during the fortification of milk, which resulted in lowering the amount of rutin present in the digested milk containing RH, thus, reducing its functional attribute as a radical scavenger.

As demonstrated in Figure 4.13, after incubating Caco-2 cells with digested milk containing FP1, FP2, and RH for 60 minutes, the fluorescence intensity was not reduced significantly ($p>0.05$). Instead, there was a spike in fluorescence (%) for all three samples when compared with 30 minutes of incubation. As discussed previously in Section 4.1.5, the efficiency of the DCFH-DA fluorescent probe after 30 minutes of incubation was reduced, and the cellular uptake of the dye occurs within 15-20 minutes of the reaction (Wolfe & Liu, 2007). Therefore, at 60 minutes of the incubation period, rutin-protein composites exhibited less antioxidant activity when compared with 30 minutes of the incubation period, indicating it as an endpoint for incubating Caco-2 cells with bioactives.

4.2.6. Summary

The current section focussed on incorporating the novel rutin-protein composites (FP1 and FP2) and rutin hydrate (RH) in a dairy beverage, which was digested by an *in vitro* gastrointestinal model and studied for the effect on its physicochemical characteristics and bioaccessibility of rutin. In addition, the cellular functionality and bioactivity of digesta were assessed through the *in vitro* TEER assay and intracellular antioxidant measurement. Physicochemical analysis showed the milk containing FP2 had a bigger particle size than FP1 during both gastric and intestinal phases of digestion, thereby reducing the surface area. This could be due to the aggregation of sodium caseinate after the breakdown of the protein complex and the release of casein from the food matrix under highly alkaline conditions. Whereas RH showed a decreasing trend in particle size from the gastric phase to the intestinal phase, which could attribute to its low dispersibility in the food matrix, thereby resulting in a higher surface area than FP1 and FP2.

At the end of the simulated intestinal digestion, the bioaccessibility of FP1 and FP2 was around 63% and 45%, respectively. When the intestinal phase was over, the loss from the initial time point was compared with the final time point; FP1 showed a loss of 16-18% whereas FP2 resulted in only a 3-4% loss, suggesting its likely higher bioaccessibility and better absorption in the small intestine. This could be due to the different structures as these composites have been manufactured using different technologies.

The digested milk containing rutin composites (i.e., FP1 and FP2) maintained higher cell viability when compared with RH. Consequently, the TEER assay confirmed that FP2 was strongest, closely followed by FP1 in maintaining barrier integrity over 24 hours of incubation even at the lowest concentration. Therefore, based on these results, as expected, FP2 exhibited higher ROS scavenging activity than FP1 and RH during 0 and 10 minutes of incubation. However, with the increase in the incubation time at 30 and 60 minutes, FP1 showed higher efficiency in scavenging ROS at a higher concentration of 25 µg/mL due to a higher amount of rutin being present in digested milk containing FP1.

Conclusion and Future Perspectives

5.1. Conclusion

The current study determined the physicochemical and functional characteristics of the novel rutin-protein composites (FP1 and FP2) and rutin hydrate (RH) by utilising *in vitro* gastrointestinal digestion and *in-vitro* cell models. The antioxidant potency, cytotoxicity, and bioaccessibility of the samples were evaluated through a functional dairy matrix.

The DPPH assay of antioxidant potency in FP1 and FP2 demonstrated a significantly ($p<0.05$) higher efficiency in scavenging free radicals compared to RH. It is worth noting that FP1, FP2, and RH were maintaining higher cell viability before subjecting them in a digestion model. After utilising the *in vitro* gastrointestinal model on FP1, FP2, and RH through a milk matrix, a reduction of 20% in cell viability was observed. The intracellular antioxidant activity of FP1 and FP2 was reduced by 40% after digestion, but their potency to scavenge ROS was significantly ($p<0.05$) higher than RH. This suggests that the addition of digestive enzymes, bile salts, and aggregation of milk proteins from the matrix attribute to cytotoxicity in cells.

The interactions between rutin and the milk matrix during digestion suggest that rutin was protected during the gastric phase thereby, resulting in a higher bioaccessibility. The absorption of rutin across Caco-2 cells monolayers for FP1 and FP2 was comparable for concentrations up to 50 µg/mL. However, increasing the concentration to 200 µg/mL resulted in a sharp decrease in absorption for FP1 while it remained unchanged for FP2. It suggests that FP2 maintains barrier integrity of Caco-2 cell monolayers even at higher concentrations.

Taken together, the results of this study suggested that both FP1 and FP2 were highly digestible and bioaccessible compared to RH, with superior intracellular antioxidant activity. These features, along with the fact that FP1 and FP2 are highly soluble, make them competitive candidates for fortifying food products in order to provide corresponding health-promoting properties to consumers.

5.2. Future perspectives and recommendations

The following recommendations are suggested for future studies:

- In this study, FP1 and FP2 showed protective effects even at the lowest concentrations in Caco-2 cells under oxidative stress. However, it is important to investigate this protective effect of FP1 and FP2 by understanding the underlying mechanisms of action through different biomarkers for inflammatory responses such as NF-κB, IL-6, IL-8, IL-10, and MAP kinases.
- To validate the bioaccessibility of rutin in the digested milk containing FP1 and FP2 through an *in vivo* model, it is recommended that the bioavailability of the novel rutin-protein composites be studied in human subjects. This may also be attributed to other hydrophobic polyphenols that can be delivered using the FlavoPlus technology.

References

Acevedo-Fani, A., Ochoa-Grimaldo, A., Loveday, S. M., & Singh, H. (2021). Digestive dynamics of yoghurt structure impacting the release and bioaccessibility of the flavonoid rutin. *Food Hydrocolloids*, *111*, 106215.

Afanas'eva, I. B., Ostrakhovitch, E. A., Mikhal'chik, E. V., Ibragimova, G. A., & Korkina, L. G. (2001). Enhancement of antioxidant and anti-inflammatory activities of bioflavonoid rutin by complexation with transition metals. *Biochemical pharmacology*, *61*(6), 677-684.

Albu, E., Lupascu, D., Cristiana, F., Jaba, I., & Zamosteanu Filip, N. (2013). The influence of a new rutin derivative on homocysteine, cholesterol and total antioxidative status in experimental diabetes in rat. *Farmacia*, *61*, 1167-1177.

Alexander, A., Patel, R. J., Saraf, S., & Saraf, S. (2016). Recent expansion of pharmaceutical nanotechnologies and targeting strategies in the field of phytopharmaceuticals for the delivery of herbal extracts and bioactives. *Journal of controlled release*, *241*, 110-124.

Alía, M., Mateos, R., Ramos, S., Lecumberri, E., Bravo, L., & Goya, L. (2006). Influence of quercetin and rutin on growth and antioxidant defense system of a human hepatoma cell line (HepG2). *European Journal of Nutrition*, *45*(1), 19-28.

Altıok, E., Bayçın, D., Bayraktar, O., & Ülkü, S. (2008). Isolation of polyphenols from the extracts of olive leaves (Olea europaea L.) by adsorption on silk fibroin. *Separation and Purification Technology*, *62*(2), 342-348.

Asgary, S., Naderi, G., Sarrafzadegan, N., Ghassemi, N., Boshtam, M., Rafie, M., & Arefian, A. (1999). Anti-oxidant effect of flavonoids on hemoglobin glycosylation. *Pharmaceutica Acta Helvetiae*, *73*(5), 223-226.

Babazadeh, A., Ghanbarzadeh, B., & Hamishehkar, H. (2016). Novel nanostructured lipid carriers as a promising food grade delivery system for rutin. *Journal of Functional Foods*, *26*, 167-175.

Babazadeh, A., Ghanbarzadeh, B., & Hamishehkar, H. (2017). Phosphatidylcholine-rutin complex as a potential nanocarrier for food applications. *Journal of Functional Foods*, *33*, 134-141.

Barbé, F., Ménard, O., Le Gouar, Y., Buffière, C., Famelart, M.-H., Laroche, B., . . . Rémond, D. (2013). The heat treatment and the gelation are strong determinants of the kinetics of milk proteins digestion and of the peripheral availability of amino acids. *Food chemistry*, *136*(3-4), 1203-1212.

Batra, P., & Sharma, A. K. (2013). Anti-cancer potential of flavonoids: recent trends and future perspectives. *3 Biotech*, *3*(6), 439-459.

Ben Sghaier, M., Pagano, A., Mousslim, M., Ammari, Y., Kovacic, H., & Luis, J. (2016). Rutin inhibits proliferation, attenuates superoxide production and decreases adhesion and migration of human cancerous cells. *Biomedicine & Pharmacotherapy*, *84*, 1972-1978.

Benavente-García, O., Castillo, J., Marin, F. R., Ortuño, A., & Del Río, J. A. (1997). Uses and Properties of Citrus Flavonoids. *Journal of Agricultural and Food Chemistry*, *45*(12), 4505-4515.

Bordenave, N., Hamaker, B. R., & Ferruzzi, M. G. (2014). Nature and consequences of non-covalent interactions between flavonoids and macronutrients in foods. *Food & Function*, *5*(1), 18-34.

Boyle, S., Dobson, V., Duthie, S. J., Hinselwood, D., Kyle, J., & Collins, A. (2000). Bioavailability and efficiency of rutin as an antioxidant: a human supplementation study. *European Journal of Clinical Nutrition*, *54*(10), 774-782.

Brolis, M., Gabetta, B., Fuzzati, N., Pace, R., Panzeri, F., & Peterlongo, F. (1998). Identification by high-performance liquid chromatography–diode array detection–mass spectrometry and quantification by high-performance liquid chromatography–UV absorbance detection of active constituents of Hypericum perforatum. *Journal of Chromatography A*, *825*(1), 9-16.

Buchner, N., Krumbein, A., Rohn, S., & Kroh, L. W. (2006). Effect of thermal processing on the flavonols rutin and quercetin. *Rapid Communications in Mass Spectrometry, 20*(21), 3229-3235.

Bucić-Kojić, A., Planinić, M., Tomas, S., Bilić, M., & Velić, D. (2007). Study of solid–liquid extraction kinetics of total polyphenols from grape seeds. *Journal of Food Engineering, 81*(1), 236-242.

Bureau, S., Renard, C. M., Reich, M., Ginies, C., & Audergon, J.-M. (2009). Change in anthocyanin concentrations in red apricot fruits during ripening. *LWT-Food Science and Technology, 42*(1), 372-377.

Celik, S. E., Özyürek, M., Güçlü, K., & Apak, R. (2015). Antioxidant capacity of quercetin and its glycosides in the presence of β-cyclodextrins: influence of glycosylation on inclusion complexation. *Journal of inclusion phenomena and macrocyclic chemistry, 83*(3), 309-319.

Chat, O. A., Najar, M. H., & Dar, A. A. (2013). Evaluation of reduction kinetics of 2,2-diphenyl-1-picrylhydrazyl radical by flavonoid glycoside Rutin in mixed solvent based micellar media. *Colloids and Surfaces A: Physicochemical and Engineering Aspects, 436*, 343-353.

Chen, S., Han, Y., Jian, L., Liao, W., Zhang, Y., & Gao, Y. (2020). Fabrication, characterization, physicochemical stability of zein-chitosan nanocomplex for co-encapsulating curcumin and resveratrol. *Carbohydrate Polymers, 236*, 116090.

Chua, L. S. (2013). A review on plant-based rutin extraction methods and its pharmacological activities. *Journal of ethnopharmacology, 150*(3), 805-817.

Clifford, M. N. (2000). Anthocyanins–nature, occurrence and dietary burden. *Journal of the Science of Food and Agriculture, 80*(7), 1063-1072.

Corrales, M., García, A. F., Butz, P., & Tauscher, B. (2009). Extraction of anthocyanins from grape skins assisted by high hydrostatic pressure. *Journal of Food Engineering, 90*(4), 415-421.

da Silva, A. B., Cerqueira Coelho, P. L., das Neves Oliveira, M., Oliveira, J. L., Oliveira Amparo, J. A., da Silva, K. C., . . . Costa, S. L. (2020). The flavonoid rutin and its aglycone quercetin modulate the microglia inflammatory profile improving antiglioma activity. *Brain, behavior, and immunity*, *85*, 170-185.

Dammak, I., & do Amaral Sobral, P. J. (2017). Formulation and stability characterization of rutin-loaded oil-in-water emulsions. *Food and Bioprocess Technology*, *10*(5), 926-939.

Das, M. K., & Kalita, B. (2014). Design and evaluation of phyto-phospholipid complexes (phytosomes) of rutin for transdermal application. *Journal of applied pharmaceutical science*, *4*(10), 051-057.

de Araújo, M. E. M. B., Franco, Y. E. M., Alberto, T. G., Sobreiro, M. A., Conrado, M. A., Priolli, D. G., . . . de Oliveira Carvalho, P. (2013). Enzymatic de-glycosylation of rutin improves its antioxidant and antiproliferative activities. *Food chemistry*, *141*(1), 266-273.

Deineka, V. I., Grigor'ev, A., & Staroverov, V. (2004). HPLC analysis of flavonoids: determining rutin in plant extracts. *Pharmaceutical Chemistry Journal*, *38*(9), 487-489.

Dey, T. K., Koley, H., Ghosh, M., Dey, S., & Dhar, P. (2019). Effects of nano-sizing on lipid bioaccessibility and ex vivo bioavailability from EPA-DHA rich oil in water nanoemulsion. *Food chemistry*, *275*, 135-142.

Dima, C., Assadpour, E., Dima, S., & Jafari, S. M. (2020). Bioactive-loaded nanocarriers for functional foods: from designing to bioavailability. *Current Opinion in Food Science*, *33*, 21-29.

Dima, C., & Dima, S. (2020). Bioaccessibility study of calcium and vitamin D3 co-microencapsulated in water-in-oil-in-water double emulsions. *Food chemistry*, *303*, 125416.

Erlund, I., Kosonen, T., Alfthan, G., Mäenpää, J., Perttunen, K., Kenraali, J., . . . Aro, A. (2000). Pharmacokinetics of quercetin from quercetin aglycone and rutin in healthy volunteers. *European Journal of Clinical Pharmacology*, *56*(8), 545-553.

Fabjan, N., Rode, J., Košir, I. J., Wang, Z., Zhang, Z., & Kreft, I. (2003). Tartary buckwheat (Fagopyrum tataricum Gaertn.) as a source of dietary rutin and quercitrin. *Journal of Agricultural and Food Chemistry*, *51*(22), 6452-6455.

Fathiazad, F., Delazar, A., Amiri, R., & Sarker, S. D. (2010). Extraction of flavonoids and quantification of rutin from waste tobacco leaves. *Iranian Journal of Pharmaceutical Research*(3), 222-227.

Frutos, M. J., Rincón-Frutos, L., & Valero-Cases, E. (2019). Chapter 2.14 - Rutin. In S. M. Nabavi & A. S. Silva (Eds.), *Nonvitamin and Nonmineral Nutritional Supplements* (pp. 111-117). Academic Press.

Ganeshpurkar, A., & Saluja, A. K. (2017). The Pharmacological Potential of Rutin. *Saudi Pharmaceutical Journal*, *25*(2), 149-164.

Gangwar, M., Gautam, M. K., Sharma, A. K., Tripathi, Y. B., Goel, R. K., & Nath, G. (2014). Antioxidant Capacity and Radical Scavenging Effect of Polyphenol Rich Mallotus philippenensis Fruit Extract on Human Erythrocytes: An In Vitro Study. *The Scientific World Journal*, *2014*, 279451.

Garcia, G., Nanni, S., Figueira, I., Ivanov, I., McDougall, G. J., Stewart, D., . . . Brites, D. (2017). Bioaccessible (poly) phenol metabolites from raspberry protect neural cells from oxidative stress and attenuate microglia activation. *Food chemistry*, *215*, 274-283.

Gera, S., Pooladanda, V., Godugu, C., Swamy Challa, V., Wankar, J., Dodoala, S., & Sampathi, S. (2020). Rutin nanosuspension for potential management of osteoporosis: effect of particle size reduction on oral bioavailability, in vitro and in vivo activity. *Pharmaceutical Development and Technology*, *25*(8), 971-988.

Ghiasi, M., Azadnia, A., Arabieh, M., & Zahedi, M. (2012). Protective effect of rutin (vitamin p) against heme oxidation: a quantum mechanical approach. *Computational and Theoretical Chemistry*, *996*, 28-36.

Gimenez-Bastida, J. A., & Zielinski, H. (2015). Buckwheat as a functional food and its effects on health. *Journal of agricultural and food chemistry*, *63*(36), 7896-7913.

Glavač, N. K., Stojilkovski, K., Kreft, S., Park, C. H., & Kreft, I. (2017). Determination of fagopyrins, rutin, and quercetin in Tartary buckwheat products. *LWT-Food Science and Technology*, *79*, 423-427.

Granja, A., Neves, A. R., Sousa, C. T., Pinheiro, M., & Reis, S. (2019). EGCG intestinal absorption and oral bioavailability enhancement using folic acid-functionalized nanostructured lipid carriers. *Heliyon*, *5*(7), e02020.

Gullón, B., Lú-Chau, T. A., Moreira, M. T., Lema, J. M., & Eibes, G. (2017). Rutin: A review on extraction, identification and purification methods, biological activities and approaches to enhance its bioavailability. *Trends in food science & technology*, *67*, 220-235.

Gutiérrez, F. J., Albillos, S. M., Casas-Sanz, E., Cruz, Z., García-Estrada, C., García-Guerra, A., . . . González-Ferrero, C. (2013). Methods for the nanoencapsulation of β-carotene in the food sector. *Trends in food science & technology*, *32*(2), 73-83.

Hao, H.-h., Shao, Z.-m., Tang, D.-q., Lu, Q., Chen, X., Yin, X.-x., . . . Chen, H. (2012). Preventive effects of rutin on the development of experimental diabetic nephropathy in rats. *Life Sciences*, *91*(19), 959-967.

He, Y., & Zeng, S. (2005). Transport characteristics of rutin deca (H-) sulfonate sodium across Caco-2 cell monolayers. *Journal of pharmacy and pharmacology*, *57*(10), 1297-1303.

Helal, A., & Tagliazucchi, D. (2018). Impact of in-vitro gastro-pancreatic digestion on polyphenols and cinnamaldehyde bioaccessibility and antioxidant activity in stirred cinnamon-fortified yogurt. *LWT*, *89*, 164-170.

Hendler, S. S., & Rorvik, D. M. (2008). *PDR for nutritional supplements*. Thomson Reuters.

Hollebeeck, S., Raas, T., Piront, N., Schneider, Y.-J., Toussaint, O., Larondelle, Y., & During, A. (2011). Dimethyl sulfoxide (DMSO) attenuates the inflammatory response in the in vitro intestinal Caco-2 cell model. *Toxicology letters*, *206*(3), 268-275.

Hollman, P. C. H., & Katan, M. B. (1999). Dietary flavonoids: intake, health effects and bioavailability. *Food and chemical toxicology*, *37*(9-10), 937-942.

Horincar, G., Aprodu, I., Barbu, V., Râpeanu, G., Bahrim, G. E., & Stănciuc, N. (2019). Interactions of flavonoids from yellow onion skins with whey proteins: Mechanisms of binding and microencapsulation with different combinations of polymers. *Spectrochimica Acta Part A: Molecular and Biomolecular Spectroscopy*, *215*, 158-167.

Hussain, M. B., Hassan, S., Waheed, M., Javed, A., Farooq, M. A., & Tahir, A. (2019). Bioavailability and metabolic pathway of phenolic compounds. In *Plant Physiological Aspects of Phenolic Compounds*. IntechOpen.

Iacopini, P., Baldi, M., Storchi, P., & Sebastiani, L. (2008). Catechin, epicatechin, quercetin, rutin and resveratrol in red grape: Content, in vitro antioxidant activity and interactions. *Journal of Food Composition and Analysis*, *21*(8), 589-598.

Ignat, I., Volf, I., & Popa, V. I. (2011). A critical review of methods for characterisation of polyphenolic compounds in fruits and vegetables. *Food Chemistry*, *126*(4), 1821-1835.

Jain, S., Dhanotiya, C., & Malviya, N. (2012). Physicochemical characterization and determination of free radical scavenging activity of rutin-phospholipid complex. *International Journal of Pharmaceutical Sciences and Research*, *3*(3), 909.

Jiang, Q., Zhang, H., Yang, R., Hui, Q., Chen, Y., Mats, L., . . . Yang, C. (2019). Red-osier dogwood extracts prevent inflammatory responses in Caco-2 cells and a Caco-2 BBe1/EA. hy926 cell co-culture model. *Antioxidants*, *8*(10), 428.

Jin, G.-Z., Yamagata, Y., & Tomita, K.-i. (1990). Structure of Rutin Pentamethanol. *CHEMICAL & PHARMACEUTICAL BULLETIN*, *38*(2), 297-300.

Kalinova, J., & Dadakova, E. (2009). Rutin and total quercetin content in amaranth (Amaranthus spp.). *Plant foods for human nutrition*, *64*(1), 68-74.

Kellett, M. E., Greenspan, P., & Pegg, R. B. (2018). Modification of the cellular antioxidant activity (CAA) assay to study phenolic antioxidants in a Caco-2 cell line. *Food chemistry*, *244*, 359-363.

Kidd, P., & Head, K. (2005). A review of the bioavailability and clinical efficacy of milk thistle phytosome: a silybin-phosphatidylcholine complex (Siliphos). *Alternative Medicine Review*, *10*(3).

Kim, G.-N., Kwon, Y.-I., & Jang, H.-D. (2011). Protective mechanism of quercetin and rutin on 2,2′-azobis(2-amidinopropane)dihydrochloride or Cu2+-induced oxidative stress in HepG2 cells. *Toxicology in Vitro*, *25*(1), 138-144.

Kim, K. H., Lee, K. W., Kim, D. Y., Park, H. H., Kwon, I. B., & Lee, H. J. (2005). Optimal recovery of high-purity rutin crystals from the whole plant of Fagopyrum esculentum Moench (buckwheat) by extraction, fractionation, and recrystallization. *Bioresource technology*, *96*(15), 1709-1712.

Knekt, P., Kumpulainen, J., Järvinen, R., Rissanen, H., Heliövaara, M., Reunanen, A., . . . Aromaa, A. (2002). Flavonoid intake and risk of chronic diseases. *The American journal of clinical nutrition*, *76*(3), 560-568.

Kumar, P., & Bhopal, A. K. P. (2012). Formulation design and evalution of rutin loaded selfemulsifying drug delivary system (SEDDs) using edible oil. *Asian Journal of Pharmaceutical and Clinical Research*, *5*(1), 76-78.

Kuntz, S., Wenzel, U., & Daniel, H. (1999). Comparative analysis of the effects of flavonoids on proliferation, cytotoxicity, and apoptosis in human colon cancer cell lines. *European Journal of Nutrition*, *38*(3), 133-142.

Kurisawa, M., Chung, J. E., Uyama, H., & Kobayashi, S. (2003). Enzymatic synthesis and antioxidant properties of poly (rutin). *Biomacromolecules*, *4*(5), 1394-1399.

Kyrø, C., Skeie, G., Loft, S., Overvad, K., Christensen, J., Tjønneland, A., & Olsen, A. (2013). Adherence to a healthy Nordic food index is associated with a lower incidence of colorectal cancer in women: the Diet, Cancer and Health cohort study. *Br J Nutr*, *109*(5), 920-927.

Lamothe, S., Azimy, N., Bazinet, L., Couillard, C., & Britten, M. (2014). Interaction of green tea polyphenols with dairy matrices in a simulated gastrointestinal environment. *Food & function*, *5*(10), 2621-2631.

Lau, T.-C., Chan, M.-W., Tan, H.-P., & Kwek, C.-L. (2012). Functional Food: A Growing Trend among the Health Conscious. *Asian Social Science*, *9*.

Lee, E.-R., Kang, G.-H., & Cho, S.-G. (2007). Effect of flavonoids on human health: old subjects but new challenges. *Recent patents on biotechnology*, *1*(2), 139-150.

Lee, W., Ku, S.-K., & Bae, J.-S. (2012). Barrier protective effects of rutin in LPS-induced inflammation in vitro and in vivo. *Food and chemical toxicology*, *50*(9), 3048-3055.

Liu, E.-H., Qi, L.-W., Cao, J., Li, P., Li, C.-Y., & Peng, Y.-B. (2008). Advances of modern chromatographic and electrophoretic methods in separation and analysis of flavonoids. *Molecules*, *13*(10), 2521-2544.

Liu, F., Ma, C., Zhang, R., Gao, Y., & McClements, D. J. (2017). Controlling the potential gastrointestinal fate of β-carotene emulsions using interfacial engineering: Impact of coating lipid droplets with polyphenol-protein-carbohydrate conjugate. *Food chemistry*, *221*, 395-403.

Liu, M., Zheng, Y., Wang, C., Xie, J., Wang, B., Wang, Z., . . . Niu, M. (2016). Improved stability of (+)-catechin and (−)-epicatechin by complexing with hydroxypropyl-β-cyclodextrin: Effect of pH, temperature and configuration. *Food chemistry*, *196*, 148-154.

Liu, Q., Cai, W., & Shao, X. (2008). Determination of seven polyphenols in water by high performance liquid chromatography combined with preconcentration. *Talanta*, *77*(2), 679-683.

Ma, J.-J., Yu, Y.-G., Yin, S.-W., Tang, C.-H., & Yang, X.-Q. (2018). Cellular uptake and intracellular antioxidant activity of zein/chitosan nanoparticles incorporated with quercetin. *Journal of agricultural and food chemistry*, *66*(48), 12783-12793.

Mahmoud, A. M. (2012). Influence of rutin on biochemical alterations in hyperammonemia in rats. *Experimental and Toxicologic Pathology*, *64*(7), 783-789.

Manach, C., Morand, C., Demigné, C., Texier, O., Régérat, F., & Rémésy, C. (1997). Bioavailability of rutin and quercetin in rats. *FEBS letters*, *409*(1), 12-16.

Mauludin, R., Müller, R. H., & Keck, C. M. (2009). Development of an oral rutin nanocrystal formulation. *International journal of pharmaceutics*, *370*(1-2), 202-209.

McClements, D. J. (2021). Advances in edible nanoemulsions: Digestion, bioavailability, and potential toxicity. *Progress in lipid research*, *81*, 101081.

McGuire, S. (2016). World cancer report 2014. Geneva, Switzerland: World Health Organization, international agency for research on cancer, WHO Press, 2015. *Advances in nutrition*, *7*(2), 418-419.

Milner, J. A. (2000). Functional foods: the US perspective. *The American journal of clinical nutrition*, *71*(6), 1654S-1659S.

Minekus, M., Alminger, M., Alvito, P., Ballance, S., Bohn, T., Bourlieu, C., . . . Dupont, D. (2014). A standardised static in vitro digestion method suitable for food–an international consensus. *Food & function*, *5*(6), 1113-1124.

Morales, A. M., Mukai, R., Murota, K., & Terao, J. (2018). Inhibitory effect of catecholic colonic metabolites of rutin on fatty acid hydroperoxide and hemoglobin dependent lipid peroxidation in Caco-2 cells. *Journal of Clinical Biochemistry and Nutrition*, 18-38.

Moughan, P. J. (2020). Holistic properties of foods: a changing paradigm in human nutrition. *Journal of the Science of Food and Agriculture*, *100*(14), 5056-5063.

Müller, E., Berger, R., Blass, E., Sluyts, D., & Pfennig, A. (2000). Liquid–liquid extraction. *Ullmann's Encyclopedia of Industrial Chemistry*.

Naczk, M., Grant, S., Zadernowski, R., & Barre, E. (2006). Protein precipitating capacity of phenolics of wild blueberry leaves and fruits. *Food chemistry*, *96*(4), 640-647.

Naczk, M., & Shahidi, F. (2006). Phenolics in cereals, fruits and vegetables: Occurrence, extraction and analysis. *Journal of pharmaceutical and biomedical analysis*, *41*(5), 1523-1542.

Nagasawa, T., Tabata, N., Ito, Y., & Nishizawa, N. (2002). Suppression of early and advanced glycation by dietary water-soluble rutin derivative in diabetic rats. *International Congress Series*, *1245*, 403-405.

Natoli, M., Leoni, B. D., D'Agnano, I., Zucco, F., & Felsani, A. (2012). Good Caco-2 cell culture practices. *Toxicology in Vitro*, *26*(8), 1243-1246.

Naveen, P., Lingaraju, H., & Anitha, K. (2017). Simultaneous determination of rutin, isoquercetin, and quercetin flavonoids in Nelumbo nucifera by high-performance liquid chromatography method. *International journal of pharmaceutical investigation*, *7*(2), 94.

Negahdari, R., Bohlouli, S., Sharifi, S., Maleki Dizaj, S., Rahbar Saadat, Y., Khezri, K., . . . Raeesi, S. (2021). Therapeutic benefits of rutin and its nanoformulations. *Phytotherapy Research*, *35*(4), 1719-1738.

Németh, K., Plumb, G. W., Berrin, J.-G., Juge, N., Jacob, R., Naim, H. Y., . . . Kroon, P. A. (2003). Deglycosylation by small intestinal epithelial cell β-glucosidases is a critical step in the absorption and metabolism of dietary flavonoid glycosides in humans. *European Journal of Nutrition*, *42*(1), 29-42.

Nguyen, T. A., Liu, B., Zhao, J., Thomas, D. S., & Hook, J. M. (2013). An investigation into the supramolecular structure, solubility, stability and antioxidant activity of rutin/cyclodextrin inclusion complex. *Food chemistry*, *136*(1), 186-192.

Nollet, L. M., & Toldrá, F. (2012). *Food analysis by HPLC*. CRC press.

Oboh, G., Ademosun, A. O., Ayeni, P. O., Omojokun, O. S., & Bello, F. (2015). Comparative effect of quercetin and rutin on α-amylase, α-glucosidase, and some pro-oxidant-induced lipid peroxidation in rat pancreas. *Comparative Clinical Pathology*, *24*(5), 1103-1110.

Olejnik, A., Rychlik, J., Kidoń, M., Czapski, J., Kowalska, K., Juzwa, W., . . . Moyer, M. P. (2016). Antioxidant effects of gastrointestinal digested purple carrot extract on the human cells of colonic mucosa. *Food chemistry*, *190*, 1069-1077.

Organization, P. A. H. (2019). *NCDs at a Glance: NCD Mortality and Risk Factor Prevalence in the Americas. Washington, D.C. : PAHO*.

Paczkowska, M., Mizera, M., Piotrowska, H., Szymanowska-Powałowska, D., Lewandowska, K., Goscianska, J., . . . Cielecka-Piontek, J. (2015). Complex of rutin with β-cyclodextrin as potential delivery system. *PLoS One*, *10*(3), e0120858.

Panche, A., Diwan, A., & Chandra, S. (2016). Flavonoids: an overview. *Journal of nutritional science*, *5*.

Patil, S. L., Somashekarappa, H., & Rajashekhar, K. (2012). Evaluation of the radioprotective action of rutin in mice exposed to gamma-radiation. *Int J Biol Pharm Res*, *3*, 12-18.

Ponnusamy, Y., Chear, N. J.-Y., Ramanathan, S., & Lai, C.-S. (2015). Polyphenols rich fraction of Dicranopteris linearis promotes fibroblast cell migration and proliferation in vitro. *Journal of Ethnopharmacology*, *168*, 305-314.

Prasad, R., & Prasad, S. (2019). A review on the chemistry and biological properties of Rutin, a promising nutraceutical agent. *Asian Journal of Pharmacy and Pharmacology*, *5*, 1-20.

Prior, R. L., Wu, X., & Schaich, K. (2005). Standardized methods for the determination of antioxidant capacity and phenolics in foods and dietary supplements. *Journal of agricultural and food chemistry*, *53*(10), 4290-4302.

Proestos, C., Boziaris, I., Nychas, G.-J., & Komaitis, M. (2006). Analysis of flavonoids and phenolic acids in Greek aromatic plants: Investigation of their antioxidant capacity and antimicrobial activity. *Food Chemistry*, *95*(4), 664-671.

Pyrzynska, K., & Pękal, A. (2013). Application of free radical diphenylpicrylhydrazyl (DPPH) to estimate the antioxidant capacity of food samples. *Analytical Methods*, *5*(17), 4288-4295.

Rashidinejad, A., Acevedo-Fani, A., Singh, H., Loveday, S., Thompson, A., and Niu, Z. (2020). *Flavonoid delivery system. WO2020095238A1 (PCT/IB2019/059560).*

Rashidinejad, A., Jameson, G. B., & Singh, H. (2022). The Effect of pH and Sodium Caseinate on the Aqueous Solubility, Stability, and Crystallinity of Rutin towards Concentrated Colloidally Stable Particles for the Incorporation into Functional Foods. *Molecules*, *27*(2), 534.

Rashidinejad, A., Loveday, S. M., Jameson, G. B., Hindmarsh, J. P., & Singh, H. (2019). Rutin-casein co-precipitates as potential delivery vehicles for flavonoid rutin. *Food Hydrocolloids*, *96*, 451-462.

Rashidinejad;, A., Fani;, A. A., & Singh;, H. (2022). *Flavonoid-enriched spray-dried powder*.

Ravi, G., Charyulu, R. N., Dubey, A., Prabhu, P., Hebbar, S., & Mathias, A. C. (2018). Nano-lipid complex of rutin: Development, characterisation and in vivo investigation of hepatoprotective, antioxidant activity and bioavailability study in rats. *Aaps Pharmscitech*, *19*(8), 3631-3649.

Rice-Evans, C. A., Miller, N. J., & Paganga, G. (1996). Structure-antioxidant activity relationships of flavonoids and phenolic acids. *Free Radical Biology and Medicine*, *20*(7), 933-956.

Roberfroid, M. B. (2002). Global view on functional foods: European perspectives. *Br J Nutr*, *88 Suppl 2*, S133-138.

Ruiz-Cruz, S., & Ornelas-Paz, J. (2017). Flavonoids: Important Biocompounds in Food. In.

Sáez-Tormo, G., Oliva, M., Muniz, P., Valls, V., Iradi, A., Ramos, M., & Climent, J. (1994). Oxidative stress and genetic damage. *Health and orange*, 51-60.

Sak, K. (2014). Cytotoxicity of dietary flavonoids on different human cancer types. *Pharmacognosy reviews*, *8*(16), 122.

Sando, C. E., & Lloyd, J. U. (1924). The isolation and identification of rutin from the flowers of elder (Sambucus canadensis L.). *Journal of Biological Chemistry*, *58*(3), 737-745.

Sen, S., & Chakraborty, R. (2017). Revival, modernization and integration of Indian traditional herbal medicine in clinical practice: Importance, challenges and future. *Journal of traditional and complementary medicine*, *7*(2), 234-244.

Serhan, C. N., Ward, P. A., & Gilroy, D. W. (2010). *Fundamentals of inflammation*. Cambridge University Press.

Sharma, S., Ali, A., Ali, J., Sahni, J. K., & Baboota, S. (2013). Rutin: therapeutic potential and recent advances in drug delivery. *Expert Opinion on Investigational Drugs*, *22*(8), 1063-1079.

Shi, J., Xue, S. J., Wang, B., Wang, W., Ye, X., & Quek, S. Y. (2015). Optimization of formulation and influence of environmental stresses on stability of lycopene-microemulsion. *LWT-Food Science and Technology*, *60*(2), 999-1008.

Shpigelman, A., Cohen, Y., & Livney, Y. D. (2012). Thermally-induced β-lactoglobulin–EGCG nanovehicles: Loading, stability, sensory and digestive-release study. *Food Hydrocolloids*, *29*(1), 57-67.

Singh, D., SM Rawat, M., Semalty, A., & Semalty, M. (2012). Rutin-phospholipid complex: an innovative technique in novel drug delivery system-NDDS. *Current drug delivery*, *9*(3), 305-314.

Sri, K. V., Kondaiah, A., Ratna, J. V., & Annapurna, A. (2007). Preparation and characterization of quercetin and rutin cyclodextrin inclusion complexes. *Drug development and industrial pharmacy*, *33*(3), 245-253.

Srinivasan, B., Kolli, A. R., Esch, M. B., Abaci, H. E., Shuler, M. L., & Hickman, J. J. (2015). TEER measurement techniques for in vitro barrier model systems. *SLAS Technology*, *20*(2), 107-126.

Stalikas, C. D. (2007). Extraction, separation, and detection methods for phenolic acids and flavonoids. *Journal of separation science*, *30*(18), 3268-3295.

Supplements, I. B. F.-F. (2021). *The global functional food and beverage market is projected to grow from $281.14 billion in 2021 to $529.66 billion in 2028 at a CAGR of 9.5%... Read More at:- https://www.fortunebusinessinsights.com/functional-foods-market-102269*.

Suzuki, T., Honda, Y., & Mukasa, Y. (2005). Effects of UV-B radiation, cold and desiccation stress on rutin concentration and rutin glucosidase activity in tartary buckwheat (Fagopyrum tataricum) leaves. *Plant Science*, *168*(5), 1303-1307.

Suzuki, T., Morishita, T., Noda, T., & Ishiguro, K. (2015). Acute and subacute toxicity studies on rutin-rich Tartary buckwheat dough in experimental animals. *Journal of nutritional science and vitaminology*, *61*(2), 175-181.

Szejtli, J. (1998). Introduction and general overview of cyclodextrin chemistry. *Chemical reviews*, *98*(5), 1743-1754.

Thiruvengadam, M., Rajakumar, G., & Chung, I.-M. (2018). Nanotechnology: current uses and future applications in the food industry. *3 Biotech*, *8*(1), 1-13.

Thompson, A. K., FANI, A. A., RASHIDINEJAD, A., Singh, H., LOVEDAY, S. D. M., & Niu, Z. (2020). Flavonoid delivery system. In: Google Patents.

Tiwari, R., Siddiqui, M. H., Mahmood, T., Farooqui, A., Bagga, P., Ahsan, F., & Shamim, A. (2020). An exploratory analysis on the toxicity & safety profile of Polyherbal

Vogrincic, M., Timoracka, M., Melichacova, S., Vollmannova, A., & Kreft, I. (2010). Degradation of rutin and polyphenols during the preparation of tartary buckwheat bread. *Journal of agricultural and food chemistry*, *58*(8), 4883-4887.

Wach, A., Pyrzyńska, K., & Biesaga, M. (2007). Quercetin content in some food and herbal samples. *Food Chemistry*, *100*(2), 699-704.

Walia, N., & Chen, L. (2020). Pea protein based vitamin D nanoemulsions: Fabrication, stability and in vitro study using Caco-2 cells. *Food chemistry*, *305*, 125475.

Wan, H., Liu, D., Yu, X., Sun, H., & Li, Y. (2015). A Caco-2 cell-based quantitative antioxidant activity assay for antioxidants. *Food chemistry*, *175*, 601-608.

Wang, C., & Li, S. (2015). Functional foods and nutraceuticals potential role in human health. *Clinical aspects of functional foods and nutraceuticals*, *2015*, 51-76.

Wang, S.-w., Wang, Y.-J., Su, Y.-j., Zhou, W.-w., Yang, S.-g., Zhang, R., . . . Liu, R.-t. (2012). Rutin inhibits β-amyloid aggregation and cytotoxicity, attenuates oxidative stress, and decreases the production of nitric oxide and proinflammatory cytokines. *NeuroToxicology*, *33*(3), 482-490.

Wei, Z., Yang, W., Fan, R., Yuan, F., & Gao, Y. (2015). Evaluation of structural and functional properties of protein–EGCG complexes and their ability of stabilizing a model β-carotene emulsion. *Food Hydrocolloids*, *45*, 337-350.

Wolfe, K. L., & Liu, R. H. (2007). Cellular antioxidant activity (CAA) assay for assessing antioxidants, foods, and dietary supplements. *Journal of agricultural and food chemistry*, *55*(22), 8896-8907.

Wu, X., & Schauss, A. G. (2012). Mitigation of Inflammation with Foods. *Journal of Agricultural and Food Chemistry*, *60*(27), 6703-6717.

Xie, J., Shi, L., Zhu, X., Wang, P., Zhao, Y., & Su, W. (2011). Mechanochemical-assisted efficient extraction of rutin from Hibiscus mutabilis L. *Innovative Food Science & Emerging Technologies*, *12*(2), 146-152.

Yang, J., Guo, J., & Yuan, J. (2008a). In vitro antioxidant properties of rutin. *LWT-Food Science and Technology*, *41*(6), 1060-1066.

Yang, J., Guo, J., & Yuan, J. (2008b). In vitro antioxidant properties of rutin. *LWT - Food Science and Technology*, *41*(6), 1060-1066.

Yang, R., Sun, G., Zhang, M., Zhou, Z., Li, Q., Strappe, P., & Blanchard, C. (2016). Epigallocatechin gallate (EGCG) decorating soybean seed ferritin as a rutin nanocarrier with prolonged release property in the gastrointestinal tract. *Plant Foods for Human Nutrition*, *71*(3), 277-285.

Ye, J., Deng, L., Wang, Y., McClements, D. J., Luo, S., & Liu, C. (2021). Impact of rutin on the foaming properties of soybean protein: Formation and characterization of flavonoid-protein complexes. *Food chemistry*, *362*, 130238.

Yildirim-Elikoglu, S., & Erdem, Y. K. (2018). Interactions between milk proteins and polyphenols: Binding mechanisms, related changes, and the future trends in the dairy industry. *Food Reviews International*, *34*(7), 665-697.

Yousefi, M., & Jafari, S. M. (2019). Recent advances in application of different hydrocolloids in dairy products to improve their techno-functional properties. *Trends in food science & technology*, *88*, 468-483.

Yu, X.-L., Li, Y.-N., Zhang, H., Su, Y.-J., Zhou, W.-W., Zhang, Z.-P., . . . Liu, R.-T. (2015). Rutin inhibits amylin-induced neurocytotoxicity and oxidative stress [10.1039/C5FO00500K]. *Food & Function*, *6*(10), 3296-3306.

Yuan, X., Xiao, J., Liu, X., McClements, D. J., Cao, Y., & Xiao, H. (2019). The gastrointestinal behavior of emulsifiers used to formulate excipient emulsions impact the bioavailability of β-carotene from spinach. *Food chemistry*, *278*, 811-819.

Zhang, R., & McClements, D. J. (2016). Enhancing nutraceutical bioavailability by controlling the composition and structure of gastrointestinal contents: Emulsion-based delivery and excipient systems. *Food structure*, *10*, 21-36.

Zhang, S., & Han, Y. (2018). Preparation, characterisation and antioxidant activities of rutin-loaded zein-sodium caseinate nanoparticles. *PLoS One*, *13*(3), e0194951.

Zhang, X., Song, J., Shi, X., Miao, S., Li, Y., & Wen, A. (2013). Absorption and metabolism characteristics of rutin in Caco-2 cells. *The Scientific World Journal*, *2013*.

Zhang, Y., Li, S.-f., & Wu, X.-w. (2008). Pressurized liquid extraction of flavonoids from Houttuynia cordata Thunb. *Separation and Purification Technology*, *58*(3), 305-310.

Zi, J., Peng, B., & Yan, W. (2007). Solubilities of rutin in eight solvents at T=283.15, 298.15, 313.15, 323.15, and 333.15K. *Fluid Phase Equilibria*, *261*(1), 111-114.

Ziaee, A., Zamansoltani, F., Nassiri-Asl, M., & Abbasi, E. (2009). Effects of Rutin on Lipid Profile in Hypercholesterolaemic Rats. *Basic & Clinical Pharmacology & Toxicology*, *104*(3), 253-258.

Zu, Y., Li, C., Fu, Y., & Zhao, C. (2006). Simultaneous determination of catechin, rutin, quercetin kaempferol and isorhamnetin in the extract of sea buckthorn (Hippophae rhamnoides L.) leaves by RP-HPLC with DAD. *Journal of pharmaceutical and biomedical analysis*, *41*(3), 714-719.

Zvezdanović, J. B., Stanojević, J. S., Marković, D. Z., & Cvetković, D. J. (2012). Irreversible UV-induced quercetin and rutin degradation in solution, studied by UV-spectrophotometry and HPLC chromatography. *Journal of the Serbian Chemical Society*, *77*(3), 297-312.

Appendices

Appendix 1: Permission to reproduce images

ELSEVIER LICENSE
TERMS AND CONDITIONS

Jul 03, 2022

This Agreement between Massey University -- Anubhavi Singh ("You") and Elsevier ("Elsevier") consists of your license details and the terms and conditions provided by Elsevier and Copyright Clearance Center.

License Number	5341670521842
License date	Jul 03, 2022
Licensed Content Publisher	Elsevier
Licensed Content Publication	Computational and Theoretical Chemistry
Licensed Content Title	Protective effect of rutin (vitamin p) against heme oxidation: A quantum mechanical approach
Licensed Content Author	Mina Ghiasi,Afsaneh Azadnia,Masoud Arabieh,Mansour Zahedi
Licensed Content Date	Sep 15, 2012
Licensed Content Volume	996
Licensed Content Issue	n/a
Licensed Content Pages	9
Start Page	28
End Page	36
Type of Use	reuse in a thesis/dissertation

Portion	figures/tables/illustrations
Number of figures/tables/illustrations	1
Format	both print and electronic
Are you the author of this Elsevier article?	No
Will you be translating?	No
Title	Bioactivity and bioaccessibility of novel rutin-protein composites incorporated into a functional dairy beverage
Institution name	Massey University
Expected presentation date	Jul 2022
Portions	Fig. 1. Chemical structure of rutin with atom's numbering system indicated.
Requestor Location	Massey University Massey University, Manawatu (Turitea) Tennent Drive Palmerston North Palmerston North, Manawatu 4474 New Zealand Attn: Massey University
Publisher Tax ID	GB 494 6272 12
Total	0.00 USD
Terms and Conditions	

Reproduced as*: **Figure 5.1** Chemical structure of rutin (quercetin-3-O-rutinoside).* Chapter 2, Literature Review, Section 2.2.1.

Appendix 2: Calibration curve of Gallic acid for Folin-Ciocâlteu method

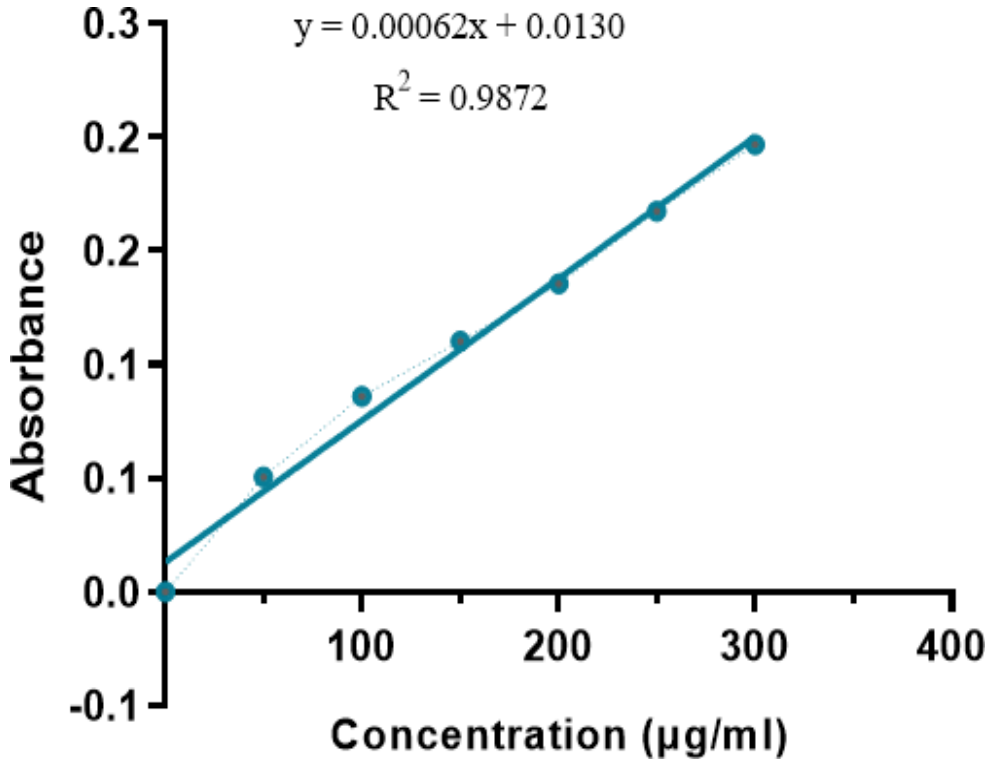

Appendix 3: Calibration curve Trolox standard for DPPH assay

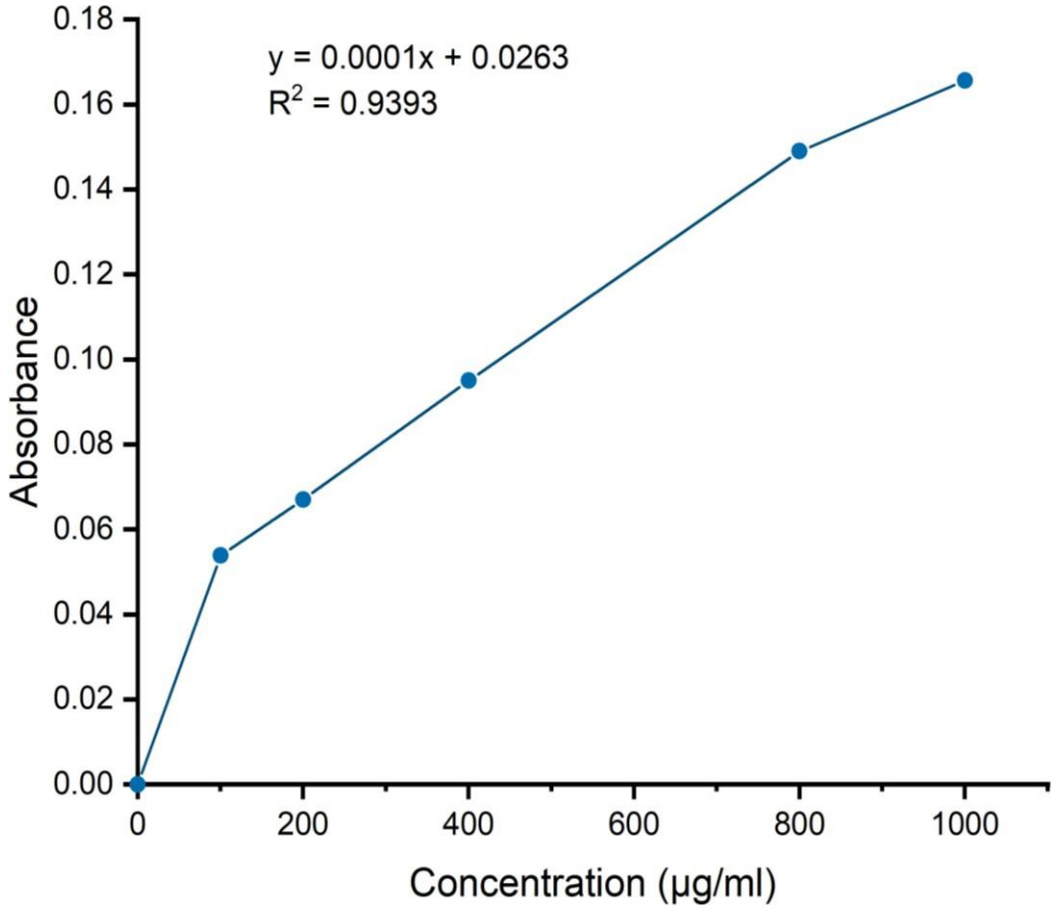

Appendix 4: Calibration curve of Rutin standard for HPLC

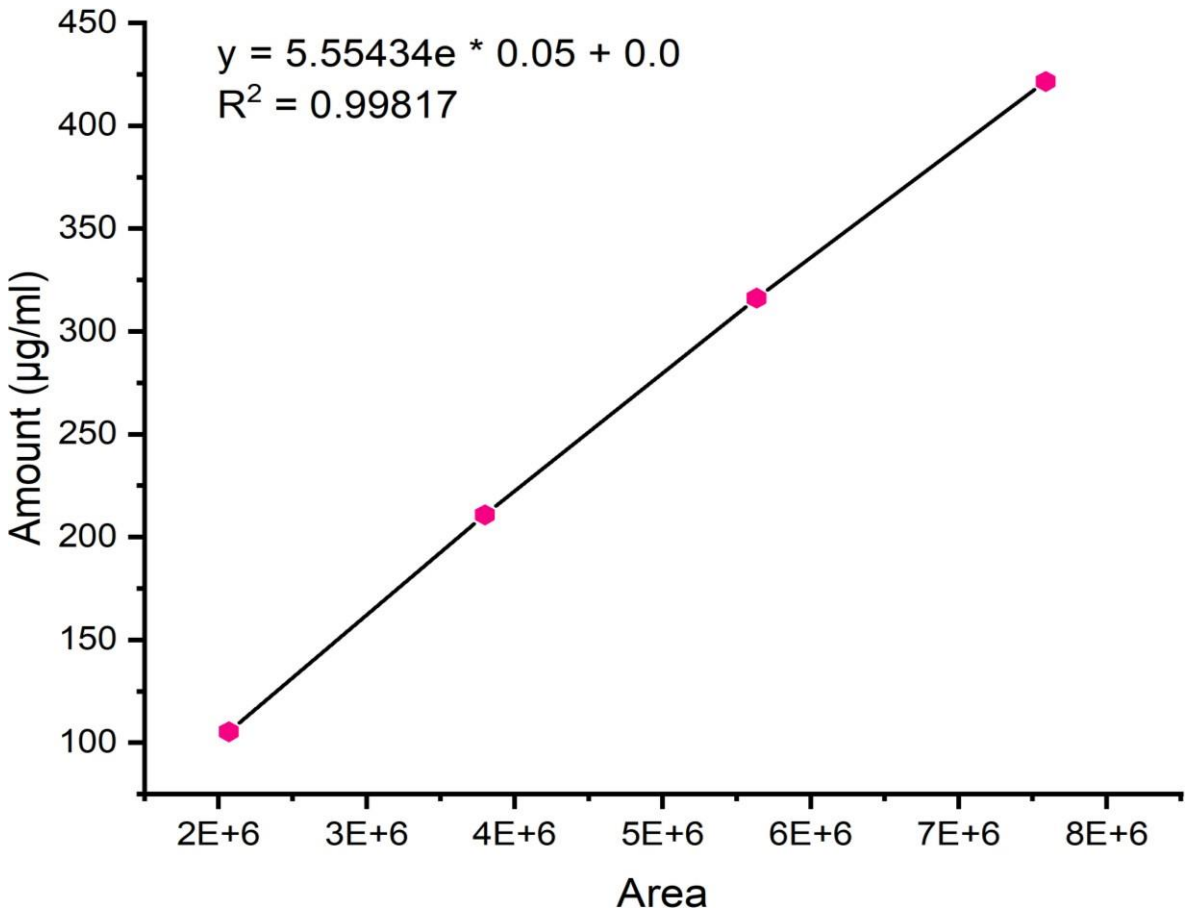

Amount	Area	RF	Last Area	Residual
105.4	2068790	5.09476553927658e-005		-9.50772
210.8	3797497	5.55102479343631e-005		-0.12606
316.2	5633609	5.61274309239424e-005		3.28996
421.6	7586625	5.55714827080553e-005		0.212724

Linear Fit ax + b
a = 5.55434e-005
b = 0.000000
Goodness of fit (r^2): 0.998177

Average RF: 5.45392e-005
RF StDev: 2.41041e-006
RF %RSD: 4.41959